

2008

# evaluation of elliptical, glass fiber reinforced polymer, and stainless steel dowel bars in concrete pavements with consideration to subgrade resilient modulus

Jason Matthew Walker  
*Iowa State University*

Follow this and additional works at: <https://lib.dr.iastate.edu/etd>

 Part of the [Civil and Environmental Engineering Commons](#)

---

## Recommended Citation

Walker, Jason Matthew, "evaluation of elliptical, glass fiber reinforced polymer, and stainless steel dowel bars in concrete pavements with consideration to subgrade resilient modulus" (2008). *Graduate Theses and Dissertations*. 11092.  
<https://lib.dr.iastate.edu/etd/11092>

This Thesis is brought to you for free and open access by the Iowa State University Capstones, Theses and Dissertations at Iowa State University Digital Repository. It has been accepted for inclusion in Graduate Theses and Dissertations by an authorized administrator of Iowa State University Digital Repository. For more information, please contact [digirep@iastate.edu](mailto:digirep@iastate.edu).

**Evaluation of elliptical, glass fiber reinforced polymer, and stainless steel dowel bars in  
concrete pavements with consideration to subgrade resilient modulus**

by

**Jason Matthew Walker**

A thesis submitted to the graduate faculty  
in partial fulfillment of the requirements for the degree of  
**MASTER OF SCIENCE**

Major: Civil Engineering (Geotechnical Engineering)

Program of Study Committee:  
James K. Cable, Major Professor  
Vernon Schaefer  
Stephen Vardeman  
Kejin Wang

Iowa State University

Ames, Iowa

2008

Copyright © Jason Matthew Walker, 2008. All rights reserved.

## Table of Contents

Table of Contents .....	ii
List of Figures .....	v
List of Tables.....	vii
Abstract .....	viii
Chapter 1. Introduction .....	1
1.1 Background .....	1
1.2 Research Needs .....	4
1.3 Research Objectives .....	5
Chapter 2. Literature Review .....	6
2.1 Falling Weight Deflectometer (FWD).....	6
2.2 Load Transfer Efficiency.....	9
2.3 Back-calculation.....	10
2.4 Modulus of Subgrade Reaction .....	11
2.5 Resilient Modulus.....	13
2.5.1 AASHTO T-307-99.....	16
2.5.2 Moisture Content Effects.....	20
2.5.3 Stress State Effects .....	22
2.5.4 Freeze-Thaw Effects.....	23
2.5.5 Compaction Method Effects.....	24
2.6 Resilient Modulus Constitutive Models .....	24
2.6.1 Power-Law Model.....	24
2.6.2 Universal Model .....	25
2.6.3 Universal Model w/ Octahedral Shear.....	26
2.6.4 Modified Universal Model w/ Octahedral Shear.....	26
Chapter 3. Research Plan .....	28
3.1 Site Reviews .....	28
3.1.1 Iowa Highway 330 Site .....	28
3.1.2 US Highway 65 Site .....	29
3.2 Dowel Materials .....	30

3.2.1	Iowa Highway 330 – Dowel Material .....	30
3.2.2	US Highway 65 – Dowel Material .....	31
3.3	Construction .....	31
3.3.1	Iowa Highway 330- Construction.....	31
3.3.2	US Highway 65 – Construction.....	33
Chapter 4.	Data Collection.....	36
4.1	FWD / Load Transfer .....	36
4.1.1	HWY 330- FWD .....	36
4.1.2	US 65- FWD.....	37
4.2	Resilient Modulus.....	38
4.2.1	Soil Sampling .....	38
4.2.2	Resilient Modulus Testing.....	40
4.3	Profile /Roughness.....	42
4.4	Faulting.....	43
Chapter 5.	Data Analysis.....	46
5.1	Soil Comparison Determination .....	46
5.2	Resilient Modulus.....	47
5.2.1	HWY 330- Resilient Modulus.....	48
5.2.2	US 65- Resilient Modulus .....	53
5.3	Load Transfer .....	54
5.3.1	HWY 330- Load Transfer .....	54
5.3.1.1	Dowel Basket Type – HWY 330 Load Transfer .....	55
5.3.1.2	Dowel Type – HWY 330 Load Transfer .....	57
5.3.1.3	Dowel Spacing – HWY 330 Load Transfer .....	59
5.3.2	US 65–Load Transfer .....	62
5.3.2.1	Dowel Type – US 65 Load Transfer .....	63
5.3.2.2	Dowel Spacing – US 65 Load Transfer.....	65
5.4	Faulting.....	67
5.4.1	HWY 330- Faulting.....	67
5.4.1.1	Dowel Basket Type – HWY 330 Faulting.....	68
5.4.1.2	Dowel Type - HWY 330 Faulting .....	70

5.4.1.3	Dowel Spacing - HWY 330 Faulting .....	73
5.4.2	US 65 - Faulting .....	76
5.5	HWY 330 Profile/ Roughness .....	77
5.5.1	Dowel Basket Type – HWY 330 IRI.....	79
5.5.2	Dowel Type – HWY 330 IRI .....	81
5.5.3	Dowel Spacing – HWY 330 IRI.....	83
Chapter 6.	Summary and Conclusions .....	87
6.1	Load Transfer .....	87
6.1.1	Dowel Basket Type – Load Transfer Conclusions .....	87
6.1.2	Dowel Type – Load Transfer Conclusions.....	88
6.1.3	Dowel Spacing – Load Transfer Conclusions .....	90
6.2	Faulting.....	92
6.2.1	Dowel Basket Type – Faulting Conclusions .....	92
6.2.2	Dowel Type – Faulting Conclusions .....	92
6.2.3	Dowel Spacing – Faulting Conclusions.....	93
6.3	Profile / Roughness.....	94
6.3.1	Dowel Basket Type – Roughness Conclusions .....	94
6.3.2	Dowel Type – Roughness Conclusions .....	94
6.3.3	Dowel Spacing – Roughness Conclusions .....	95
6.4	Overall Summary and Conclusions .....	95
Chapter 7.	Recommendations .....	98
7.1	Design Considerations.....	98
7.2	Further Study.....	98
References	.....	99
Appendix A	.....	102
Appendix B	.....	106
Appendix C	.....	107
Appendix D	.....	108

## List of Figures

Figure 1: Falling Weight Deflectometer Schematic (Darter & Barenberg, 1977).....	7
Figure 2: Typical FWD Sensor Spacing and Deflection Basin .....	8
Figure 3: Possible shapes of a deflection basin (McDaniel, 1998).....	9
Figure 4: Typical Triaxial Chamber with External LVDTs and Load Cell.....	16
Figure 5: Principal Stresses Acting on Finite Soil Specimen .....	17
Figure 6: Strain Diagram per Loading Sequence .....	19
Figure 7: Deviator Stress vs. Strain for Resilient Modulus Testing .....	19
Figure 8: Three Phase Soil Diagram .....	21
Figure 9: Effects of Post-Compaction Saturation on Resilient Modulus .....	21
Figure 10: Typical Deviator Stress vs. Resilient Modulus.....	22
Figure 11: HWY 330 Test Section Plan View .....	29
Figure 12: US 65 Test Section Plan View.....	30
Figure 13: HWY 330 Typical Dowel Spacing Configurations .....	32
Figure 14: HWY 330 Typical Pavement Profile .....	33
Figure 15: US 65 Typical Dowel Spacing Configurations.....	34
Figure 16: US 65 Typical Pavement Profile.....	35
Figure 17: Falling Weight Deflectometer (Cable J. K., et al. 2003).....	37
Figure 18: HWY 330 and US 65 Typical Shelby Tube Boring Depth.....	39
Figure 19: Shelby Tube Extruder .....	40
Figure 20: Actual Triaxial Chamber with External LVDT and Load Cell.....	41
Figure 21: Georgia Faultmeter (Hoffman, 2002) .....	43
Figure 22: Positive and Negative Faulting Schematic.....	44
Figure 23: Faultmeter Application Diagram .....	45
Figure 24: HWY 330 Example of Actual vs. Predicted Resilient Modulus.....	50
Figure 25: HWY 330 Load Transfer vs. Resilient Modulus .....	55
Figure 26: HWY 330 Load Transfer by Basket Type - Medium Elliptical Dowels.....	56
Figure 27: HWY 330 Load Transfer by Basket Type – Standard Round Dowels .....	57
Figure 28: HWY 330 Load Transfer Performance by Dowel Type @ 12 inch Spacing.....	58
Figure 29: HWY 330 Load Transfer Performance by Dowel Type @ 15 inch Spacing.....	59
Figure 30: HWY 330 Load Transfer by Dowel Spacing - Heavy Elliptical Dowels .....	60
Figure 31: HWY 330 Load Transfer by Dowel Spacing - Medium Elliptical Dowels .....	61
Figure 32: HWY 330 Load Transfer by Dowel Spacing - Standard Round Dowels .....	62
Figure 33: US 65 Load Transfer vs. Resilient Modulus.....	63
Figure 34: US 65 Load Transfer Performance by Dowel Type @ 12 inch Spacing .....	64
Figure 35: US 65 Load Transfer Performance by Dowel Type @ Eight Inch Spacing .....	65
Figure 36: US 65 Load Transfer Performance by Dowel Spacing.....	66
Figure 37: HWY 330 Joint Faulting vs. Resilient Modulus .....	67
Figure 38: HWY 330 Joint Faulting by Basket Type - Medium Elliptical Dowels .....	69
Figure 39: HWY 330 Joint Faulting by Basket Type – Standard Round Dowels.....	69

Figure 40: HWY 330 Joint Faulting by Bar Type @ 12 inch Spacing.....	70
Figure 41: HWY 330 Joint Faulting by Bar Type @ 15 inch Spacing.....	71
Figure 42: HWY 330 Joint Faulting by Bar Type @ 18 inch Spacing.....	72
Figure 43: HWY 330 Joint Faulting by Dowel Spacing – Heavy Elliptical Dowels .....	73
Figure 44: HWY 330 Joint Faulting by Dowel Spacing – Medium Elliptical Dowels .....	74
Figure 45: HWY 330 Joint Faulting Medium Elliptical Dowels (Mr Sections Only).....	75
Figure 46: HWY 330 Joint Faulting by Dowel Spacing - Standard Round Dowels .....	75
Figure 47: HWY 330 Joint Faulting Standard Round Dowels (Mr Sections Only).....	76
Figure 48: US 65 Joint Faulting Performance by Dowel Type and Spacing.....	77
Figure 49: HWY 330 Roughness vs. Resilient Modulus.....	79
Figure 50: HWY 330 Roughness by Basket Type - Medium Elliptical Dowels.....	80
Figure 51: HWY 330 Roughness by Basket Type – Standard Round Dowels .....	81
Figure 52: HWY 330 Roughness Performance by Dowel Type @ 12 inch Spacing.....	82
Figure 53: HWY 330 Roughness Performance by Dowel Type @ 15 inch Spacing.....	82
Figure 54: HWY 330 Roughness Performance by Dowel Type @ 18 inch Spacing.....	83
Figure 55: HWY 330 Roughness by Dowel Spacing - Heavy Elliptical Dowels.....	84
Figure 56: HWY 330 Roughness by Dowel Spacing - Medium Elliptical Dowels .....	85
Figure 57: HWY 330 Roughness by Dowel Spacing – Standard Round Dowels .....	86
Figure 58: HWY 330 Load Transfer by Bar Type @ 18 inch Spacing .....	107
Figure 59: HWY 330 Joint Faulting by Bar Type @ 18 inch Spacing.....	107

## List of Tables

Table 1: Recommended k-value ranges for various soil types (AASHTO, 1998) .....	13
Table 2: Typical Mr values for unbound granular and subgrade materials .....	15
Table 3: Resilient Modulus Triaxial Loading Sequences.....	18
Table 4: HWY 330 Dowel Bar Cross-Sections .....	31
Table 5: US 65 Dowel Bar Cross-Section .....	31
Table 6: HWY 330 FWD Machine Sensor Location .....	36
Table 7: US 65 FWD Machine Sensor Locations .....	37
Table 8: HWY 330 Borings with Constitutive Model Used.....	50
Table 9: US 65 Borings with Constitutive Model Used.....	53
Table 10: HWY 330 Steel Used per Joint by Dowel Type and Spacing.....	97
Table 11: HWY 330 Dowel Basket Locations .....	102
Table 12: US 65 Dowel Basket Locations .....	106
Table 13: HWY 330 Performance Data Summary .....	108
Table 14: US 65 Performance Data Summary .....	110



## **Abstract**

Jointed plain concrete pavements use dowel bars to transfer load across transverse joints. The job of the designer is to optimize the number, size, and location of the dowels in a given pavement. This research used data from two different construction locations. The first project evaluated the performance of standard 1.5 inch round and elliptical shaped dowel bars at different spacing intervals using full dowel baskets. The performance potential of standard 1.5 inch round and elliptical dowels placed in the wheel paths only was also evaluated on the same project. The second project compared corrosion resistant dowel bar (stainless steel and glass fiber reinforced polymer (GFRP) dowel bars) performance to round 1.5 inch epoxy-coated steel dowel bars. The stainless steel and GFRP bars are for possible use in environments where steel corrosion may be an issue.

Performance data was measured on both projects in terms of deflections, using falling weight deflectometer (FWD) data collected biannually. Joint faulting data was collected over the five-year test period for both projects. Roughness data was collected for only the elliptical dowel bar project over the five-year test period. Resilient modulus values were found by triaxial testing of the pavement subgrade samples. Performance criteria graphed verses resilient modulus allowed for the comparison of different dowels as the subgrade resilient modulus changed.

The elliptical dowel bar study indicated medium elliptical dowel bars at 12 inch or 15 inch spacing perform equally to the standard 1.5 inch round dowel bars at 12 inch spacing. The elliptical study also indicated the potential use of medium elliptical dowel bars in wheel paths only. The corrosion resistance study indicated stainless steel dowels spaced at eight inch intervals were the only dowels to outperform the 12 inch spaced round 1.5 inch epoxy-coated bars.

## Chapter 1. Introduction

### 1.1 Background

Concrete pavements were first developed in the 19<sup>th</sup> century. Since then, much has been done to try and increase the performance of Portland Cement Concrete (PCC) pavements.

There are three main types of Portland Cement Concrete (PCC) pavements that are being utilized in concrete paving construction: Jointed Reinforced Concrete Pavements (JRCP), Continuously Reinforced Concrete Pavements (CRCP), and Jointed Plain Concrete Pavements (JPCP).

The JRCPs are noted for having fairly long joints, typically spaced at 30 to 100 foot increments. They utilize dowel bars at joints to transfer load from one slab to the next. JRCPs also use reinforcing within the slab to control cracking and to hold the slab together in the event of cracking (Huang, 2003).

The CRCPs are characterized by concrete laid in a continuous slab. This continuous slab is reinforced with rebar. The idea of the CRCP is to prevent large cracks by allowing the steel reinforcing to take the tensile stresses induced on the concrete. The original idea was that the joints in JPCP pavements were the weak link in pavement and by eliminating the joint a thinner pavement would be possible to construct (Huang, 2003). The drawback to CRCP construction is the higher material and labor costs compared to JPCP construction.

The more commonly used concrete pavement of the JRCP, CRCP and JPCP is the JPCP. A JPCP is characterized by a series of concrete slabs which are typically 15 to 30 feet

in length (Huang, 2003). The concept behind JPCP is to control where cracking occurs (at the joints), so failure mechanisms can be more closely controlled. One reason concrete pavements can fail is due to lack of load transfer across transverse joints in the pavement. When jointed concrete pavements were first introduced they relied on a mechanism called aggregate interlock to transfer load across the slab's transverse joints. The idea was that the rough aggregate at the vertical interface between two pavement slabs would form alternating groves that in turn transfer load from one slab to the other as the load is applied. This was fairly effective when concrete pavements were first introduced due to much lower magnitude truck loads. Today, the magnitude of truck loads and heavy vehicle loads are often too high for the aggregate interlock mechanism to be effective. Failure of load transfer mechanism can result in loss of subgrade support (caused by pumping) and faulting, which can contribute to other forms of pavement failure (Huang, 2003). The JPCP pavement relies on what are called dowel bars to transfer load across pavement joints. The main purpose of the dowel bar is to help prevent unnecessary cracking of the pavement and to prevent faulting at pavement joints. Traditional bars consist of the 1 inch to 1 7/8 inch diameter round steel dowel bars. However, recent advances in technology and materials have brought rise to the possibilities of using other materials for pavement dowel bars. Epoxy-coated steel, fiber-reinforced polymer (FRP), and stainless steel are among some of the recently proposed materials.

In recent history more attention has been given to the protection of the dowel from corrosion. The use of deicers (i.e. salt) on concrete pavements speeds up the corrosion (oxidation) process when the deicer comes in contact with steel dowels. Dowel bars work by allowing movement of joints in the horizontal direction so when slabs expand and contract

due to temperature effects they do not put horizontal stress on one another. When metal oxidizes it expands. If the dowel bar corrodes and expands it can lock the free-moving joint and create tensile stresses in the concrete that can cause cracking failures of the pavement. Thus, two different methods have been used to protect the dowel bars from corroding. First, epoxy coated steel dowels have been employed to seal the steel dowel from coming in contact with water and air. They were first used for the first time in bridge decks on a bridge in West Conshohocken, Pennsylvania for corrosion protection in 1973 (Kilareski, 1982). Also, joint sealants have been used for some time to keep water out of the joints. These joint sealants are typically asphalt based rubbery seals. In 1998, McDaniel estimated it would cost approximately \$212 billion to fix all the pavements in the United States damaged by corrosion (McDaniel, 1998). This indicates the magnitude of the problem of dowel bar corrosion.

Dowel spacing and size have been changed and tested in the past. The first reported use of dowel bars to transfer load in concrete pavement was in a pavement near Newport News, Virginia in 1917. The bars were  $\frac{3}{4}$  inch diameter and placed at five-foot increments on a 20-foot-wide road. The pavement held up well to heavy truck traffic during World War I (Sutherland & Teller, 1935). This helped spread the use of steel dowel bars in concrete pavements. These  $\frac{3}{4}$  inch diameter bars placed at five-foot increments are a far cry from where pavements are today for carrying heavy loads. Today, the most frequently used dowels are still round steel dowel bars (Colley & Tayabji, 1968). In 1986, Iowa standard practice for dowel joints was to use dowels with a diameter of  $\frac{1}{8}$  the slab thickness, a 12 inch dowel spacing, and a 15 inch to 18 inch long dowel (Colley & Tayabji, 1968). New techniques and

material are being tested all the time to try and increase the performance of concrete pavements.

## **1.2 Research Needs**

There is always a cost associated with using a certain material or size of dowel for transferring load across the transverse joint. The cost can be associated with actual material cost, or in a lack of dowel performance.

It has been proposed that the cross-sectional area of a steel dowel bar may be reduced to obtain equal, if not better performance, if a shape other than a circle is used. One of the proposed shapes is that of an ellipse. Reducing the cross-sectional area of each dowel in a paving project could have significant cost savings to the contractor building the pavement. The cost and availability of materials must be addressed when considering pavement design alternatives. Different shapes or sizes of dowel bars could potentially outperform current round dowels and create a better load transfer mechanism.

The negative effects that corrosion of steel dowels across the transverse joint has had on JPCPs performance record has been cause for concern. State DOTs and pavement design agencies need to be aware of new materials and practices that may help with the issue of corrosion. Potential non-corrosive or less corrosive load transfer mechanism materials need to be evaluated for their feasibility in addressing this important economic issue. However, these materials need to be evaluated for their performance properties in order to determine their potential in future pavement design methods.

### **1.3 Research Objectives**

This research consists of the evaluation of heavy elliptical steel, medium elliptical steel, stainless steel, 1.5 inch fiber composite, and 1.88 inch fiber composite dowel bars compared with standard round 1.5 inch epoxy coated steel dowel bars in PCC pavements of four lane highways. This research is aimed at determining the suitability of using these different dowel types spaced at different intervals for practical use in highway pavement design. The research is also aimed at taking the effects of subgrade resilient modulus into account for analysis. The project accounts for installation during construction, visual distress surveying, and pavement performance evaluation. There are two projects involved in this research. One project, Iowa Highway 330, has heavy elliptical steel and medium elliptical steel dowel bars compared with standard round epoxy coated steel dowel bars spaced at 12 inch, 15 inch, and 18 inch intervals. The same project also includes the evaluation of medium elliptical steel dowels and standard round steel dowels placed in baskets of the wheel path only to determine whether the use of dowel bars in the wheel path only is an effective way to save money in pavement construction. The other project, US Highway 65, has stainless steel, 1.5 inch fiber composite, and 1.88 inch fiber composite dowel bars compared with standard epoxy coated steel dowel bars spaced at eight inch and 12 inch intervals. In each project the test sections are located in a close enough proximity to assume climate and seasonal effects to be consistent across each project. The understanding of how these different dowel bar types and configurations perform could lead to potential economic benefits for pavement construction.

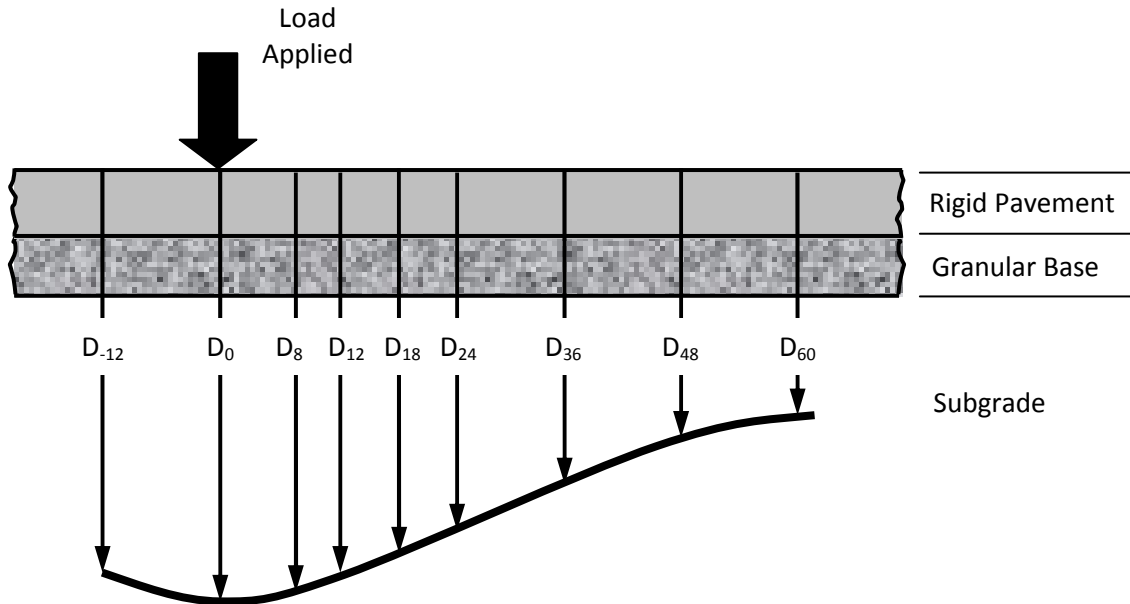
## **Chapter 2. Literature Review**

### **2.1 Falling Weight Deflectometer (FWD)**

A Falling Weight Deflectometer (FWD) is used to perform non-destructive tests (NDT) on pavements through dynamic plate loading tests. A mass from the device is dropped onto a circular pad that is put on the surface of the pavement. The result is a dynamic load on the plate by the falling weight. The purpose of the falling weight deflectometer is to simulate a single heavy vehicle dynamic load. The peak load and surface pavement displacement responses are measured under the loading plate and at several distances from the load center (Thölen, 1982) (Liang & Zeng, 2002). These displacement responses are measured by various sensors. The response at each sensor is collected and stored by the computer attached to the FWD machine. The response of the pavement can be used to calculate failure criteria or to determine properties of the pavement or underlying materials. The load test is typically run three times at three different load magnitudes. These are approximately 6 kip, 9 kip, and 12 kip loads. However, some FWD tests are run with 9 kip, 12 kip, and 16 kip loads. A schematic of a typical trailer mounted FWD machine can be seen in Figure 1.





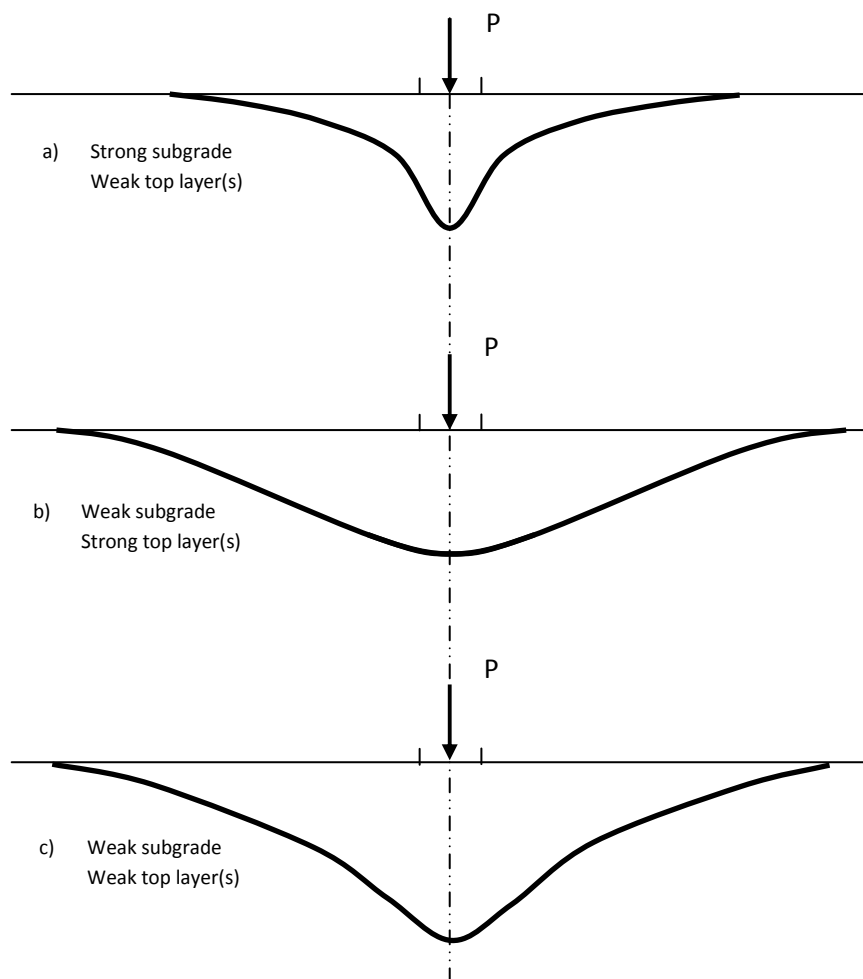


**Figure 2: Typical FWD Sensor Spacing and Deflection Basin**

The FWD test can be used for varying purposes. There are two main places on a concrete pavement where FWD data are taken.

First, FWD data can be collected over the joint of two adjacent slabs. This data can be used to calculate a very commonly used failure mechanism, load transfer efficiency, in jointed plain concrete pavements. The process of determining load transfer efficiency across a joint will be discussed further in section 2.2 later in the paper.

The second place FWD data can be collected in the section between two joints, also known as the mid-slab. FWD data taken at the mid-slab can be used to back-calculate a modulus of subgrade reaction or other subgrade parameters used in pavement design. The process of back-calculating a modulus of subgrade reaction will be discussed later in section 2.3. A schematic of different combinations of subgrade and top layer strength and how that affects the deflection basic shape can be seen below in Figure 3.



**Figure 3: Possible shapes of a deflection basin (McDaniel, 1998)**

Common errors associated with the FWD testing are generally due to poor machine maintenance, lack of calibration, and user error. Error in testing can be substantially reduced by paying attention to these key FWD issues (Brigg, 2000).

## 2.2 Load Transfer Efficiency

Load transfer efficiency is a measure of how well the joint transfer mechanism is transferring the load to the next concrete slab in a jointed concrete pavement. FWD data used for load transfer efficiency calculation is taken from the 9,000 pound loading sequence. The actual load applied is not exactly 9,000 lbs., so the data is normalized to ensure that the

energy going into each test is standardized. This allows for the comparison of load transfer efficiency between joints. The deflection-based load transfer is determined by dividing the deflection at sensor three (12 inches from load application) by the deflection at sensor one (over center of load application) and multiplying by 100 to get a percent of load transfer (Ioannides & Korovesis, 1992). The formula can be seen below in *Equation 1*.

$$LTE = \frac{D_3}{D_1} \times 100\% \quad \text{Equation 1}$$

Where,

LTE = load transfer efficiency (%)

$D_3$  = deflection reading 12 inches from the applied load (in)

$D_1$  = deflection reading 0 inches or at the center of the applied load (in)

The load transfer efficiency is on a scale of 0 to 100%. Zero meaning that there is absolutely no load transfer taking place across the joints. One hundred percent load transfer means the load is being transferred completely between the two slabs.

### 2.3 Back-calculation

Back-calculation is a method of using known information to determine unknown information about pavement layers. Nondestructive test results may be used to determine subgrade properties. For example, in a pavement profile where concrete properties, concrete thickness, base properties, and base thickness are the same, back-calculation may be used to determine the properties of the unknown subgrade soil. After measuring the deflection caused by a FWD, the deflection basin area is calculated by the equation (AASHTO, 1998):

$$AREA_7 = 4 + 6 \left( \frac{d_8}{d_0} \right) + 5 \left( \frac{d_{12}}{d_0} \right) + 6 \left( \frac{d_{18}}{d_0} \right) + 9 \left( \frac{d_{24}}{d_0} \right) + 18 \left( \frac{d_{36}}{d_0} \right) + 12 \left( \frac{d_{60}}{d_0} \right) \quad \text{Equation 2}$$

Where,

$d_0$  = deflection in center of loading plate, inches

$d_i$  = deflection at 0, 8, 12, 18, 24, 36, and 60 in from plate center, inches

If there is different sensor spacing arrangement for the FWD machine the trapezoidal rule allows for the use of the following equation to estimate the deflection basin area under the pavement (Hoffman, 2002):

$$AREA = 6 + 12 \left( \frac{d_{12}}{d_0} \right) + 12 \left( \frac{d_{24}}{d_0} \right) + 12 \left( \frac{d_{36}}{d_0} \right) + 12 \left( \frac{d_{48}}{d_0} \right) + 12 \left( \frac{d_{60}}{d_0} \right) + 6 \left( \frac{d_{72}}{d_0} \right) \quad \text{Equation 3}$$

Where,

$d_0$  = deflection in center of loading plate, inches

$d_i$  = deflection at 0, 12, 24, 36, 48, 60, and 72 in from plate center, inches

The next step in the back-calculation process according to the AASHTO Design of Pavement Structures (1998) is to calculate the radius of relative stiffness,  $\ell_{est}$ . The radius of relative stiffness is able to be estimated according to the following equation (Hall, 1992):

$$\ell_{est} = \left( \frac{\ln \left( \frac{72 - AREA}{242.385} \right)}{-0.442} \right)^{2.205} \quad \text{Equation 4}$$

The next step in back calculation is to calculate an estimate of the initial modulus of subgrade reaction,  $k$ .

## 2.4 Modulus of Subgrade Reaction

The modulus of subgrade reaction is calculated with the equation (AASHTO, 1998):

$$k_{est} = \frac{P \times d_0^*}{d_0 (\ell_{est})^2} \quad \text{Equation 5}$$

Where,

$k_{est}$  = back-calculated dynamic k-value, psi/in

P = load, lb

$d_0$  = deflection in center of loading plate, inches

$\ell_{est}$  = estimated radius of relative stiffness, inches

$d_0^*$  = nondimensional coefficient of deflection at center of load plate

The  $d_0^*$  value is calculated by (AASHTO, 1998):

$$d_0^* = 0.1245e^{[-0.14707e^{(-0.07565 \ell_{est})}]} \quad \text{Equation 6}$$

After the initial estimated modulus of subgrade reaction is calculated adjustment factors must be calculated for finite slab effects. The two equations used for adjustment are (AASHTO, 1998):

$$AF_{d_0} = 1 - 1.15085e^{-0.71878\left(\frac{L}{\ell_{est}}\right)^{0.80151}} \quad \text{Equation 7}$$

$$AF_{\ell} = 1 - 0.89434e^{-0.61662\left(\frac{L}{\ell_{est}}\right)^{1.04831}} \quad \text{Equation 8}$$

Where,

$$L = \sqrt{L_l L_w} \quad \text{if } L_l \leq 2 * L_w$$

$$L = \sqrt{2} * L_l \quad \text{if } L_l > 2 * L_w$$

$L_l$  = Slab length, inches

$L_w$  = Slab width, inches

Once the correction factors are calculated the adjusted k value can be calculated with the equation (AASHTO, 1998):

$$k = \frac{k_{est}}{AF_{\phi}^2 AF_{d_o}} \quad \text{Equation 9}$$

This yields a mean dynamic k-value. In order to get a static k-value for design the dynamic k-value should be divided by two.

A table containing typical k-values by soil type can be seen in Table 1 below.

**Table 1: Recommended k-value ranges for various soil types (AASHTO, 1998)**

AASHTO class	Description	Unified class	Dry density (lb/ft <sup>3</sup> )	CBR (percent)	k-value (psi/in)
Fine-grained soils:					
A-4	silt	ML, OL	90-105	4 - 8	25 - 165*
	silt/sand/gravel mixture		100-125	5 - 15	40 - 220*
A-5	poorly graded silt	MH	80-100	4 - 8	25 - 190*
A-6	plastic clay	CL	100-125	5 - 15	20 - 255*
A-7-5	moderately plastic elastic clay	CL, OL	90-125	4 - 15	25 - 215*
A-7-6	highly plastic elastic clay	CH, OH	80-110	3 - 5	40 - 220*

\* k-value of fine-grained soil is highly dependent on degree of saturation

## 2.5 Resilient Modulus

Resilient modulus is defined as the unloading modulus after many cycles of repeated loading (Andrei, et al. 2004). The resilient modulus is a standardized roadbed soil parameter used to gather a basic relationship between stress and strain of pavement materials. The

resilient modulus can be found for subgrade soil as well as the granular pavement base. The traditional definition of resilient modulus in a triaxial test setting is the applied axial deviator stress over the recoverable axial strain of the sample. This is represented by the following equation:

$$M_R = \frac{\sigma_d}{\varepsilon_r} \quad \text{Equation 10}$$

Where,

$M_R$  = resilient modulus, psi

$\sigma_d$  = deviator stress, psi

$\varepsilon_r$  = recoverable axial strain

Typically, the resilient modulus of a pavement subgrade is a function of the following factors: moisture content, deviator stress, confining pressure, freeze-thaw cycles, and compaction methodology (Kim & Siddiki, 2006). However, the resilient modulus of a sample is mainly a function of applied deviator stress when only one confining pressure is considered (Santha, 1994). According to the new Mechanistic Empirical Design Guide, (MEPDG) the resilient modulus values can vary considerably (ARA Inc. E. C., 2004).

Typical resilient modulus values suggested for design by part two chapter two of the upcoming mechanistic empirical design guide are shown in Table 2 below.

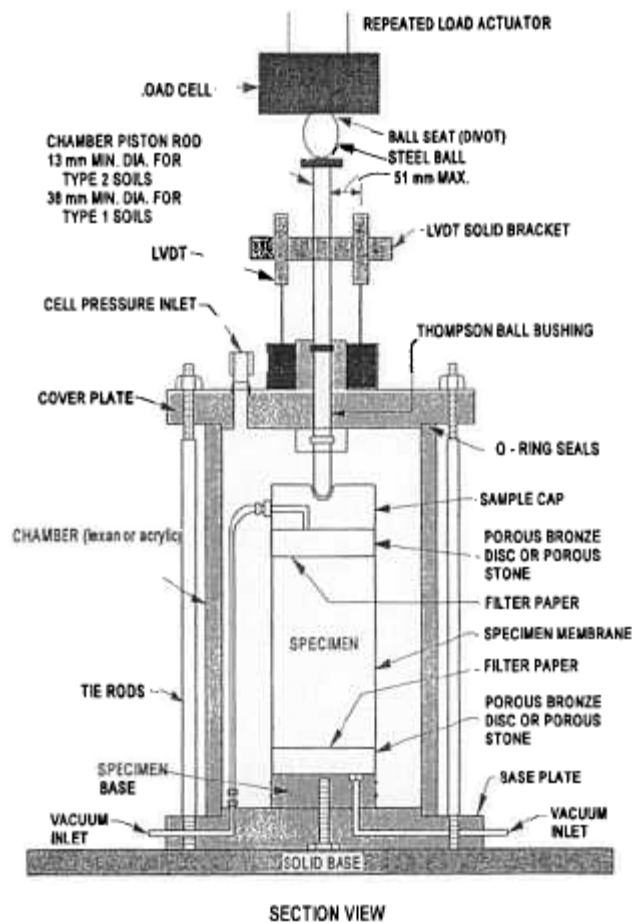
**Table 2: Typical  $M_r$  values for unbound granular and subgrade materials [resilient modulus at optimum moisture content] (ARA Inc. E. C., 2004)**

<b>Material Classification</b>	<b><math>M_r</math> Range</b>	<b>Typical <math>M_r</math></b>
A-1-a	38,500 - 42,000	40,000
A-1-b	35,500 - 40,000	38,000
A-2-4	28,000 - 37,500	32,000
A-2-5	24,000 - 33,000	28,000
A-2-6	21,500 - 31,000	26,000
A-2-7	21,500 - 28,000	24,000
A-3	24,500 - 35,500	29,000
A-4	21,500 - 29,000	24,000
A-5	17,000 - 25,500	20,000
A-6	13,500 - 24,000	17,000
A-7-5	8,000 - 17,500	12,000
A-7-6	5,000 - 13,500	8,000
CH	5,000 - 13,500	8,000
MH	8,000 - 17,500	11,500
CL	13,500 - 24,000	17,000
ML	17,000 - 25,500	20,000
SW	28,000 - 37,500	32,000
SP	24,000 - 33,000	28,000
SW-SC	21,500 - 31,000	25,500
SW-SM	24,000 - 33,000	28,000
SP-SC	21,500 - 31,000	25,500
SP-SM	24,000 - 33,000	28,000
SC	21,500 - 28,000	24,000
SM	28,000 - 37,500	32,000
GW	39,500 - 42,000	41,000
GP	35,500 - 40,000	38,000
GW-GC	28,000 - 40,000	34,500
GW-GM	35,500 - 40,500	38,500
GP-GC	28,000 - 39,000	34,000
GP-GM	31,000 - 40,000	36,000
GC	24,000 - 37,500	31,000
GM	33,000 - 42,000	38,500



### 2.5.1 AASHTO T-307-99

AASHTO T-307-99 is the current standard procedure used to collect data and calculate resilient modulus values for soils and aggregate materials. A triaxial test machine is used to carry out the resilient modulus testing. A diagram of a typical triaxial test machine can be seen in Figure 4 below.

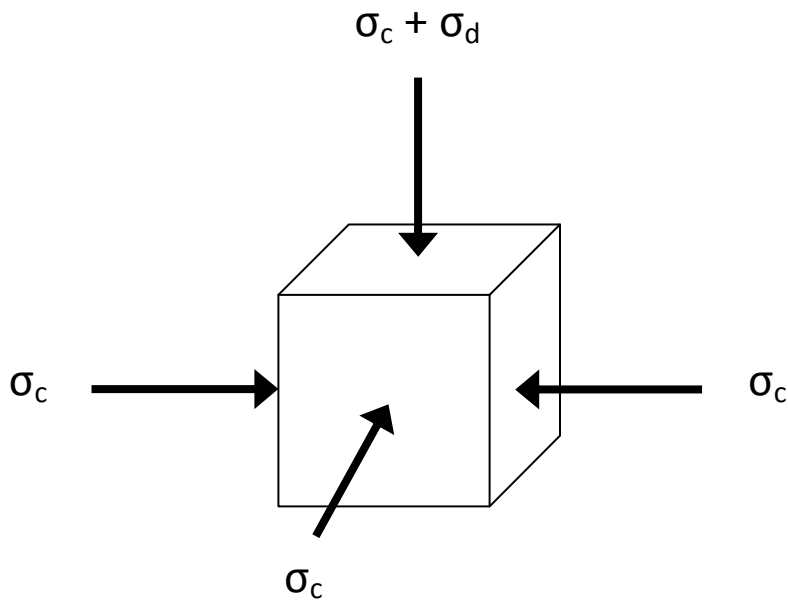


**Figure 4: Typical Triaxial Chamber with External LVDTs and Load Cell (AASHTO T-307-99 , 2000)**

The test can be conducted on a 2.8 in (71mm), 3.94 in (100mm), or 5.98 in (152mm) cylindrical sample that has been prepared according to the standard's specifications.

However, undisturbed Shelby-tube samples may also be used to conduct the test. The

diameter of a Shelby-tube sample is approximately 2.8 inches. The test requires that the specimen be at least twice as long as the diameter of the specimen. During the test, a fixed magnitude, axial cyclic stress is repeatedly applied to the cylindrical test sample. The stress is applied for duration 0.1 seconds, with a cyclic duration of 1.0 seconds. This allows for a 0.9 second recovery time for the sample between each cyclic load application. Different confining and deviator stresses are applied to the specimen. The principal stresses that are acting on the soil specimen can be represented by the illustration in Figure 5 below. Note that  $\sigma_c$  and  $\sigma_d$  are the confining stress and deviator stress respectively.



**Figure 5: Principal Stresses Acting on Finite Soil Specimen**

Each confining and deviator stress combination is called a sequence. The resilient modulus test is run in 16 different sequences. The first sequence is called the pre-conditioning sequence of the resilient modulus test. This sequence is run at a confining pressure of six psi and a deviator stress of four psi. The purpose of the first sequence is to eliminate the effects of the interval between compaction and loading. Also, the first sequence

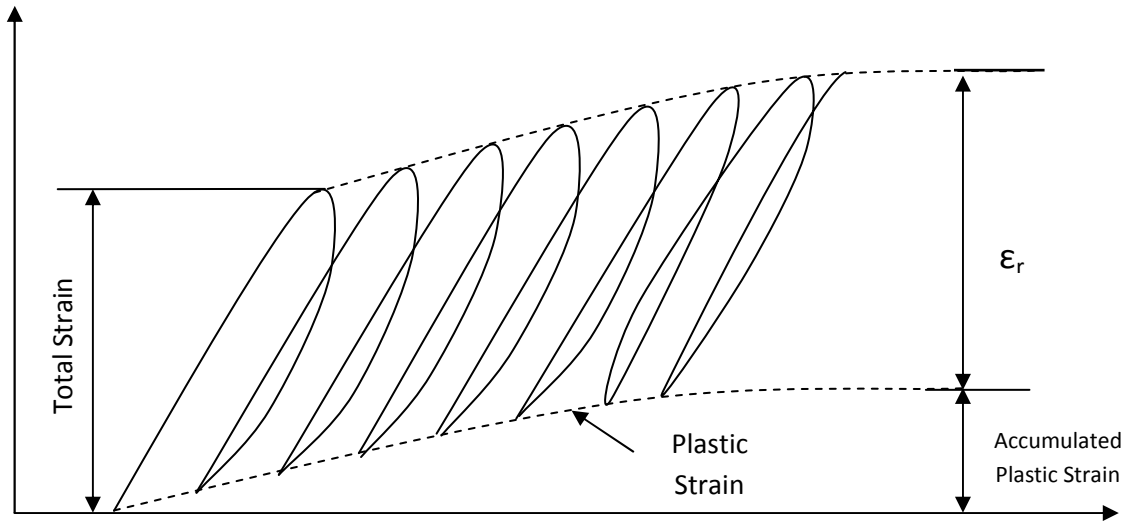
eliminates the effects of initial loading versus reloading. The first sequence is also used to minimize the effects of the imperfect contact between the sample and the sample cap.

(AASHTO T-307-99 , 2000) The next 15 sequences are useable data. A table of the different confining pressures, deviator stresses (maximum axial stresses), and number of repetitions per sequence can be seen below in Table 3.

**Table 3: Resilient Modulus Triaxial Loading Sequences**

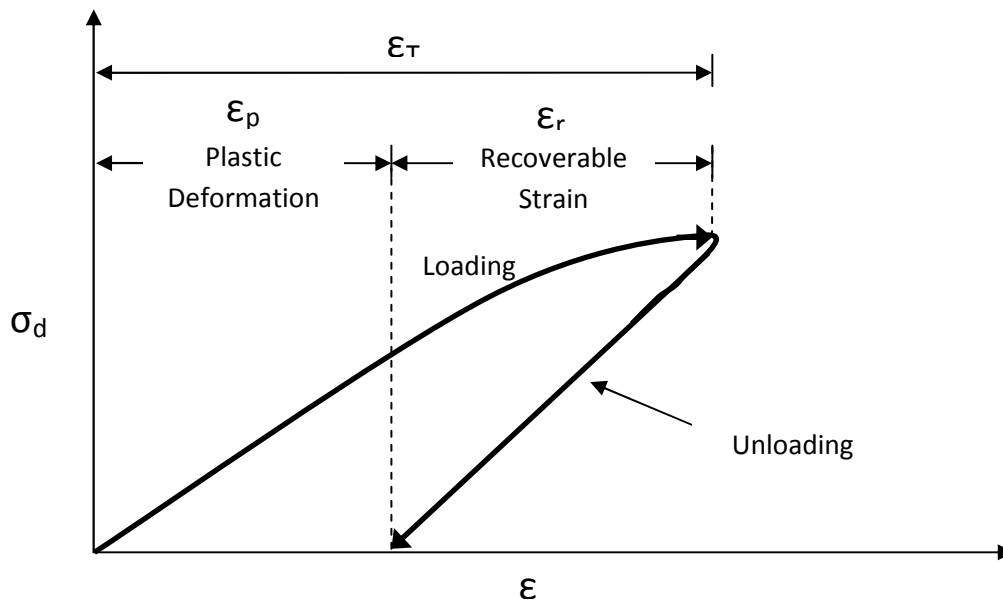
Sequence #	Confining Pressure (psi)	Maximum Axial Stress (psi)	Number of Load Repetitions
1	6	4	500
2	6	2	100
3	6	4	100
4	6	6	100
5	6	8	100
6	6	10	100
7	4	2	100
8	4	4	100
9	4	6	100
10	4	8	100
11	4	10	100
12	2	2	100
13	2	4	100
14	2	6	100
15	2	8	100
16	2	10	100

The response of the specimen is recorded for each cycle. The linear variable differential transducer (LVDT) measures the strain of the sample during the test. The results of the test are used to calculate the resilient modulus of the soil. A typical graphical representation of the plastic and elastic strain that occurs during a cyclic loading sequence can be seen in Figure 6.



**Figure 6: Strain Diagram per Loading Sequence**

When each sequence is run a deviator stress is applied to the sample. A typical graph of deviator stress versus strain over two sequences can be seen below in Figure 7. In the graph  $\epsilon_p$  represents the plastic strain of the sample. This is essentially strain that is permanent. The  $\epsilon_r$  represents the recoverable strain which is basically the elastic strain of the specimen. The  $\epsilon_T$  represents the total amount of strain seen by the specimen during the sequence.



**Figure 7: Deviator Stress vs. Strain for Resilient Modulus Testing**

### 2.5.2 Moisture Content Effects

Moisture content of the soil sample plays a key role in the resilient modulus value. As the moisture content of a soil sample increases the resilient modulus of that sample is going to decrease (Drumm, et al. 1997). The equation for determining the moisture content of a soil sample is found below in *Equation 11*.

$$w = \frac{W_w}{W_s} \quad \text{Equation 11}$$

Where,

$w$  = moisture content

$W_w$  = weight of water

$W_s$  = weight of soil solids

Another way to describe a soil's moisture condition is by its degree of saturation. The degree of saturation can be calculated with the following equation (Das, 2001):

$$S = \frac{V_w}{V_v} \quad \text{Equation 12}$$

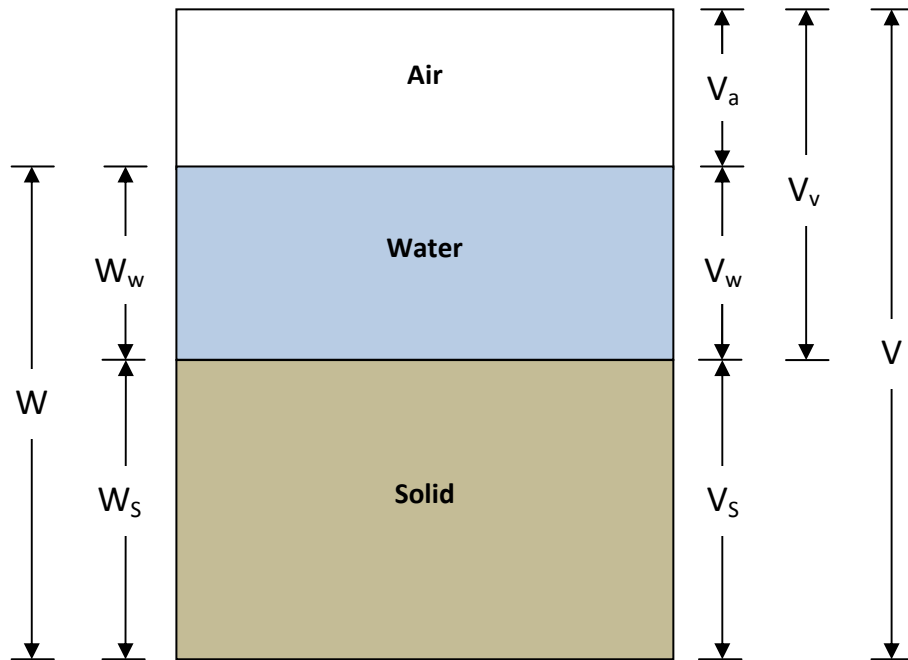
Where,

$S$  = degree of saturation

$V_w$  = volume of water in specimen

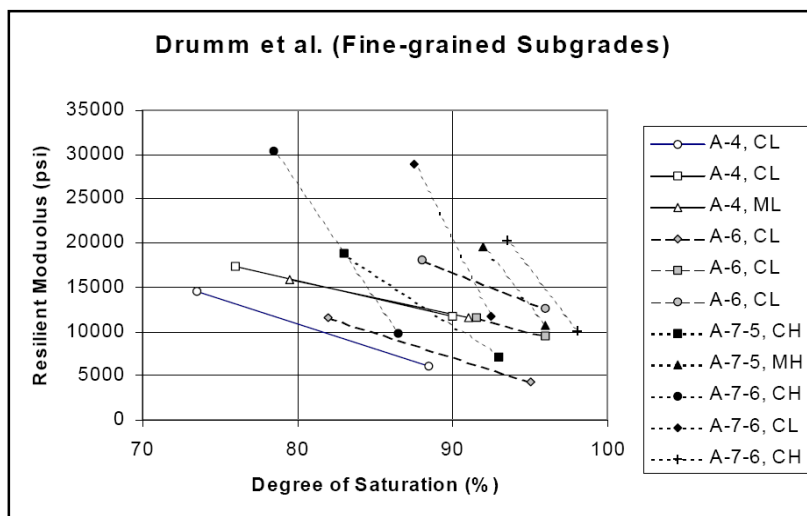
$V_v$  = volume of voids in specimen

In order to calculate the volume of water and volume of voids a phase diagram is typically used. Known values of specimen weight and volume are used to fill in the unknown values of the phase diagram. An example of a soil phase diagram can be seen below in Figure 8.



**Figure 8: Three Phase Soil Diagram**

As the degree of saturation increases for fine-grained soils, the resilient modulus decreases. Some fine-grained soils are more sensitive to an increase in the degree of saturation. A graph of the effect of the degree of saturation has on resilient modulus values can be seen in Figure 9 below.

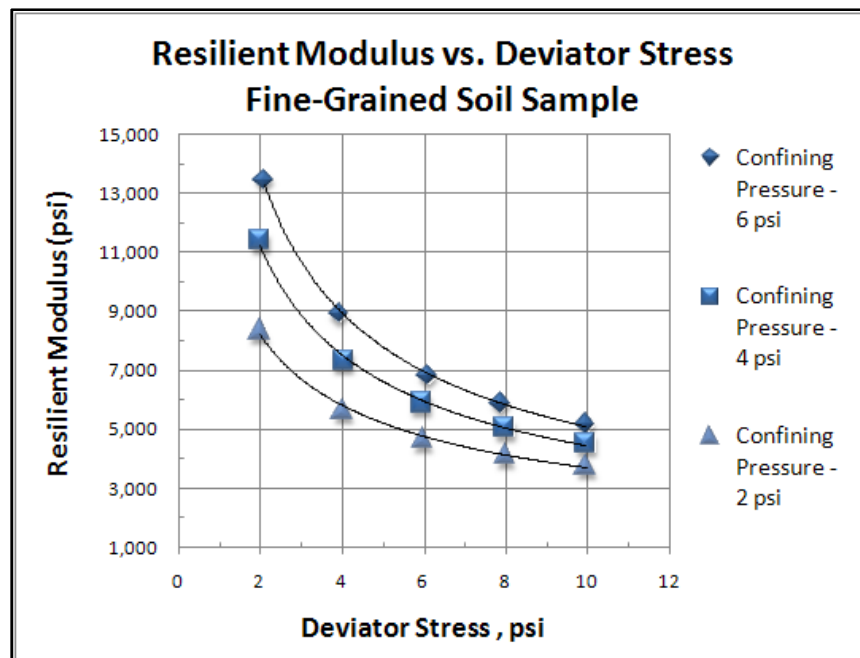


**Figure 9: Effects of Post-Compaction Saturation on Resilient Modulus (ARA Inc. E. D., 2000)**

Figure 9 is showing that one must go on a case-by-case basis to determine what the saturation effects to the soil will be for a particular fine-grained soil.

### 2.5.3 Stress State Effects

The stress state that the specimen is put under during each sequence determines what the resilient modulus value will be at that particular confining pressure and deviator stress. In other words, the resilient modulus value obtained from the triaxial repetitive loading is a function of the particular confining and deviator stresses used in the test. Therefore, to report accurate resilient modulus values, not just relative resilient modulus values, for a particular stretch of pavement, it would be essential to use the test data that has similar stress state to the in-situ conditions. A graphical representation of how the resilient modulus can change with deviator stress and confining pressure can be seen in Figure 10 below. Figure 10 was a product of the testing done in this research.



**Figure 10: Typical Deviator Stress vs. Resilient Modulus**

The graph indicates that for a typical fine-grained soil the resilient modulus will increase as the deviator stress decreases. Also, the resilient modulus increases as the confining pressure increases. This relationship is non-linear in most cases.

Multiple studies have been done in the past to address the issue of simplifying the resilient modulus test to make it more simple and feasible to use for design purposes. In 1988, the resilient modulus standard was AASHTO T274, which called for the use of zero, three, and six psi confining pressures. The deviator stresses tested in the standard were one, two, four, eight, and 10 psi. A study from the University of Arkansas proposed that the resilient modulus test could be run at a single confining pressure of three psi and a single deviator stress of eight psi for the purpose of roadway design (Elliott & Thornton, 1988). Another study done more recently at Purdue University proposed simplification of AASHTO T307 by using a two psi confining pressure and two, four, six, eight, 10, and 15 psi deviator stresses (Kim & Siddiki, 2006). These studies indicate that typical in-situ confining pressures are in the area of two to four psi and typical deviator stresses find their way to the eight to 15 psi range for asphalt pavements. However, it is generally known that at low levels of repeated deviator stress the resilient modulus decreases sharply as the deviator stress increases. At higher levels of repeated deviator stress the resilient modulus has what appears to be an asymptotic behavior (Wilson, et al. 1990). Different soils achieve this at different deviator stresses.

#### 2.5.4 *Freeze-Thaw Effects*

Freeze-thaw effects play a role in in-situ resilient modulus values. However, this variable will not need to be addressed in this study since the pavement sections for both



projects are geographically located in what could be considered the same area. Therefore, the freeze-thaw cycles of the section subgrades will be considered constant.

#### 2.5.5 *Compaction Method Effects*

Compaction method used also effects resilient modulus values for the pavement. Construction techniques were likely similar on both projects. Therefore, the effects of compaction method will be considered constant.

## 2.6 **Resilient Modulus Constitutive Models**

The behavior of soils during a triaxial resilient modulus test varies from soil to soil. The relationships can be linear, but generally are not linear. The purpose of a constitutive model is to describe the behavior of the soil using a standard form of an equation. This allows engineers and technicians to talk in a universal language when they report constitutive model coefficients. Constitutive models can also be used to help eliminate anomalies in the data. Numerous constitutive models have been proposed to try and account for the large variability in soil behavior from soil type to soil type. There have been several fine-grained soil constitutive models developed to model the behavior of various fine-grained soils.

### 2.6.1 *Power-Law Model*

A successful model used to describe the behavior of fine-grained soils is the power-law model, also known as the semi-log model. The equation for fitting the triaxial resilient modulus data into this model is shown below in *Equation 13* (Witczak & Uzan, 1988).

$$M_R = k_1 p_a \left( \frac{\sigma_d}{p_a} \right)^{k_3} \quad \text{Equation 13}$$

Where,

$M_R$  = resilient modulus

$\sigma_d$  = deviator stress

$k_1, k_3$  = material parameters, with  $k_1 > 0$  and  $k_3 \leq 0$

$p_a$  = atmospheric pressure, same units as  $\theta$  and  $M_R$

This model mainly represents the decrease in stiffness of fine-grained soils as the deviator stress increases. This model can be effective for some fine-grained soils. However, other factors may need to be taken into effect in order to accurately model the soil behavior under repetitive loading.

### 2.6.2 Universal Model

As the confining pressure increases on the soil, the stiffness generally increases. Also, with increasing shear comes a decrease in stiffness (Andrei, et al. 2004). The “universal” model was proposed by May and Witczak (1981) to combine these two effects into a single equation (May & Witczak, 1981):

$$M_R = k_1 p_a \left( \frac{\theta}{p_a} \right)^{k_2} \left( \frac{\sigma_d}{p_a} \right)^{k_3} \quad \text{Equation 14}$$

Where,

$M_R$  = resilient modulus

$\theta$  = bulk stress ( $\sigma_1 + \sigma_2 + \sigma_3$ )

$\sigma_d$  = deviator stress

$k_1, k_2, k_3$  = material parameters, with  $k_1 > 0$ ,  $k_2 \geq 0$  and  $k_3 \leq 0$

$p_a$  = atmospheric pressure, same units as  $\theta$  and  $M_R$

This constitutive model has been tested extensively. Studies found the model to be pretty comprehensive for determining resilient modulus values for cohesive and non-cohesive subgrade soils (George, 2004).

### 2.6.3 Universal Model w/ Octahedral Shear

The universal model was modified in 1985 by to adjust for effect of change normal shear stress during testing (Uzan, 1985). In this proposed model the deviator stress is replaced with what is referred to as the octahedral shear stress. This model was tested on some cohesive and non-cohesive soils and found to be effective (Malla & Joshi, 2007). The general form of the proposed model can be seen below in *Equation 15*.

$$M_R = k_1 p_a \left( \frac{\theta}{p_a} \right)^{k_2} \left( \frac{\tau_{\text{oct}}}{p_a} \right)^{k_3} \quad \text{Equation 15}$$

Where,

$M_R$  = resilient modulus

$\theta$  = bulk stress ( $\sigma_1 + \sigma_2 + \sigma_3$ )

$\tau_{\text{oct}}$  = octahedral shear stress  $\left( \frac{1}{3} \right) \sqrt{(\sigma_1 - \sigma_2)^2 + (\sigma_1 - \sigma_3)^2 + (\sigma_2 - \sigma_3)^2}$

$k_1, k_2, k_3$  = material parameters, with  $k_1 > 0$ ,  $k_2 \geq 0$  and  $k_3 \leq 0$

$p_a$  = atmospheric pressure, same units as  $\theta$  and  $M_R$

### 2.6.4 Modified Universal Model w/ Octahedral Shear

Sometime the octahedral stress of certain soils will approach zero. A modified version of the octahedral shear equation can be seen below.

$$M_R = k_1 p_a \left( \frac{\theta}{p_a} \right)^{k_2} \left( \frac{\tau_{\text{oct}}}{p_a} + 1 \right)^{k_3} \quad \text{Equation 16}$$

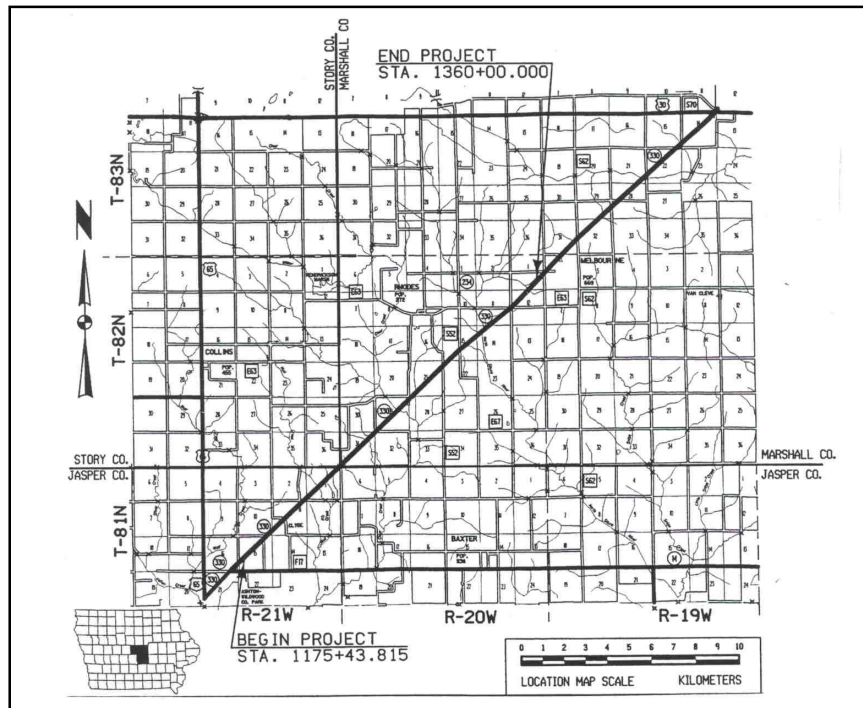
This equation was developed to avoid numerical problems when  $\tau_{\text{oct}}$  goes to zero. This equation has been adopted by the new MEPDG to act as the default constitutive model for fine-grained subgrade materials (ARA Inc. E. C., 2004). The equation can be found in part two of chapter two in the new design guide.

## Chapter 3. Research Plan

### 3.1 Site Reviews

#### 3.1.1 *Iowa Highway 330 Site*

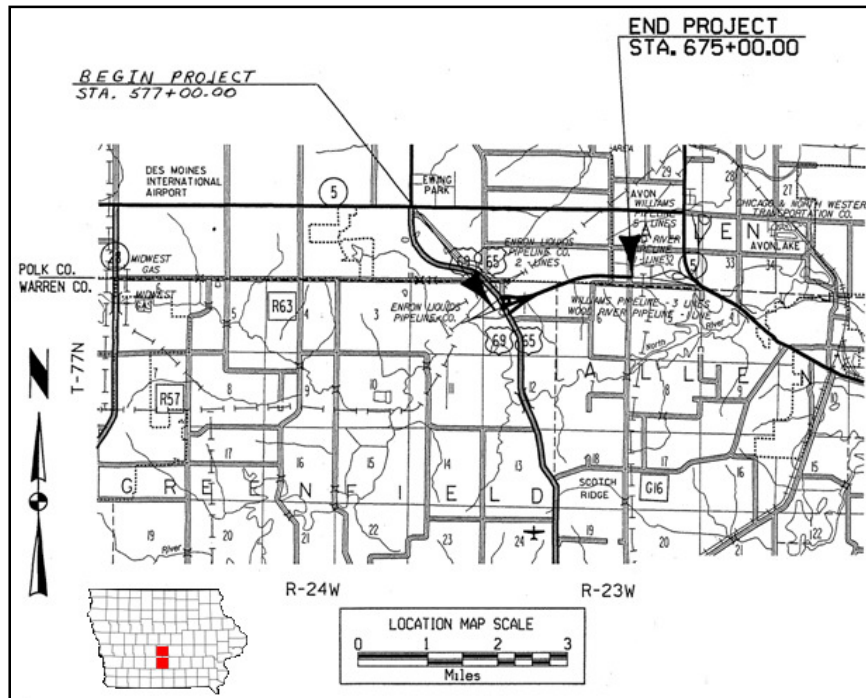
Highway 330 is a four lane highway in Iowa. The test section is located in Marshall, Jasper, and Story Counties in central Iowa. The PCC (Portland Concrete Cement) paving project is approximately 11.5 miles long with a portion having been tested. The pavement was constructed in 2001. The direction of travel of the tested pavement section is southwest. The pavement in the northeast direction of travel was the two-way existing section of Highway 330 that was converted into northbound lanes upon the completion of the two new lanes of Highway 330. These northeast bound lanes were not included in the study. The test sections begin about 0.4 miles northeast of the intersection of Fairman Avenue and 295<sup>th</sup> Street. The Fairman Avenue and 295<sup>th</sup> Street intersection is located approximately 1.6 miles southwest of the Gerhart Avenue and 285<sup>th</sup> Street intersection, just west of Melbourne, IA. The project was done in metric units. These values were converted to Standard English units for convenience and consistency reasons. A plan view of the roadway section in which the Iowa Highway 330 project is contained can be seen in Figure 11 below. Notice the plan sheet overview extends beyond the ranges of the tested sections.



**Figure 11: HWY 330 Test Section Plan View**

### 3.1.2 US Highway 65 Site

US Highway 65 is a four lane highway in Iowa. The research area is located in Polk and Warren Counties in central Iowa. The PCC (Portland Concrete Cement) paving project is approximately 2.69 miles in length. It is located between the Iowa Highway 5 interchange and the US 65/69 interchange west of Carlisle, IA. The test pavement sections make up about 0.5 miles of the construction project. These test sections are in the southwest bound lanes. The pavement in the northeast direction of travel was not included in the study. The project was done in Standard English units. A plan view of the US Highway 65 project containing the test sections can be seen in Figure 12 below.






**Figure 12: US 65 Test Section Plan View**

## 3.2 Dowel Materials

### 3.2.1 Iowa Highway 330 – Dowel Material

The 3.5 miles of test sections on the Iowa Highway 330 project consists of a combination of bar types such as standard 1.5 inch round epoxy-coated steel dowel bars (area = 1.767 in<sup>2</sup>), medium elliptical dowel bars (major axis = 1.654 in., minor axis = 1.115 in., and area = 1.473 in<sup>2</sup>), and heavy elliptical dowel bars (major axis = 1.969 in., minor axis = 1.338 in., and area = 2.084 in<sup>2</sup>). A cross section of the different bars used on the project can be seen below in Table 4.


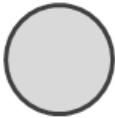


**Table 4: HWY 330 Dowel Bar Cross-Sections**

HWY 330 Dowel Bar Cross Sections					
1.50"	Standard Round	1.65"	Medium Elliptical	1.97"	Heavy Elliptical
	1.50"		1.12"		1.34"

*3.2.2 US Highway 65 – Dowel Material*

The project consists of a combination of bar types such as standard round epoxy-coated steel, 1.5 inch stainless steel round, 1.5 inch GFRP (Glass Fiber Reinforced Polymer), and 1.88 inch GFRP dowel bars. A cross section of the different bars used on the project can be seen below in Table 5.

**Table 5: US 65 Dowel Bar Cross-Section**

US 65 Dowel Bar Cross Sections							
1.50"	Standard Round	1.50"	Stainless Round	1.50"	GFRP Round	1.88"	GFRP Round
	1.50"		1.50"		1.50"		1.88"

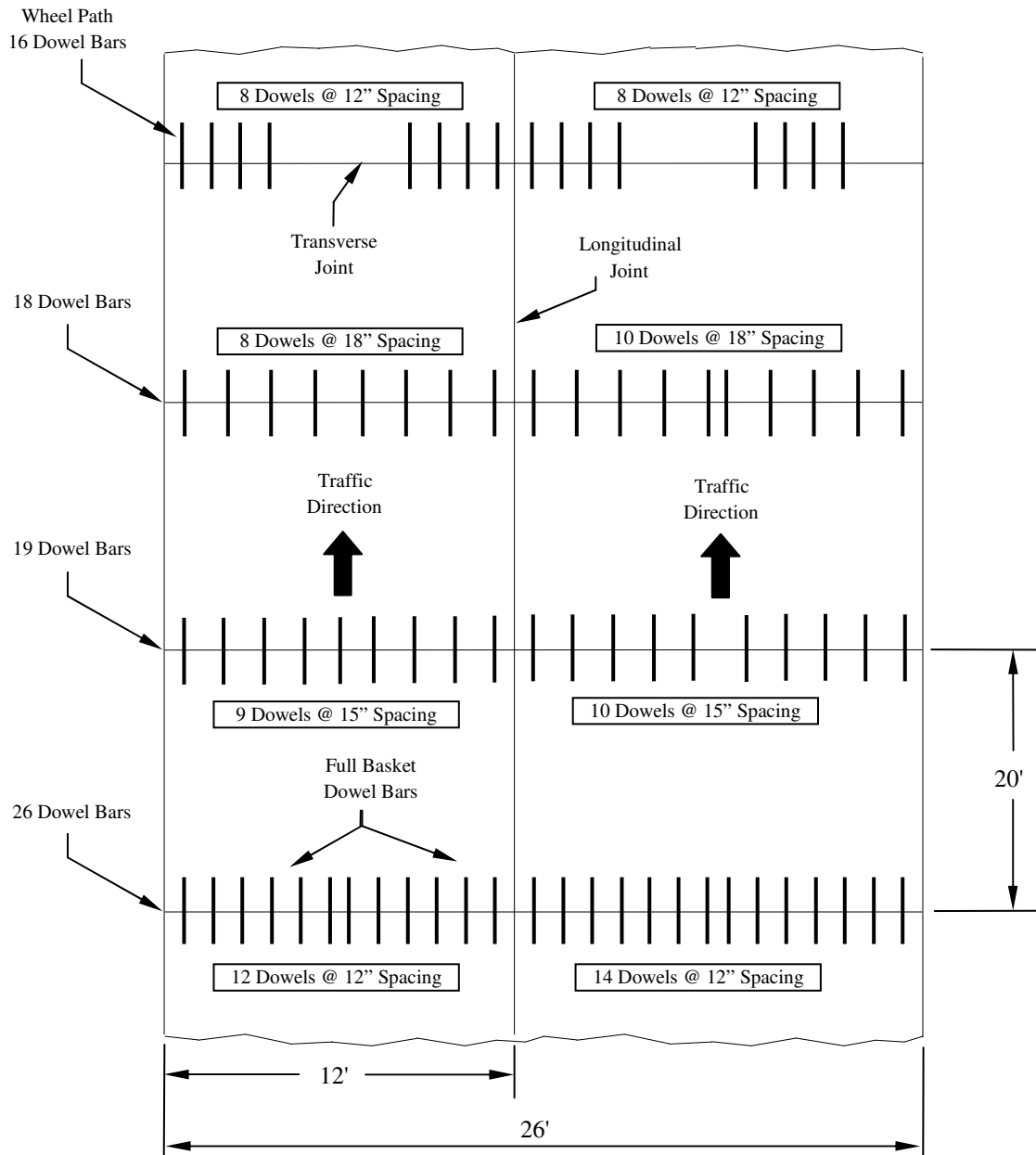
**3.3 Construction**

*3.3.1 Iowa Highway 330- Construction*

The Iowa Highway 330 project contained dowels spaced at 12 inch, 15 inch, and 18 inch intervals. The typical joint spacing is approximately 20 feet. There were also some test sections that contain dowel bars only in the wheel paths. These sections have four dowel bars



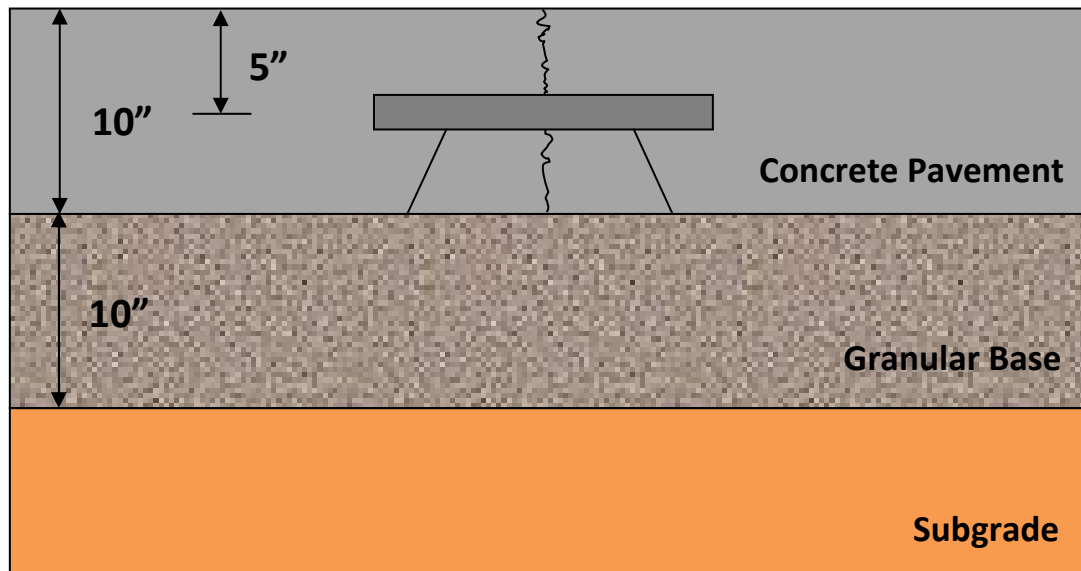
put in each wheel path, spaced 12 inches apart (Cable, et al 2008). A typical plan view of the different bar spacing configurations found on the Iowa Highway 330 project can be seen below in Figure 13.



**Figure 13: HWY 330 Typical Dowel Spacing Configurations**

The section dowel locations and configurations of Iowa Highway 330 can be found in Appendix A.

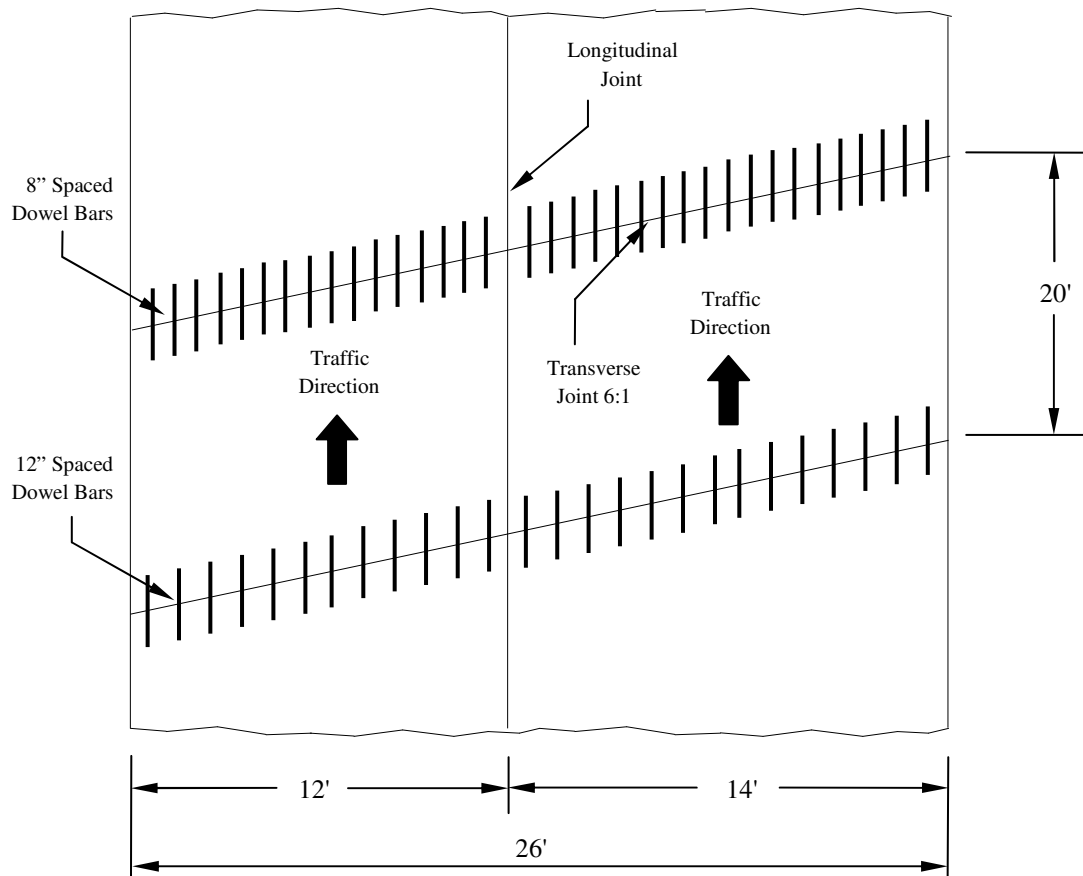
The 11.47 mile section on Iowa Highway 330 where testing took place has a typical profile that consists of a three layer system. The top layer is a 10 inch thick concrete pavement which overlies a 10 inch granular base. Beneath the granular base is the subgrade soil. The dowel bars were placed at approximately half the depth of the concrete pavement. A visual representation of a typical profile from the Iowa Highway 330 pavement can be seen in Figure 14 below.



**Figure 14: HWY 330 Typical Pavement Profile**

### 3.3.2 US Highway 65 – Construction

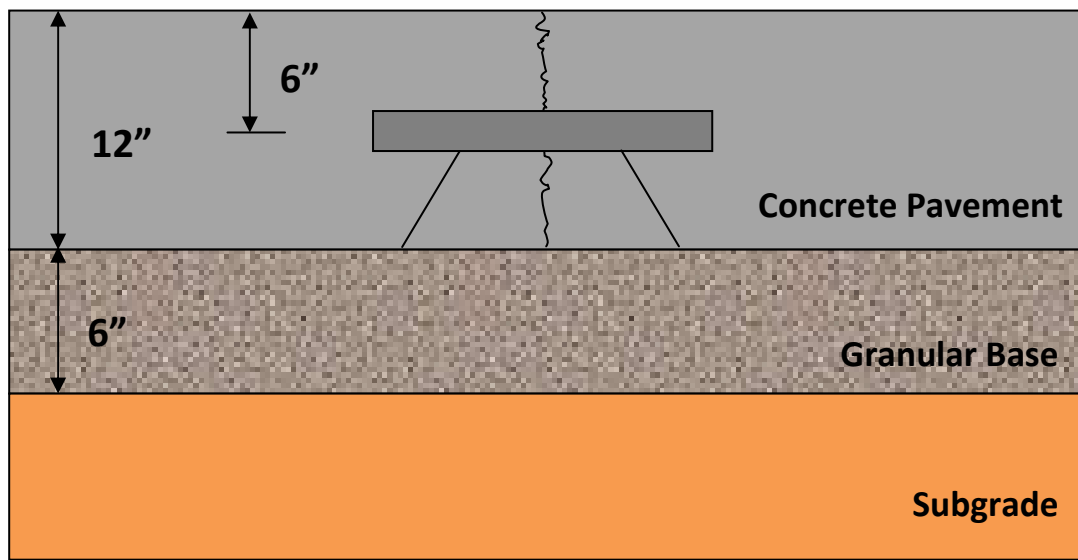
The US Highway 65 project contained dowels spaced at eight inches and 12 inches. The typical joint spacing was approximately 20 feet. The joints were skewed at a ratio of six to one. A typical plan view of the different bar spacing configurations can be seen below in Figure 15.



**Figure 15: US 65 Typical Dowel Spacing Configurations**

The section dowel locations and configurations can be found in Appendix B.

The 0.5 mile of pavement section where testing took place has a typical profile that consists of a three layer system. The top layer is a 12 inch thick concrete pavement which overlies a six inch granular base. Beneath the granular base is the subgrade soil. The dowel bars were placed at approximately half the depth of the concrete pavement. A visual representation of a typical profile from the US Highway 65 pavement can be seen in Figure 16.



**Figure 16: US 65 Typical Pavement Profile**

## Chapter 4. Data Collection

### 4.1 FWD / Load Transfer

Load transfer efficiency of a joint is calculated using FWD data. The following sections explain how FWD data was collected for the two projects.

#### 4.1.1 HWY 330- FWD

The HWY 330 and US 65 project locations have different sensor spacing setups for the FWD machine. The FWD data taken on Iowa 330 has sensors spaced at 0, 8, 12, 18, 24, 36, 48, 60, and -12 inches (12 inches back) from the applied load. The sensor spacing for Iowa Highway 330 is summarized in Table 6 below.

**Table 6: HWY 330 FWD Machine Sensor Location**

Project Site	Distance from Applied Load, inches								
	Sensor 1	Sensor 2	Sensor 3	Sensor 4	Sensor 5	Sensor 6	Sensor 7	Sensor 8	Sensor 9
IA 330	0	8	12	18	24	36	48	60	-12

Deflection testing was located within sections composed of 20 joints. Deflection readings were conducted in both lanes at three of the twenty joints in each test section. These tests were run in the outer wheel path only. In each 20 joint test section, deflection testing was run on the three joints collectively labeled 12–15 (measured from the southernmost test section joint). Dynamic loads of approximately 6, 9, and 12 kips were applied in each test (Cable J. K., et al. 2008). The results of the nine kip load were used for the analysis. The sensor readings under the load and 12 inches from the load were used to calculate the load transfer as shown in *Equation 1*. Load transfer data for Iowa Highway 330 was taken at several different dates. Raw data was collected in the driving and passing lanes in; Fall 2002, Spring 2003, Fall 2003, Spring 2004, Fall 2004, Spring 2005, Fall 2005, Spring 2007, and Fall 2007.

#### 4.1.2 US 65- FWD

The FWD data taken on US Highway 65 has sensors spaced at 0, 12, 24, 36, 48, 60, and 72 inches from the applied load. The sensor spacing for US Highway 65 is summarized in Table 7 below.

**Table 7: US 65 FWD Machine Sensor Locations**

Project Site	Distance from Applied Load, inches								
	Sensor 1	Sensor 2	Sensor 3	Sensor 4	Sensor 5	Sensor 6	Sensor 7	Sensor 8	Sensor 9
US 65	0	12	24	36	48	60	72	-	-

FWD tests were run on three joints and three mid-slabs in each section. Deflection readings were conducted at three of the twenty joints in each test section and each lane. These tests were run in the outer wheel path only, approximately two feet from the edge of the slab. Dynamic loads of approximately 9, 12, and 16 kips were applied in each test (Hoffman, 2002). The results of the nine kip load were used for the analysis. The sensor readings under the load and 12 inches from the load were used to calculate the load transfer. Data was collected in the driving and passing lanes in; Fall 1997, Spring 1998, Fall 1998, Spring 1999, Fall 1999, Spring 2000, Fall 2000, Spring 2001. Figure 17 below shows a picture of the FWD machine used to collect the data for the US 65 project.



**Figure 17: Falling Weight Deflectometer (Cable J. K., et al. 2003)**

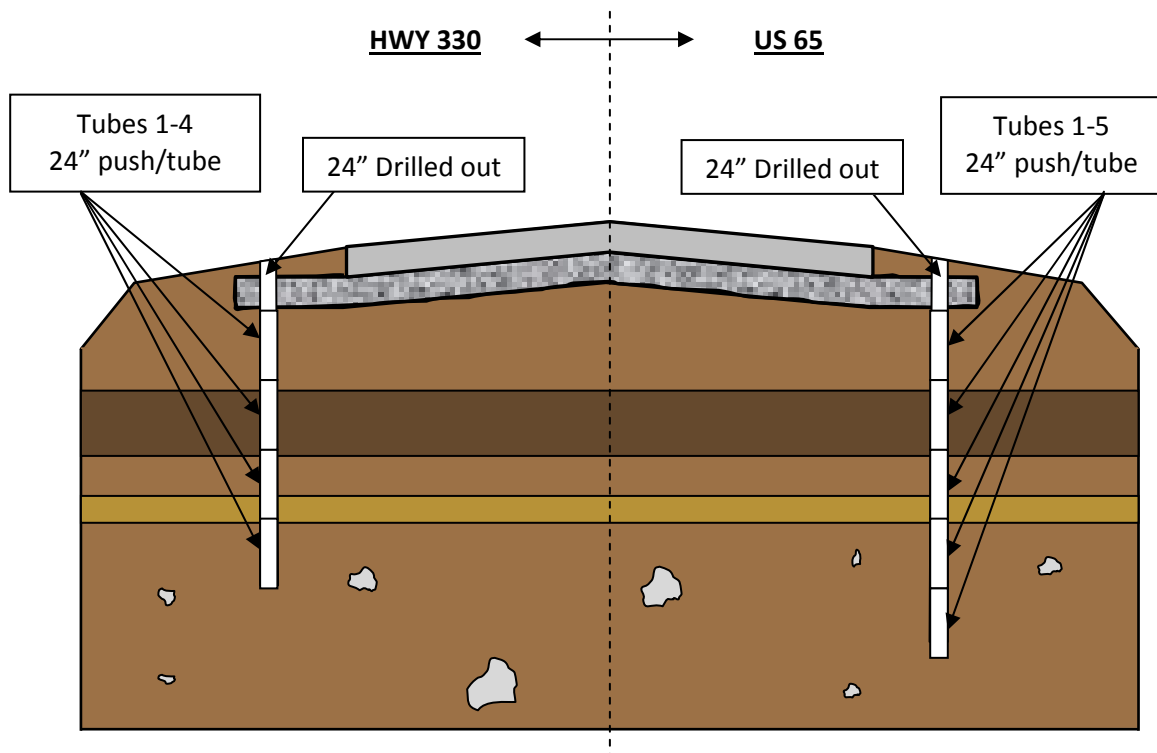
## **4.2 Resilient Modulus**

### *4.2.1 Soil Sampling*

Resilient modulus testing is an expensive process. Since a limited number of soil samples were to be collected and tested, an extensive amount of time was put into determining the soil sampling locations. The first step to determining how to get soil testing data to be inclusive of all test sections was to get a map of the natural soil deposits in the area. The Web Soil Survey (2008) program for the counties mentioned in the two projects was utilized for this purpose. The construction plan sheets were then used to determine the location of cut and fill sections. This gave a good indication where native soils and fill soils would be found under the pavement. Pavement test sections within the same overall fill areas were considered likely to have similar soil layering due to typical Iowa subgrade construction. This is why part of the Highway 330 project has such a low soil sampling to pavement section ratio. More soil sampling was done in areas where soil types were less certain.

AASHTO T-307-99 allows the use of undisturbed Shelby-tube samples or compacted samples for the resilient modulus test. Shelby tube samples were used for the purpose of this project. The samples were collected in mid-July 2008 for both projects. A total of 127 Shelby tube samples were collected on Iowa Highway 330. Another 20 tubes were collected for US Highway 65. It was determined that the boring data would start at two feet below the surface of the pavement shoulder. After construction of the pavement base course and topsoil can be found in the shoulder of the road, above the soil similar to that under the pavement. Therefore, the first 24 inches of shoulder material and topsoil was drilled through the use of a solid-stem continuous flight auger to get down to the soil that is representative of the soil

under the pavement. Shelby tubes for Iowa Highway 330 were collected from two to ten feet below the surface of the highway shoulder. Shelby tubes for US Highway 65 were collected from two to 12 feet below the surface of the highway shoulder. The thin-walled Shelby tube sampling was performed in accordance to ASTM D1587. Procedures for sampling and shipment were observed. Figure 18 below shows a visual representation of how deep the Shelby tubes were pushed on the Iowa Highway 330 and US Highway 65 projects. Keep in mind that for both sites Shelby tube samples were taken off the shoulder of the driving lane.



**Figure 18: HWY 330 and US 65 Typical Shelby Tube Boring Depth**

The samples were taken and sealed in the field to prevent moisture loss during storage time. The Shelby tube samples were stored upright and great care was taken during the transportation of the samples to the laboratory. There were no significant events (i.e. bumps,



quick turns, etc.) during that transportation that would have led to disturbance of the samples. The samples were extruded with the aid of a hydraulic extruder seen in Figure 19 below.



**Figure 19: Shelby Tube Extruder**

Upon extrusion the samples were carefully transported by a halved PVC pipe to a stainless steel table. The samples were then visually classified using color and texture. Pictures were taken of the samples as well. Moisture content was taken by way of oven dried sampling. The samples were then carefully wrapped in plastic wrap and aluminum foil. The samples were stored in plastic tubs with limited samples per tub to avoid disturbance until resilient modulus testing was conducted.

#### *4.2.2 Resilient Modulus Testing*

As stated in the literature review section of the report, the resilient modulus test can be run on fine-grained or coarse-grained soils. In the case of this study, the resilient modulus

is for the subgrade soils, which are fine-grained. The test requires that the specimen be at least twice as long as the diameter of the specimen. Therefore, the Shelby tube samples were trimmed to a length of approximately 5.6 inches in length. A picture of the actual triaxial chamber used in the testing can be seen below in Figure 20.



**Figure 20: Actual Triaxial Chamber with External LVDT and Load Cell**

The triaxial resilient modulus testing was done in the Iowa State University Geotechnical Mobile Lab according to the AASHTO T-307-99 standard test. It was very important during the test that the LVDT was not obstructed by having tangled chords. This would have prevented the test from producing meaningful strain readings. LVDT

obstructions were monitored very closely by the technician running the tests. Once the test was done, the sample was then removed from the chamber and a moisture content of the sample was taken by means of oven-drying. There were a total of 25 samples tested. Resilient modulus tests were conducted on 20 samples from Iowa Highway 330 and five samples from US Highway 65.

### **4.3 Profile /Roughness**

Profile measurements are essentially the measure of the how rough a pavement feels to the user of a typical vehicle. Before profiling machines, users would rate how rough the pavement felt. This was a very subjective process. Now, profiling machines are used to obtain an International Roughness Index (IRI) value of the pavement section (FHWA, Pavement Smoothness Methodologies, 2008). The IRI value is a quantitative measure of how much vertical movement a vehicle is subjected to within a pavement section. This value is measured by taking continuous readings through the use of transducers mounted to the test vehicle. The IRI value is said to have a direct correlation with the user's perception of the pavement roughness. There is a pavement temperature reading device on the profiling vehicle that allows the data to be normalized for pavement temperature.

The Iowa Highway 330 project was the only project to have profile data taken during the study period. Data was taken in the driving and passing lanes as well as the inside and outside wheel paths. The normalized values obtained by the profiling vehicle were imported into a computer program to determine IRI values over a specific section of road. ProVal 2.7 (Transtec Group, 2007) was the program used to convert the profile data readings into an IRI value. Driving lane, passing lane, inside wheel path, and outside wheel path data were

combined to do the analysis of IRI to dowel performance. IRI values were established for each section containing different dowel types and spacing intervals.

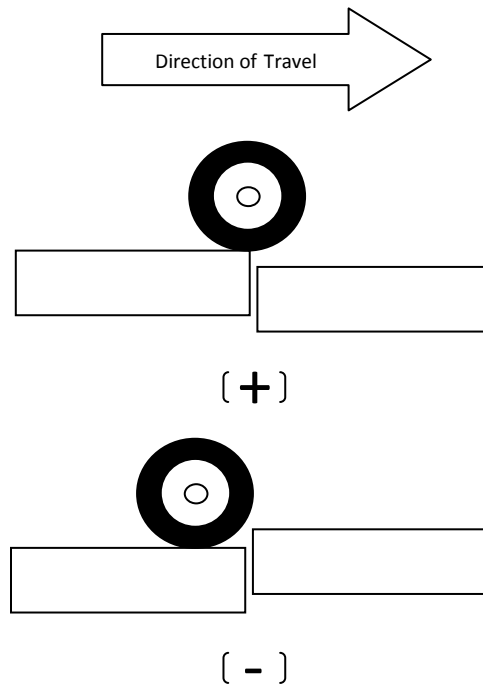
#### 4.4 Faulting

Joint faulting is essentially the measure of the difference in elevation at the joint from one slab to another. As a concrete pavement ages and is exposed to loading conditions and wear, faulting may result at the transverse joint between slabs. Georgia faultmeters were used to conduct faulting measurements on both projects. These meters are used according to the Federal Highway faulting measurement manual (FHWA, 2008). The faultmeters used on the two projects were the same type of faultmeter, however, they were different faultmeter units. A picture of the Georgia faultmeter used on the US 65 project can be seen in Figure 21 below.



**Figure 21: Georgia Faultmeter (Hoffman, 2002)**

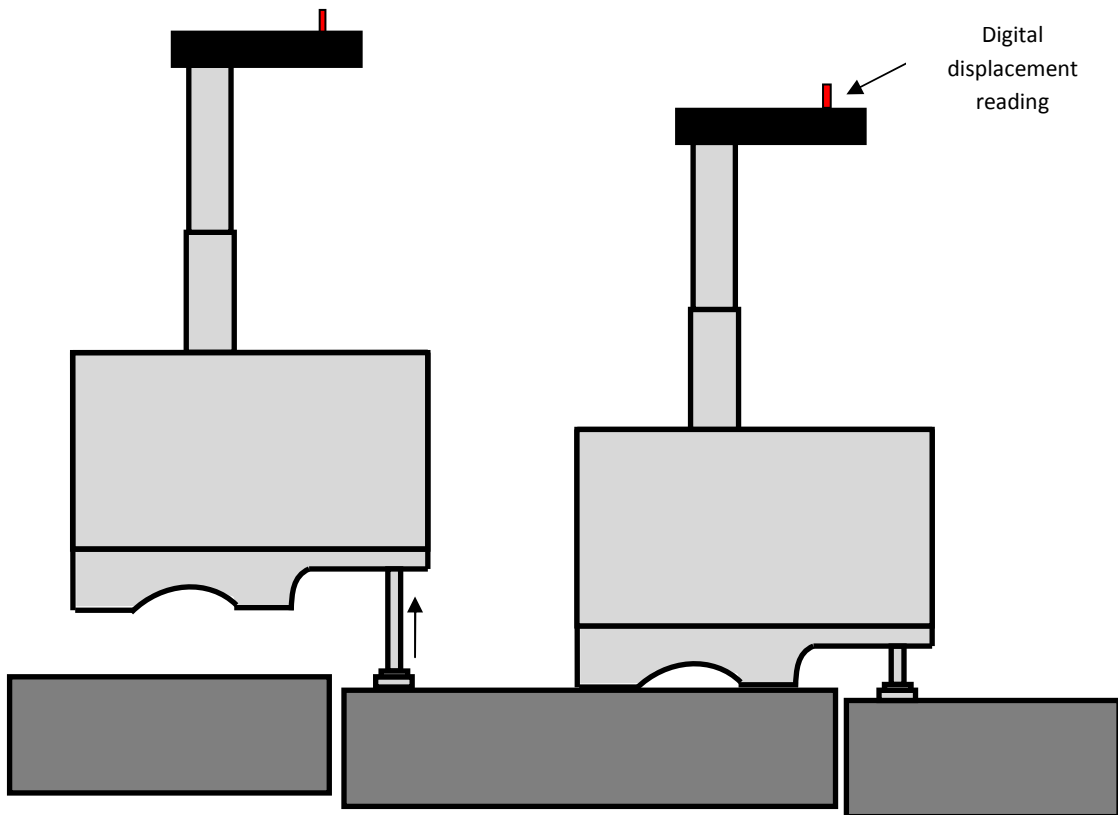
This joint faulting can be considered positive or negative depending upon the direction of travel. Figure 22 shows the difference between positive and negative faulting.



**Figure 22: Positive and Negative Faulting Schematic**

Positive faulting has a more significant effect on driver comfort than negative faulting. This comfort issue caused by positive faulting is due to the tire running into the adjacent slab whereas in negative faulting the vehicle simply drops off the slab.

The faultmeter is utilized by placing it over the transverse joint in the same direction each time. The measuring probe on the faultmeter is long enough that any reasonable faulting levels will not max out the machine. Upon being placed over the joint the measuring probe is pushed upward and transmits a reading to an LVDT within the faultmeter. The faulting value is then digitally sent and displayed on the faultmeter screen. This reading will be a positive or negative number depending upon which way the slabs are faulting. Figure 23 below shows a diagram of the faultmeter application process.



**Figure 23: Faultmeter Application Diagram**

Faulting measurements for the Iowa Highway 330 project were taken in the Spring 2003, Fall 2003, Spring 2004, Fall 2004, Spring 2005, Fall 2005, Spring 2006, Spring 2007, and Fall 2007. These faulting readings were taken at a distance of 18 inches from the edge of the pavement in the driving and passing lanes. Faulting measurements were taken at 10 joints in the middle of each dowel section.

Faulting measurements for the US Highway 65 project were taken in the Spring 1998, Fall 1998, Spring 1999, Fall 1999, Spring 2000, and Spring 2001. These faulting readings were taken for the inside and outside wheel paths of the driving lane at a distance of 30 inches and 18 inches from the edge of the pavement lane, respectively (Hoffman, 2002). Faulting measurements were taken at three joints in each dowel section.

## **Chapter 5. Data Analysis**

### **5.1 Soil Comparison Determination**

Resilient modulus testing equipment is very expensive and rare to come across. This makes it very expensive if large quantities of resilient modulus tests are run. For this reason, it was only economically feasible to run resilient modulus tests on a select amount of soil samples. Though many more soil samples were obtained, only a few were tested. In order to increase the amount of comparable data, several techniques were used to relate different pavement sections with a pavement section which had resilient modulus tests run. Four different techniques were used to match subgrade soil sections that were not tested for resilient modulus with those sections that had resilient modulus testing done.

First, soils data was taken from the plan sheets. All sections on the project that were in cut sections were able to be identified by AASHTO classification according to the plan sheet boring logs.

Second, the Web Soil Survey, from the National Resource Conservation Service (NRCS) website, was used to get soils data. The Web Soil Survey will give a typical soil profile for the first five feet of soil. The aerial photographs were calibrated and scaled. Then, major features from the plan sheets were scaled and overlaid on the aerial maps. This enabled the determination of soil types in each test section across the Iowa Highway 330 and US Highway 65 projects.

Third, FWD data was used to help estimate soil characteristics. For the Iowa 330 project the deflection basin under the joint deflection was used since no mid-slab data was available. The idea is if the deflection basin area underneath the pavement is calculated, the

larger the area under the pavement would correlate to a lower the resilient modulus of the section. Deflection basin areas on each project were compared with deflection basin areas from other sections on the same project. This was done to verify or establish the section's resilient modulus relationship to the resilient modulus of the sections where resilient modulus testing was conducted. On the US 65 project mid-slab data was available for three time periods. This made the calculation of modulus of subgrade reaction possible. These values were used to help assign resilient modulus values to the soils for the US 65 project.

Last, visual description data from the extruded Shelby tube samples was used to compare the different soils. A tentative general soil matching plan was set up before the borings were done based on the plan sheets and Web Soil Survey data. The tentative soil matching plan was revised once the soils were extruded from the Shelby tubes. Soil borings supposedly having similar properties of other soil sections were looked at especially close.

The four techniques above were used and cross-referenced with each other in order to obtain the best results with the limited resilient modulus data available.

## **5.2 Resilient Modulus**

The resilient modulus is dependent upon stress state, as stated earlier. The proper stress state conditions were found through the use of the program Kenlayer (Huang, 2004). This is a layer analysis where layer thickness, modulus, and Poisson's ratio are input. Inputting modulus values of typical concrete, base, and soils in the respective layers of the system should yield accurate results to determine the stress state conditions of the projects. The stress conditions at 18 inches into the soil layer of the pavement system on both projects were calculated. The maximum vertical (deviator) and horizontal (confining) stresses were



below two psi each. Therefore, the results from the resilient modulus test for the two psi deviator and two psi confining pressure were used to yield the most representative resilient modulus values.

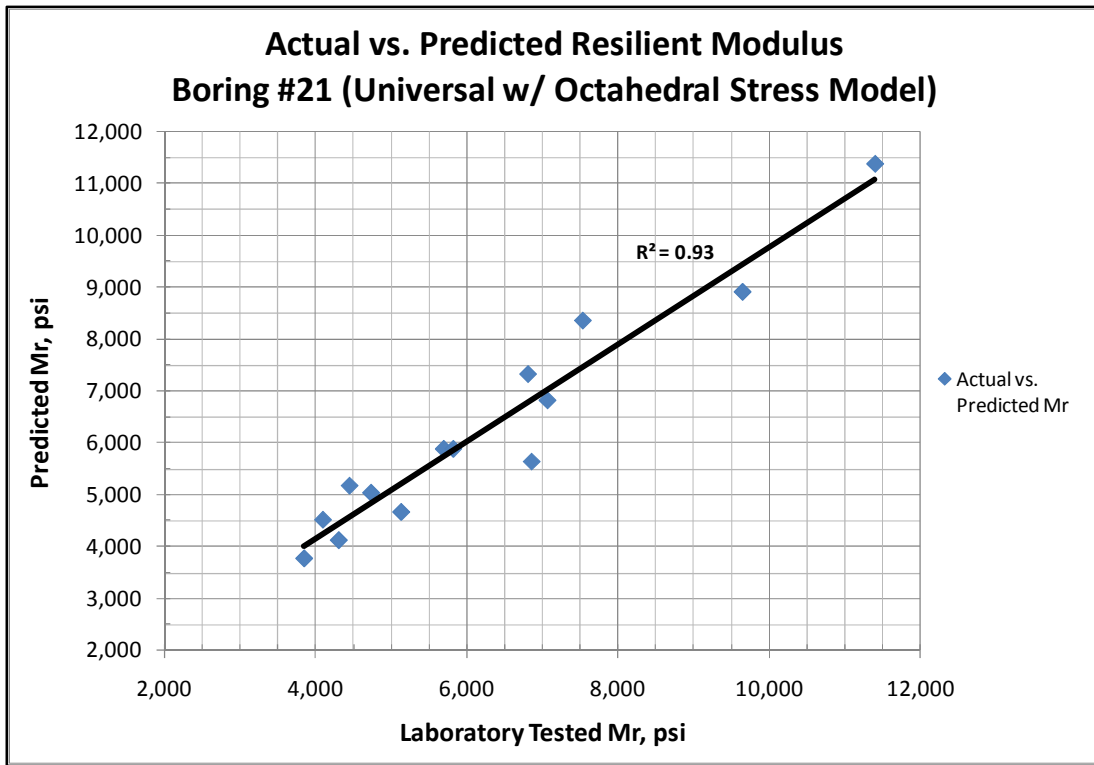
The degree of saturation was looked at as a factor in determining resilient modulus. A specific gravity of soil solids was taken to be 2.70 for all soils. The degree of saturation for the soils on Iowa Highway 330 ranged from about 89 to 96% degree of saturation. There was an exception of one sample tested that had a degree of saturation of 76%. This sample had more silt and sand than the other samples, so the lower degree of saturation was expected. The degree of saturation of the US 65 samples ranged from 94% to 100%. Due to the small difference in degree of saturation the effects of saturation were not incorporated into the results.

#### *5.2.1 HWY 330- Resilient Modulus*

The resilient modulus data was transferred to an Excel spreadsheet format. Once the data was in Excel format, each sequence of the data was hand sifted to make sure there were not any significant outliers in the data. There were only a handful of outliers of the hundreds of repetitions used for calculations, but they did exist. The irregular data was typically due to the machine sensor reading invalid numbers or applying a stress that did not fit the sequence being run. For example, the resilient modulus sequence being run may have been for a confining pressure of four psi and a deviator stress of two psi. The data used for the sequence is taken as the last five applications of the repetitive load. One of those last five repetitions may have had a deviator stress of 6.05psi. This is in the neighborhood of four psi higher than the deviator stress was supposed to be for the sequence. The relationship of resilient modulus

and stress dependence dictates that the resilient modulus for that particular repetition is typically going to be significantly lower due to its high deviator stress. Therefore, in cases like this, the irregular repetition is discarded from the last five repetitions. This still leaves four values to be used to calculate the average resilient modulus of the sequence.

In order to eliminate some of the variability encountered by the resilient modulus testing, different models were used to match the behavior of the soil under repetitive loading. The different constitutive models used were the Power-law, Universal, Universal w/ Octahedral Shear, and the Modified Universal w/ Octahedral Shear found in sections; 2.6.1, 2.6.2, 2.6.3, and 2.6.4 respectively. Each boring was model in all four models to produce the best model fit for each soil. JMP 7.0 (SAS, 2007) was the computer program used to generate the constants in each model. This was done by inputting the form of the desired equation into the model with the observed field data. The nonlinear modeling function iterates until it comes up with the exponential coefficients of the nonlinear prediction formula that give the highest  $R^2$  value (best fit) for the observed data input. The modeled resilient modulus values were graphed against the actual resilient modulus values. A straight line was fit to the graph to see how well the model predicted resilient modulus behavior of the soil. An example of actual resilient modulus data graphed verses modeled resilient modulus data can be seen below in Figure 24. The graph happens to be for boring 21 which was best modeled by the Universal with Octahedral Shear model. The  $R^2$  value that appears on the chart represents one way of measuring how well the trendline fits the data. The larger the  $R^2$  value the better the data fit the trendline. The highest achievable  $R^2$  value is one.



**Figure 24: HWY 330 Example of Actual vs. Predicted Resilient Modulus**

A summary of the results of the best constitutive model used and how well it fit the measured data for each tested boring can be seen below in Table 8. Boring 20 had an unusual soil behavior and was not able to be modeled by any of the proposed constitutive models. Therefore, for comparison purposes the original data was used instead of modeled data. All other borings were analyzed using their modeled values.

**Table 8: HWY 330 Borings with Constitutive Model Used**

<b>HWY 330 Resilient Modulus Constitutive Models and Parameters</b>						
<b>Boring #</b>	<b>Model</b>	<b>Equation</b>	<b>k<sub>1</sub></b>	<b>k<sub>2</sub></b>	<b>k<sub>3</sub></b>	<b>R<sup>2</sup></b>
3	Universal w/ Octahedral Stress	$M_R = k_1 p_a \left(\frac{\theta}{p_a}\right)^{k_2} \left(\frac{\tau_{oct}}{p_a}\right)^{k_3}$	178	0.372	-0.408	0.89

<b>HWY 330 Resilient Modulus Constitutive Models and Parameters</b>						
<b>Boring #</b>	<b>Model</b>	<b>Equation</b>	<b>k<sub>1</sub></b>	<b>k<sub>2</sub></b>	<b>k<sub>3</sub></b>	<b>R<sup>2</sup></b>
5	Universal	$M_R = k_1 p_a \left(\frac{\theta}{p_a}\right)^{k_2} \left(\frac{\sigma_d}{p_a}\right)^{k_3}$	282	0.513	-0.655	0.97
6	Universal	$M_R = k_1 p_a \left(\frac{\theta}{p_a}\right)^{k_2} \left(\frac{\sigma_d}{p_a}\right)^{k_3}$	418	0.369	-0.552	0.93
8	Universal	$M_R = k_1 p_a \left(\frac{\theta}{p_a}\right)^{k_2} \left(\frac{\sigma_d}{p_a}\right)^{k_3}$	727	0.285	-0.394	0.93
10	Universal	$M_R = k_1 p_a \left(\frac{\theta}{p_a}\right)^{k_2} \left(\frac{\sigma_d}{p_a}\right)^{k_3}$	114	0.568	-0.661	0.94
11	Universal w/ Octahedral Stress	$M_R = k_1 p_a \left(\frac{\theta}{p_a}\right)^{k_2} \left(\frac{\tau_{oct}}{p_a}\right)^{k_3}$	260	0.170	-0.395	0.96
13	Universal	$M_R = k_1 p_a \left(\frac{\theta}{p_a}\right)^{k_2} \left(\frac{\sigma_d}{p_a}\right)^{k_3}$	343	0.419	-0.359	0.89
14	Universal	$M_R = k_1 p_a \left(\frac{\theta}{p_a}\right)^{k_2} \left(\frac{\sigma_d}{p_a}\right)^{k_3}$	371	0.504	-0.403	0.76
15	Universal	$M_R = k_1 p_a \left(\frac{\theta}{p_a}\right)^{k_2} \left(\frac{\sigma_d}{p_a}\right)^{k_3}$	512	0.569	-0.513	0.69
18	Universal	$M_R = k_1 p_a \left(\frac{\theta}{p_a}\right)^{k_2} \left(\frac{\sigma_d}{p_a}\right)^{k_3}$	602	0.361	-0.359	0.86
19	Universal	$M_R = k_1 p_a \left(\frac{\theta}{p_a}\right)^{k_2} \left(\frac{\sigma_d}{p_a}\right)^{k_3}$	421	0.393	-0.319	0.81
20	None	None	None	None	None	None
21	Universal w/ Octahedral Stress	$M_R = k_1 p_a \left(\frac{\theta}{p_a}\right)^{k_2} \left(\frac{\tau_{oct}}{p_a}\right)^{k_3}$	106	0.562	-0.733	0.93
23	Universal w/ Octahedral Stress	$M_R = k_1 p_a \left(\frac{\theta}{p_a}\right)^{k_2} \left(\frac{\tau_{oct}}{p_a}\right)^{k_3}$	58	0.424	-0.686	0.98

<b>HWY 330 Resilient Modulus Constitutive Models and Parameters</b>						
<b>Boring #</b>	<b>Model</b>	<b>Equation</b>	<b>k<sub>1</sub></b>	<b>k<sub>2</sub></b>	<b>k<sub>3</sub></b>	<b>R<sup>2</sup></b>
24	Universal	$M_R = k_1 p_a \left(\frac{\theta}{p_a}\right)^{k_2} \left(\frac{\sigma_d}{p_a}\right)^{k_3}$	116	0.357	-0.674	0.94
25	Universal	$M_R = k_1 p_a \left(\frac{\theta}{p_a}\right)^{k_2} \left(\frac{\sigma_d}{p_a}\right)^{k_3}$	315	0.243	-0.442	0.95
28	Universal	$M_R = k_1 p_a \left(\frac{\theta}{p_a}\right)^{k_2} \left(\frac{\sigma_d}{p_a}\right)^{k_3}$	141	0.457	-0.533	0.94
30	Universal Modified w/ Octahedral	$M_R = k_1 p_a \left(\frac{\theta}{p_a}\right)^{k_2} \left(\frac{\tau_{oct}}{p_a} + 1\right)^{k_3}$	77	0.139	3.791	0.87
32	Universal w/ Octahedral Stress	$M_R = k_1 p_a \left(\frac{\theta}{p_a}\right)^{k_2} \left(\frac{\tau_{oct}}{p_a}\right)^{k_3}$	142	0.574	-0.671	0.99
33	Universal	$M_R = k_1 p_a \left(\frac{\theta}{p_a}\right)^{k_2} \left(\frac{\sigma_d}{p_a}\right)^{k_3}$	270	0.350	-0.520	0.96

The R<sup>2</sup> values for the soils tested on Iowa Highway 330 were in the range of 0.69 to 0.99 with a majority being in the upper 0.80's to 0.90's. The R<sup>2</sup> values were at an appropriate level to use the modeled resilient modulus values for comparison purposes. Again, using these models helps weed out a little variability in the machine testing as well as gives a standard equation by which others may later model the soil.

The modeled resilient modulus values from the two psi confining pressure and two psi deviator stress were used in the analysis. The soil type determination, described earlier in Chapter 5.1, performed on the road sections where resilient modulus data was not run was used to assign resilient modulus values to those sections.

### 5.2.2 US 65- Resilient Modulus

The same procedures were used for the US Highway 65 section for determining resilient modulus data that were stated in Chapter 5.2.1 for the Iowa Highway 330 sections. The resilient modulus data was placed in excel spreadsheet format. The data was hand sifted for outliers in the same manner as the Iowa Highway 330 resilient modulus data. The same four constitutive models were used to predict the behavior of the soil at each US 65 boring.

A summary of the results of the best constitutive model used and how well it fit the measured data for each boring can be seen below in Table 9. All US 65 borings were analyzed using their modeled values.

**Table 9: US 65 Borings with Constitutive Model Used**

<b>US 65 Resilient Modulus Constitutive Models and Parameters</b>						
<b>Boring #</b>	<b>Model</b>	<b>Equation</b>	<b>k<sub>1</sub></b>	<b>k<sub>2</sub></b>	<b>k<sub>3</sub></b>	<b>R<sup>2</sup></b>
1	Universal w/ Octahedral Stress	$M_R = k_1 p_a \left(\frac{\theta}{p_a}\right)^{k_2} \left(\frac{\tau_{oct}}{p_a}\right)^{k_3}$	226	0.377	-0.449	0.85
2	Universal	$M_R = k_1 p_a \left(\frac{\theta}{p_a}\right)^{k_2} \left(\frac{\sigma_d}{p_a}\right)^{k_3}$	664	0.103	-0.193	0.89
3	Universal w/ Octahedral Stress	$M_R = k_1 p_a \left(\frac{\theta}{p_a}\right)^{k_2} \left(\frac{\tau_{oct}}{p_a}\right)^{k_3}$	265	0.029	-0.365	0.91
4	Universal	$M_R = k_1 p_a \left(\frac{\theta}{p_a}\right)^{k_2} \left(\frac{\sigma_d}{p_a}\right)^{k_3}$	391	0.322	-0.361	0.92
5	Universal	$M_R = k_1 p_a \left(\frac{\theta}{p_a}\right)^{k_2} \left(\frac{\sigma_d}{p_a}\right)^{k_3}$	364	0.340	-0.465	0.95

The R<sup>2</sup> values for the soils tested on US Highway 65 were in the range of 0.85 to 0.95. These R<sup>2</sup> values were also at an appropriate level to use the modeled resilient modulus values for comparison purposes.

The modeled resilient modulus values from the two psi confining pressure and two psi deviator stress were used in the analysis. As in the IA 330 project, the soil type determination, described in Chapter 5.1, was performed on the road sections to assign resilient modulus data to section in which resilient modulus tests were not run.

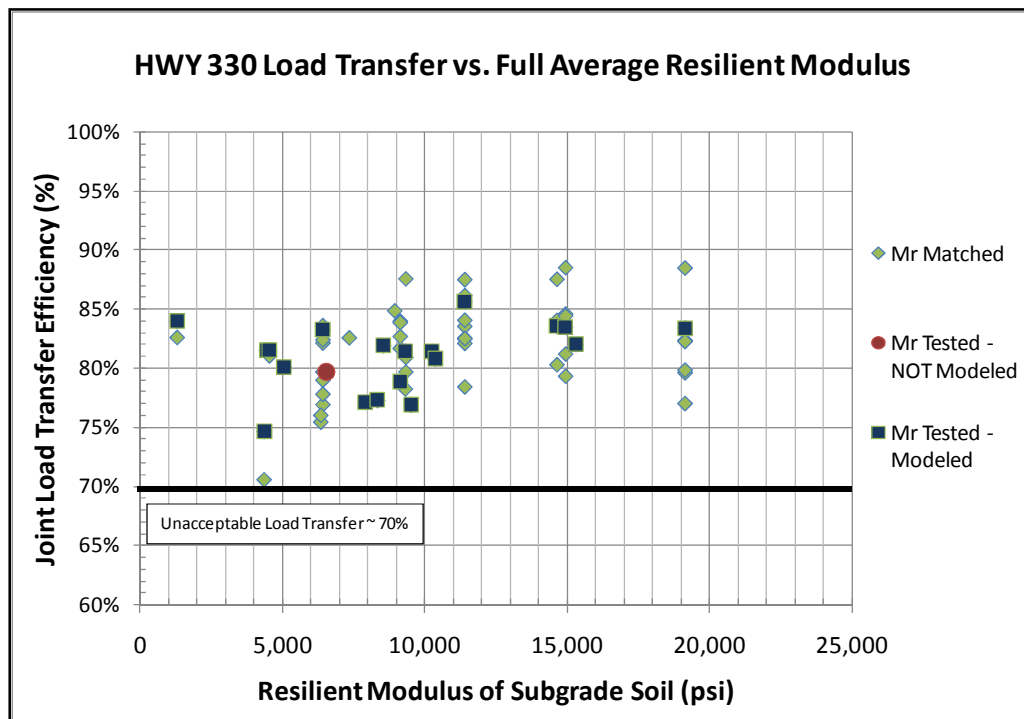
### **5.3 Load Transfer**

One way to compare performance by bar type and spacing, while accounting for effects from subgrade resilient modulus, would be to plot load transfer efficiency of sections with different bar types and spacing intervals versus resilient modulus. Another way to compare performance of different treatment combinations could be done by keeping the resilient modulus value constant and seeing how that affects performance. Ideally, one would be able to control the resilient modulus variable to better compare pavement performance. However, since resilient modulus was not a controllable variable in this study (testing was not originally designed for resilient modulus considerations), comparisons must be done with what resilient modulus values resulted from testing. Since the resilient modulus of a section was essentially left up to chance during construction, it was foreseen that difficulties in matching resilient modulus values was a possibility. However, since there is a large amount of performance data for Iowa Highway 330, results from any sections with matching resilient modulus values would have strong implications.

#### *5.3.1 HWY 330- Load Transfer*

Load transfer data is determined through the use of FWD data, as previously stated. Data at sensors under the applied load and 12 inches from the applied load are used to make this calculation. An overall load transfer versus resilient modulus graph of all the dowel

sections can be seen below in Figure 25. This graph does not differentiate sections with different dowel types and spacing. Notice the increasing trend of load transfer as the resilient modulus increases in Figure 25. This occurs until a resilient modulus of about 10,000 psi, at which point, only small improvement of load transfer is achieved as resilient modulus increases.



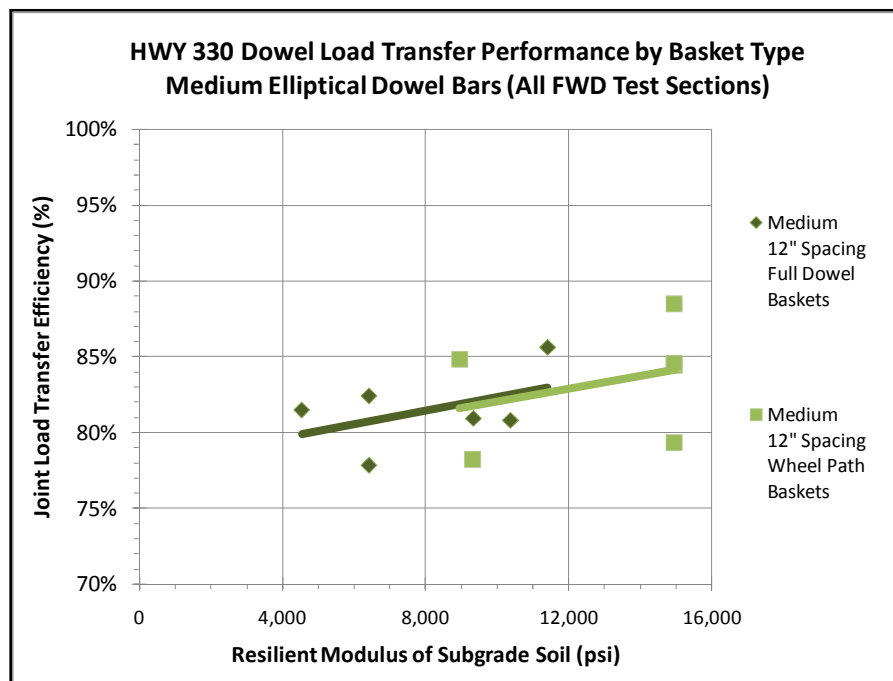
**Figure 25: HWY 330 Load Transfer vs. Resilient Modulus**

#### 5.3.1.1 Dowel Basket Type – HWY 330 Load Transfer

One of the objectives of the Iowa Highway 330 research project was to determine if the use of dowel bars in the wheel paths only was a viable option compared with full dowel baskets across the transverse joint. Wheel path baskets were placed using four bars per wheel path (See Figure 13). These bars were spaced 12 inches apart. There were a total of 12 sections having dowels in the wheel paths only. Half of the wheel path dowels were



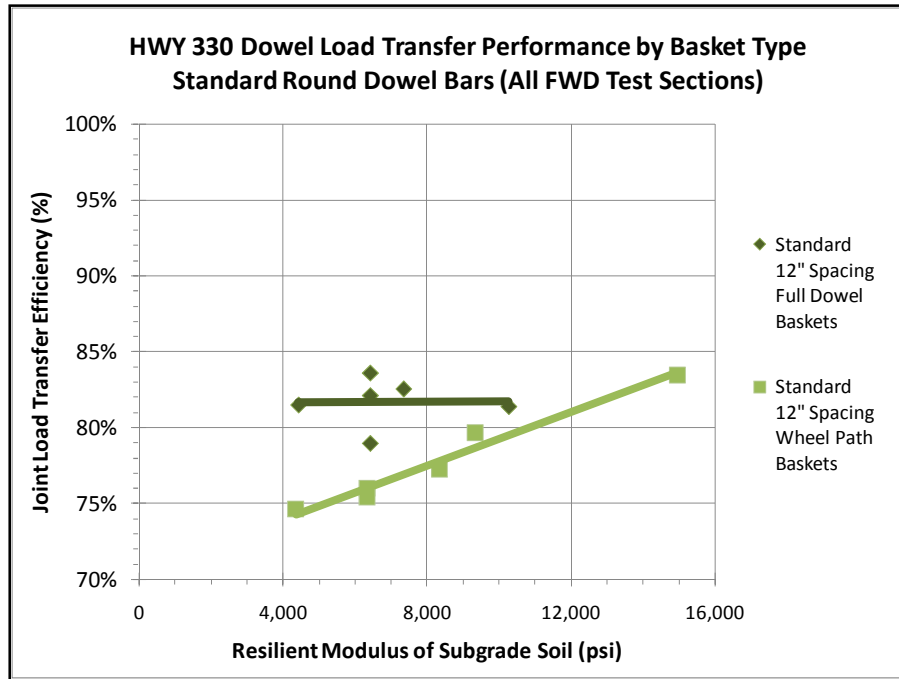
constructed using medium elliptical dowel bars. The other half were constructed using standard round dowel bars. A linear trendline will be placed on the majority of the graphs to assume an average value of performance by resilient modulus value. Figure 26 below shows similar performance between the load transfer performance of full dowel basket sections and wheel path dowel basket sections for medium elliptical dowel bars spaced 12 inches apart. Since the relationship between full dowel baskets and wheel path dowel baskets is so similar with medium elliptical dowel bars, the wheel path dowel sections will be accounted for in the overall comparisons of full dowel baskets for the medium elliptical 12 inch spaced dowels.



**Figure 26: HWY 330 Load Transfer by Basket Type - Medium Elliptical Dowels**

The load transfer performance of standard round dowel bars showed slightly different results from the medium elliptical dowel bars when full baskets were compared with the wheel path baskets. Figure 27 shows the full dowel basket sections having higher load transfer efficiency than the wheel path sections. Since there is difference in the wheel path

section compared with full dowel baskets for the standard round dowel bars; the wheel path sections will not be included in the overall data analysis of bar types and spacing.

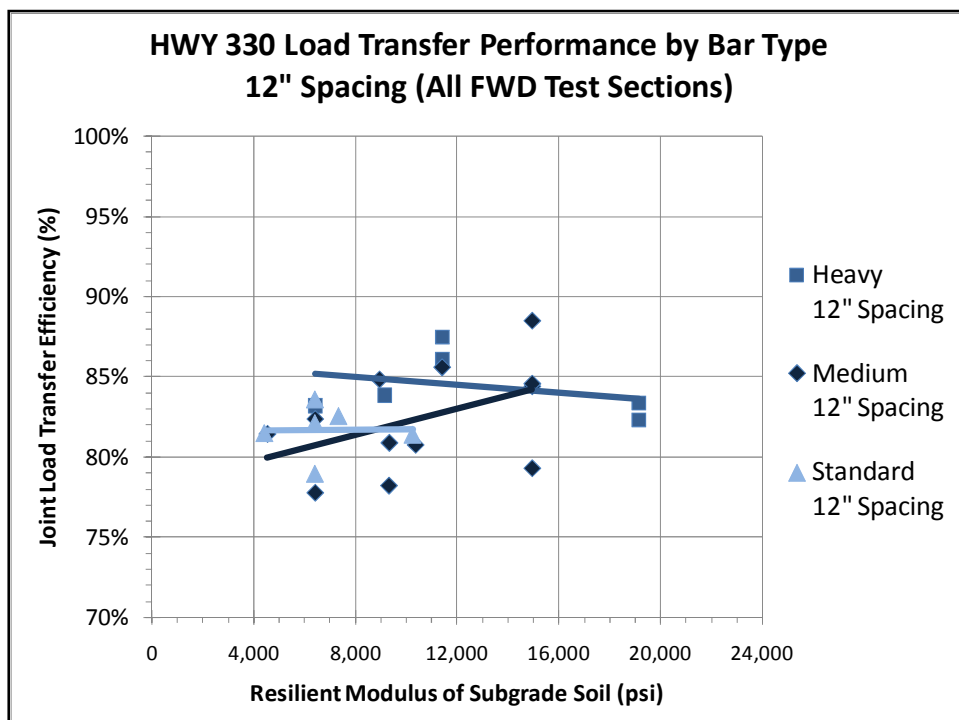


**Figure 27: HWY 330 Load Transfer by Basket Type – Standard Round Dowels**

### 5.3.1.2 Dowel Type – HWY 330 Load Transfer

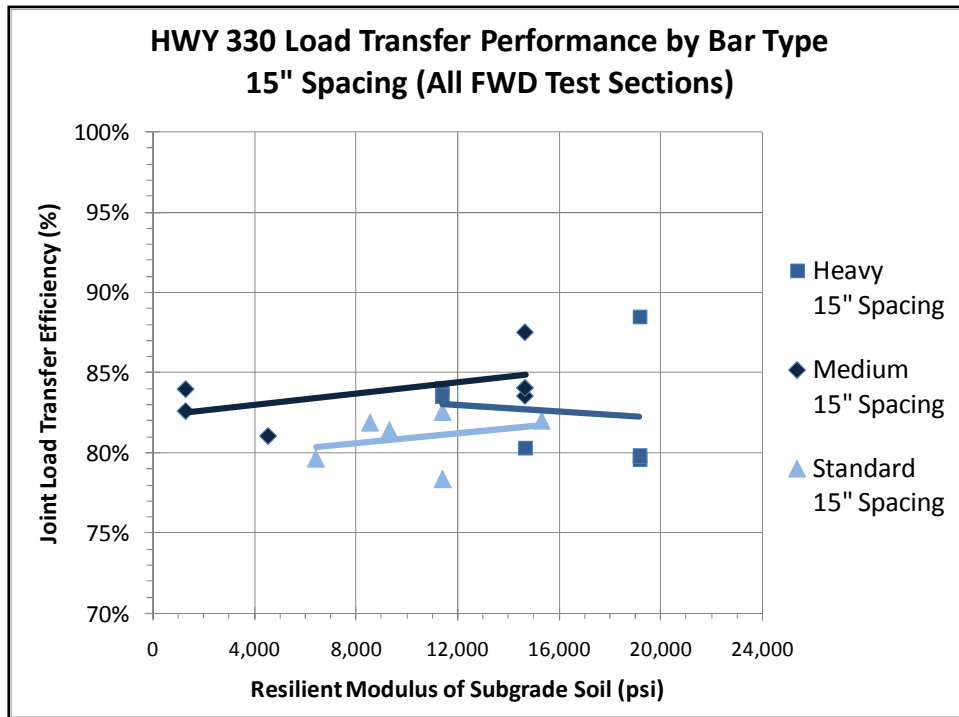
Another objective of the Iowa Highway 330 research project was to determine how standard round, medium elliptical, and heavy elliptical bars performed compared to one another. According to research done by Porter (2001) on elliptical dowel bars and optimization, the concrete bearing stress of the standard round 1.5 inch bars and medium elliptical bars in the lab are about the same. This makes it possible to attribute performance of the standard round and medium elliptical dowel directly to the dowel shape. In order to determine whether using a particular bar is better at carrying the load across a joint in the field, resilient modulus and spacing must be taken into account. Figure 28 below indicates that heavy elliptical dowel bars are performing better than medium elliptical and standard

round bars at 12 inch spacing when resilient modulus is taken into account. This is likely due to the heavy elliptical dowel's ability to handle more bearing stress (Porter, et al 2001). The graph also shows for each standard round dowel section with 12 inch spaced dowels there is essentially an equal counterpart of medium elliptical performance. This indicates medium elliptical dowels are transferring load equally with standard round dowel bars with 12 inch dowel spacing.



**Figure 28: HWY 330 Load Transfer Performance by Dowel Type @ 12 inch Spacing**

Figure 29 below shows heavy and medium elliptical dowels perform better than standard round dowels at 15 inch spaced dowels. Also, the overall load transfer is lower than the dowels spaced 12 inches apart. This seems to confirm the idea that the more bars put into the joint, the better the performance of the joint.



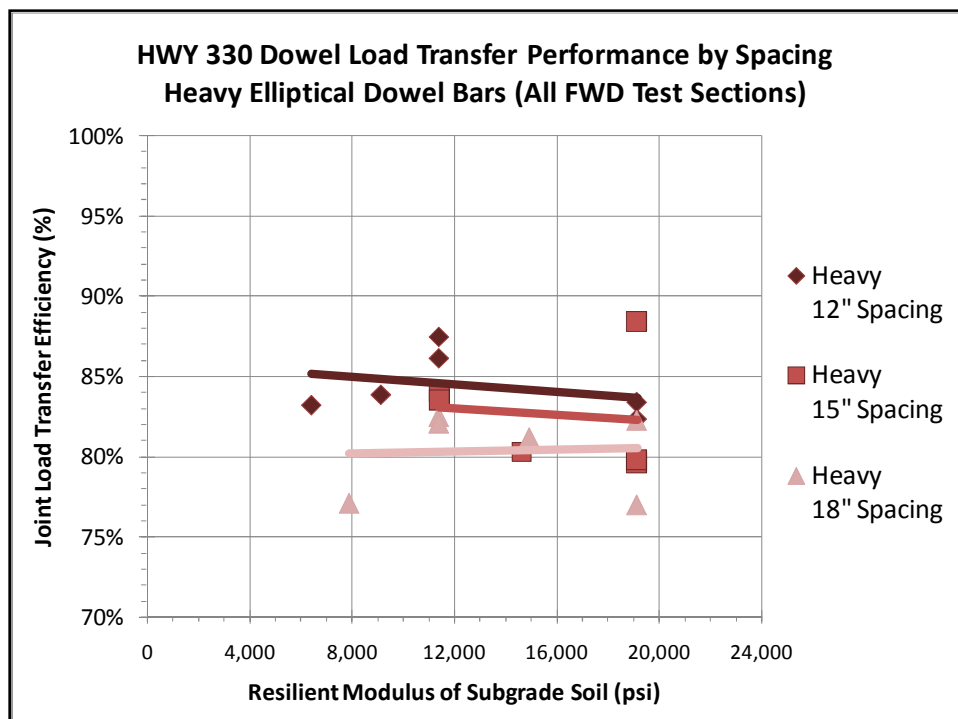
**Figure 29: HWY 330 Load Transfer Performance by Dowel Type @ 15 inch Spacing**

The results of the 18 inch spacing comparison were not conclusive. Nearly all the 18 inch spaced medium elliptical dowel bars were in sections having 8,000 to 9,000 psi resilient modulus values. The lack of range for the resilient modulus values makes it difficult to draw any reasonable conclusions. The heavy elliptical dowels had a majority of sections with high resilient modulus values. The standard round bars had a majority of sections with low resilient modulus values. This made for very little overlap for comparison between the heavy elliptical dowels and standard round dowels at the 18 inch spacing. A graph can be found in Appendix C.

### 5.3.1.3 Dowel Spacing – HWY 330 Load Transfer

Another objective of the Iowa Highway 330 research project was to determine how the spacing of standard round, medium elliptical, and heavy elliptical bars affected the

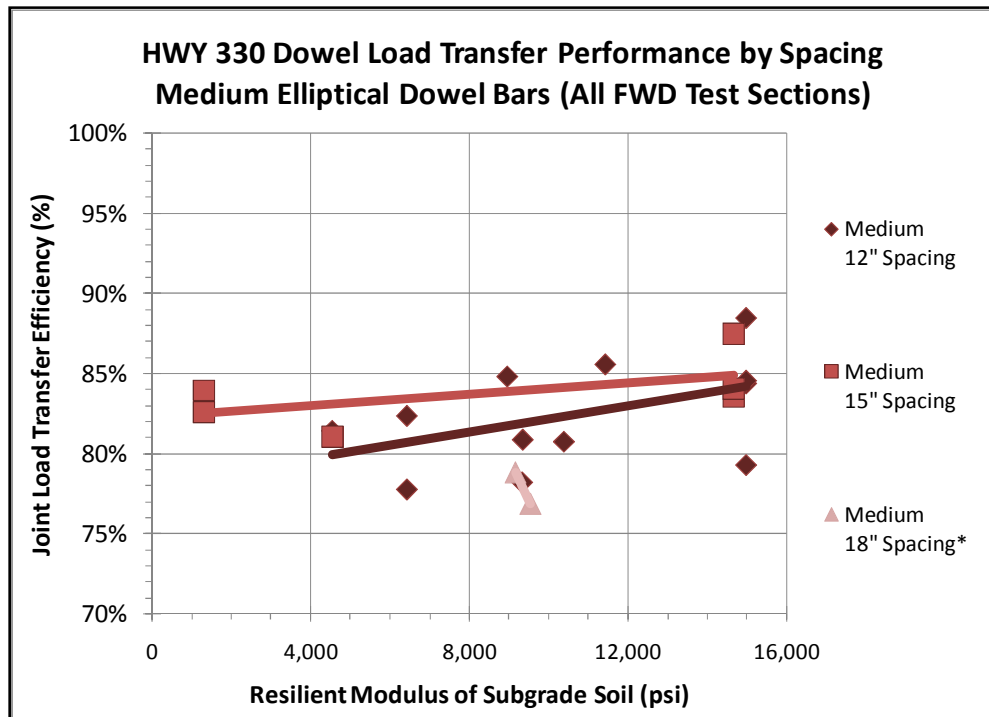
performance of the different sections. In order to determine whether using a particular spacing is better at carrying the load across a joint, resilient modulus and dowel type are taken into account. The results of the heavy dowel bars spaced at 12 inches, 15 inches, and 18 inches can be seen in Figure 30 below. The graph shows the load transfer efficiency decreasing as the spacing of the dowel bars increases. This is to be expected. The purpose of the dowel bar is to transfer load. So, the closer the dowel bars are spaced, the more dowel bars being used. The more dowel bars used, the more transfer mechanism across the joint.



**Figure 30: HWY 330 Load Transfer by Dowel Spacing - Heavy Elliptical Dowels**

Medium elliptical dowel bars were tested for load transfer efficiency as well. The results of the medium elliptical dowel bars spaced at 12 inches, 15 inches, and 18 inches can be seen in Figure 31 below. Figure 31 shows the medium elliptical dowels spaced at 15 inches performing just as well as the medium elliptical dowels spaced 12 inches apart. The

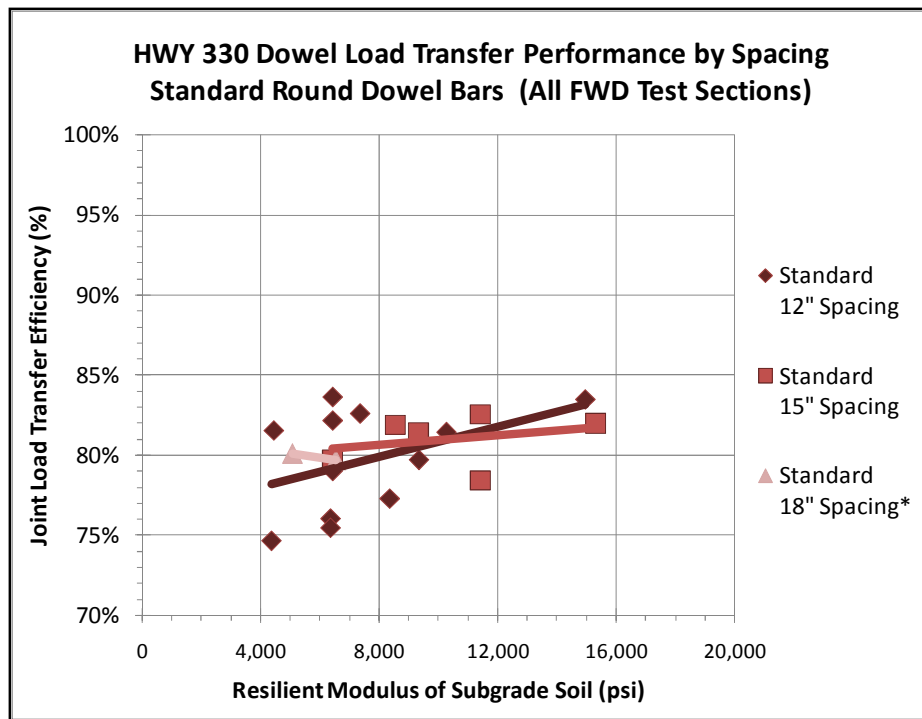
medium elliptical dowels spaced 18 inches apart do not perform as well as the 12 inch and 15 inch spaced dowels.



Note: \* means only Mr tested data used

**Figure 31: HWY 330 Load Transfer by Dowel Spacing - Medium Elliptical Dowels**

The results of the standard round dowel bars spaced at 12 inches, 15 inches, and 18 inches can be seen in Figure 32 below. The results appear to show the 12 inch spaced standard round dowel bars perform slightly better than the 15 inch and 18 inch spaced standard round dowels. This is to be expected since there are more dowel bars transferring load in the 12 inch spaced sections. Figure 32 shows the standard round dowels spaced at 18 inches performing just as well as the standard round dowels spaced 15 inches apart. However, there is not enough data for the 18 inch spaced dowels to draw that conclusion. It is likely that the 18 inch spaced standard round bars transfer load at a lower efficiency than the dowels spaced 15 inches apart.

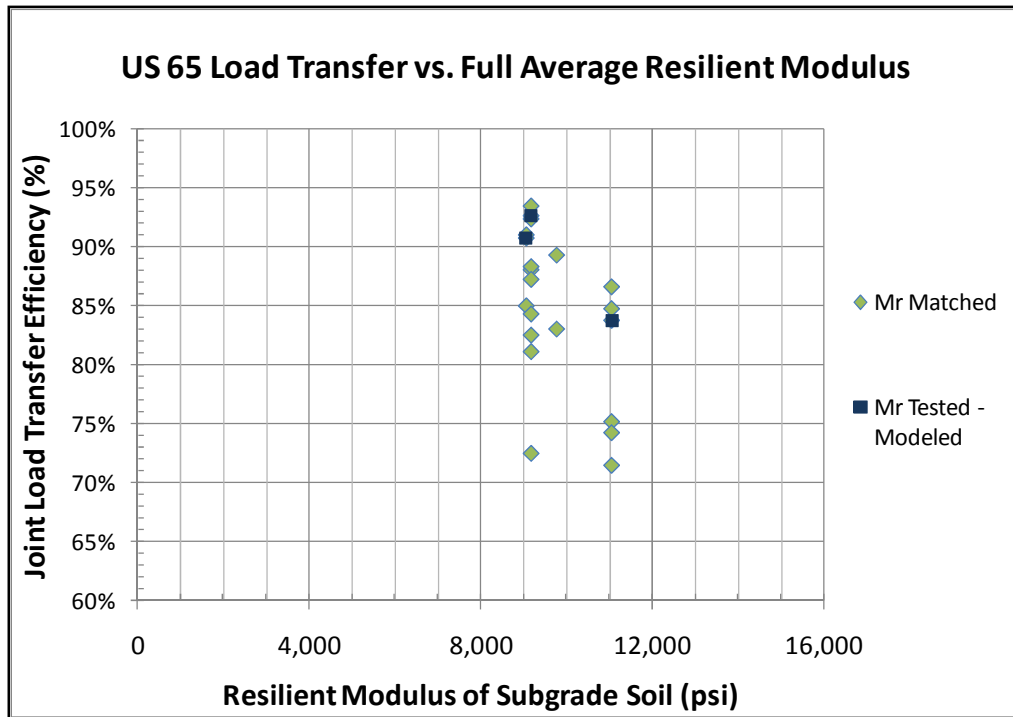


Note: \* means only Mr tested data used

**Figure 32: HWY 330 Load Transfer by Dowel Spacing - Standard Round Dowels**

### 5.3.2 US 65–Load Transfer

The US Highway 65 project had considerably less data than the Iowa Highway 330 project. There were a total of 21 test sections on US Highway 65 where FWD data was taken. Each dowel bar type and spacing had three sections used for testing. The load transfer (FWD) performance data for the sections was taken at eight different times during the length of the study. This means that there would be approximately 24 different load transfer values used to calculate an overall average of load transfer performance of a particular bar type and spacing combination during the course of the study. Figure 33 below shows the soils on the US 65 project have a much smaller range of resilient modulus (Mr) values than the HWY 330 project. This is partially due to the significantly smaller scale of the US 65 project.



**Figure 33: US 65 Load Transfer vs. Resilient Modulus**

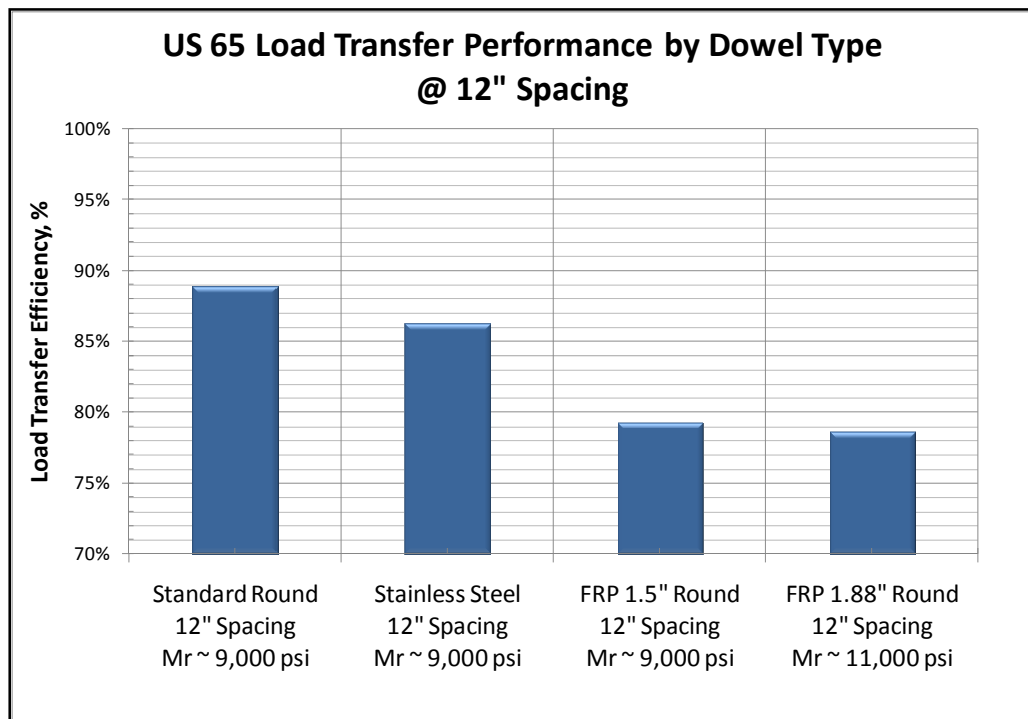
Five strategically placed boring were used for the resilient modulus determination of these sections. This data coupled with AREA calculations from mid-slab FWD data and plan sheet soil data were used to get resilient modulus data for each section. Since there was not enough difference in resilient modulus values from section to section, the method of keeping the resilient modulus value constant and comparing the dowel sections was used.

#### 5.3.2.1 Dowel Type – US 65 Load Transfer

One of the objectives of the US Highway 65 research project was to determine how standard round, stainless steel, 1.5 inch round GFRP, and 1.88 inch round GFRP dowel bars performed compared to one another. In order to determine whether using a particular bar is better at carrying the load across a joint, resilient modulus (Mr) and spacing were taken into account. Figure 34 ,below, indicates that standard round and stainless steel dowel bars are performing better than both sizes of GFRP dowel bars at 12 inch spacing when resilient



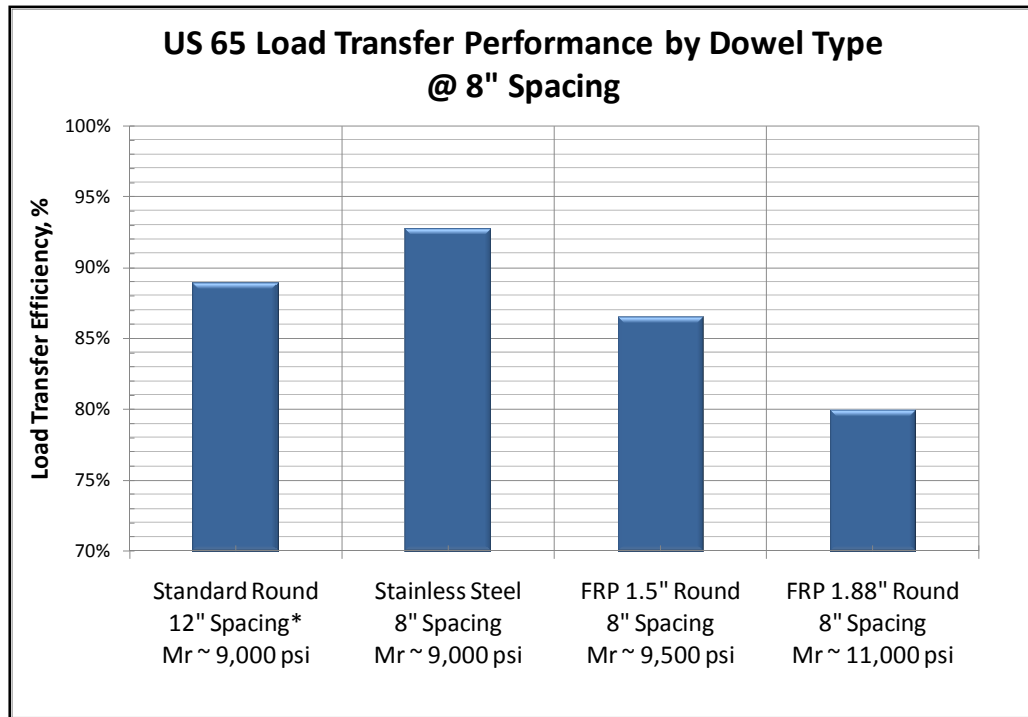
modulus is taken into account. Even with an increased diameter (1.88 inch bars) the GFRP bars are still not performing as well as the standard round and stainless steel dowels, in terms of load transfer. This may be due to the low modulus of elasticity of GFRP. The slightly lower performance of the stainless steel dowel bars may be due to their lower bond strength. The lower bond strength of stainless steel bars was determined in a study by Porter (2001).



**Figure 34: US 65 Load Transfer Performance by Dowel Type @ 12 inch Spacing**

Figure 35, below, indicates that stainless steel dowel bars are performing better than both sizes of GFRP dowel bars at eight inch spacing when resilient modulus is taken into account. There were no sections of standard dowels spaced at eight inches, so the 12 inch spacing was used in the figure as a reference point. However, if standard round dowels spaced eight inches apart had been used, one would expect the standard round load transfer to be close to or a little above the stainless steel dowels. In Figure 35 notice the resilient

modulus value of the 1.88 inch round GFRP dowel section is higher than the other sections. Even with the higher subgrade resilient modulus and closer spacing, the 1.88 inch round GFRP dowel bars are still not performing as well as the standard round or stainless steel dowel bars spaced farther apart.

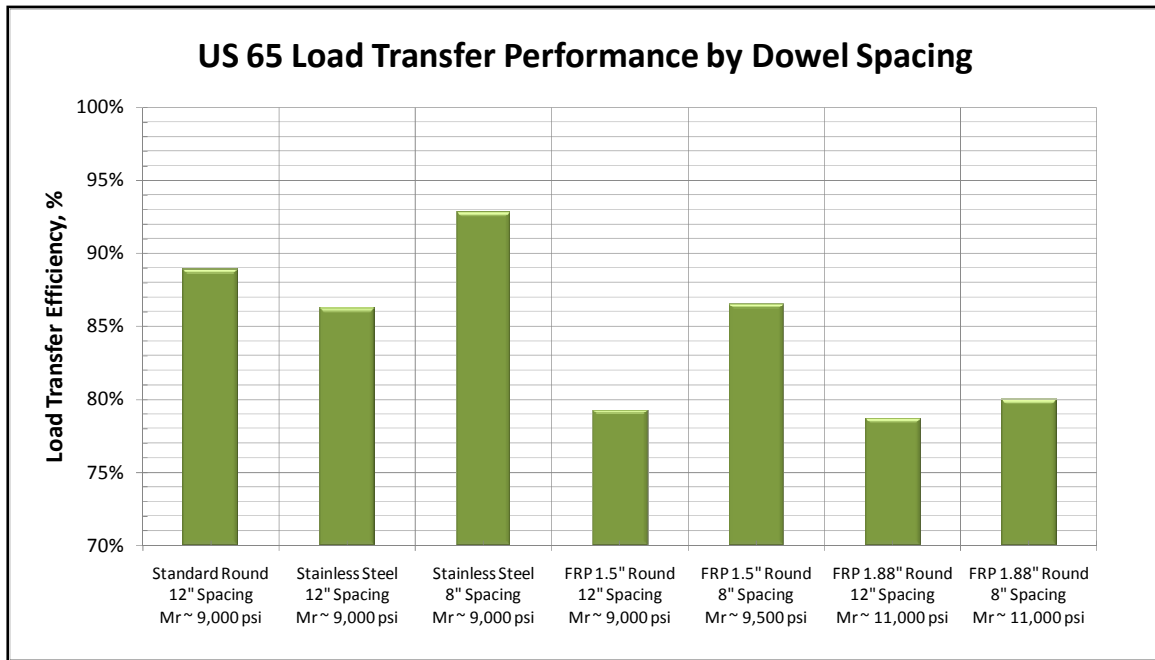


Note: \* indicates different spacing

**Figure 35: US 65 Load Transfer Performance by Dowel Type @ Eight Inch Spacing**

### 5.3.2.2 Dowel Spacing – US 65 Load Transfer

Another objective of the US Highway 65 research project was to determine how standard round, stainless steel, 1.5 inch round GFRP, and 1.88 inch round GFRP dowel bars performed when dowel bars were spaced at eight inch and 12 inch intervals. The results of the standard round, stainless steel, 1.5 inch GFRP, and 1.88 inch GFRP dowels spaced at eight inches and 12 inches can be seen in Figure 36 below. Figure 36 shows the increase in load transfer achieved by spacing dowels closer together.



**Figure 36: US 65 Load Transfer Performance by Dowel Spacing**

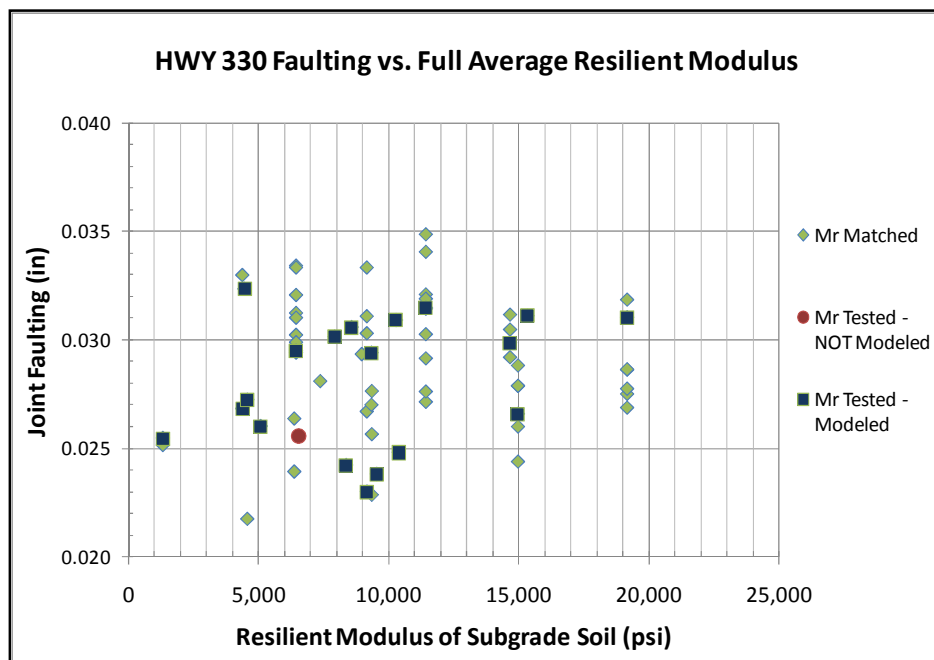
The largest benefits were attained by the stainless steel and 1.5 inch GFRP dowel bar being spaced closer together. The 1.88 inch GFRP dowel bars showed improvement with closer spacing, but not nearly as significant as the improvement shown by the other bar types. Stainless steel dowel bars spaced eight inches apart showed to have the highest level of load transfer of all the dowel type and spacing combinations. The stainless steel bars at eight inch spacing would have the highest stiffness of the tested sections. This is likely the reason for the best load transfer performance of the tested bar type and spacing combinations. The stainless steel sections also had the lowest subgrade resilient modulus values of all the tested sections. This helps solidify the statement that the stainless steel dowel bars spaced eight inches apart transferred load across the joint better than any other dowel type and spacing combination tested. However, if standard round epoxy-coated bars had been tested at an eight inch spacing, it is conceivable that they may have transferred load better than the stainless steel bars at eight inch spacing.

## 5.4 Faulting

### 5.4.1 HWY 330- Faulting

The faulting measurements for the Iowa Highway 330 project were taken at a distance of 18 inches from the edge of the pavement in the driving and passing lanes. These faulting measurements were taken at 10 joints in the middle of each dowel section. The overall average of faulting for each section was taken as the average of the driving and passing lane faulting values of all 10 joints in the section over the study period. There were nine different data collection periods. Therefore, each overall average faulting value for the section is a combination of about 180 readings.

An overall faulting versus resilient modulus graph of all the dowel sections on Iowa Highway 330 can be seen below in Figure 37. The graph does not differentiate sections with different dowel types and spacing.



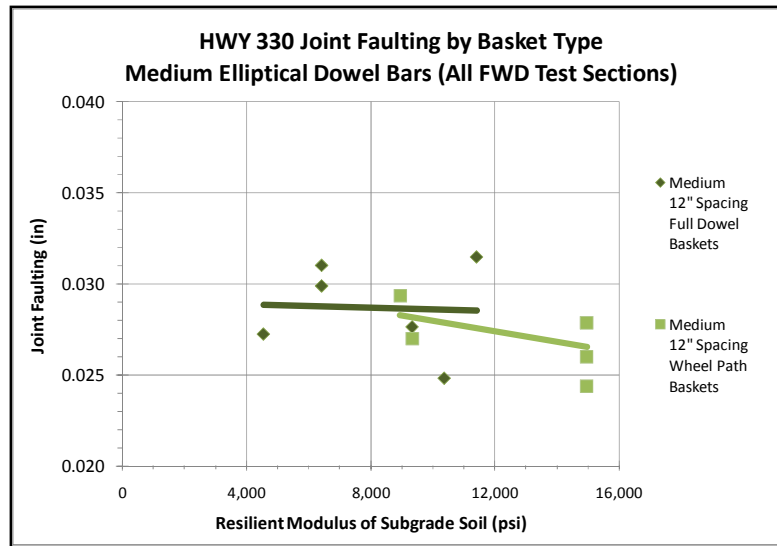
**Figure 37: HWY 330 Joint Faulting vs. Resilient Modulus**

Notice Figure 37 does not appear to have any significantly noticeable trends of joint faulting to resilient modulus when dowel type and spacing are not considered. The results will become clearer as the dowel type and spacing are taken into consideration.

The faulting performance of heavy elliptical, medium elliptical, and standard round dowel bars at 12 inch, 15 inch and 18 inch spaced intervals were analyzed and will be discussed further in the following sections. The faulting performance of the Iowa Highway 330 dowel sections with wheel path baskets was also analyzed. The values obtained by the faultmeters were in the range of 0.02 inches to 0.04 inches. The small faulting values are not necessarily surprising as the pavement has only been monitored for the first five years of its existence. Faulting values taken at later dates may indicate more significant faulting patterns between the dowel types and spacing intervals of the Iowa Highway 330 project.

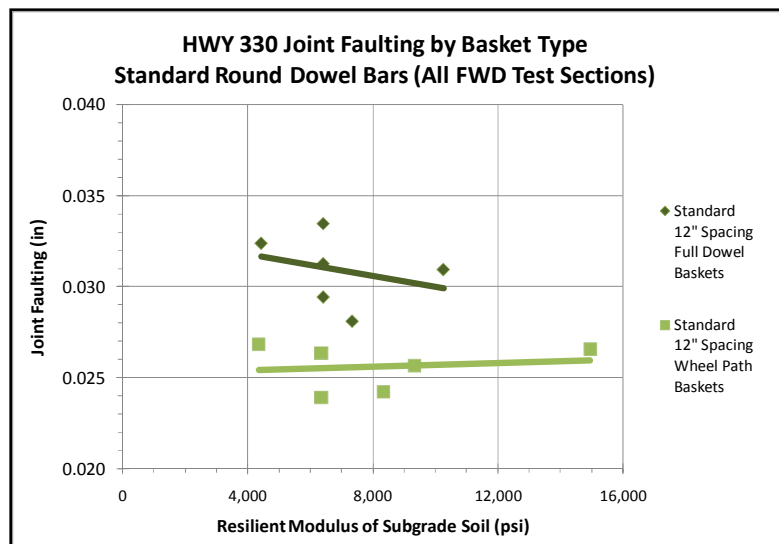
#### *5.4.1.1 Dowel Basket Type – HWY 330 Faulting*

The effects of using a wheel path dowel basket verses a full dowel basket for medium elliptical dowel bars can be seen below in Figure 38. The figure shows the wheel path baskets having less faulting than the full dowel baskets. This indicates medium elliptical dowel bars placed in the wheel paths only perform just as well as medium elliptical full dowel baskets in terms of faulting.



**Figure 38: HWY 330 Joint Faulting by Basket Type - Medium Elliptical Dowels**

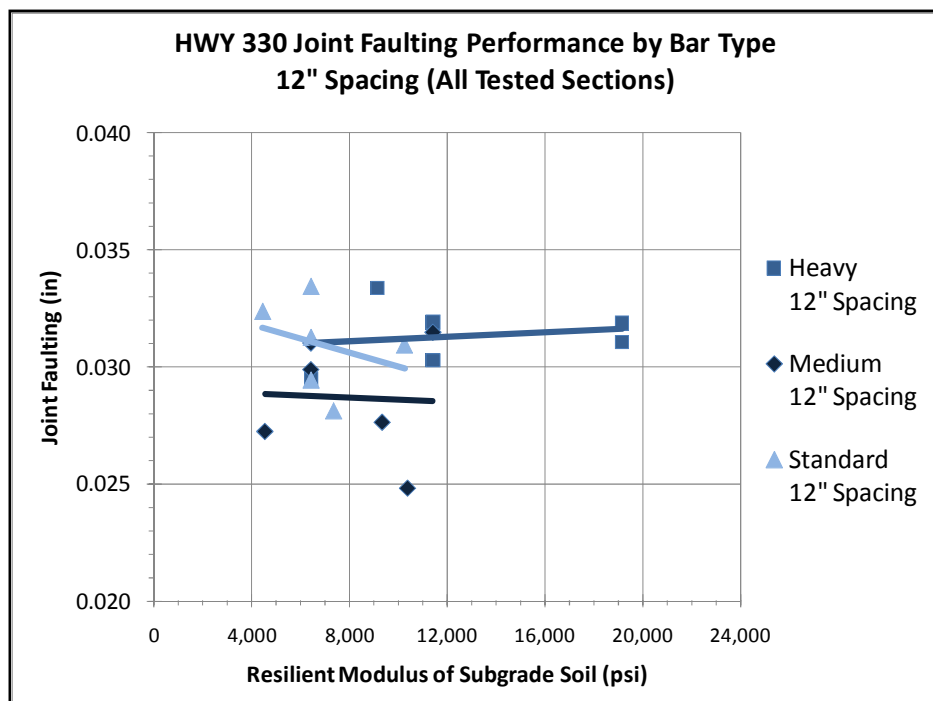
The plot of standard round wheel path basket sections and standard round full basket sections in terms of faulting can be seen below in Figure 39. The figure shows the standard round wheel path basket sections performing just as well, if not better than the standard round full basket sections. This indicates standard round dowels placed in the wheel paths only will perform just as well as full dowel basket section in terms of faulting.



**Figure 39: HWY 330 Joint Faulting by Basket Type – Standard Round Dowels**

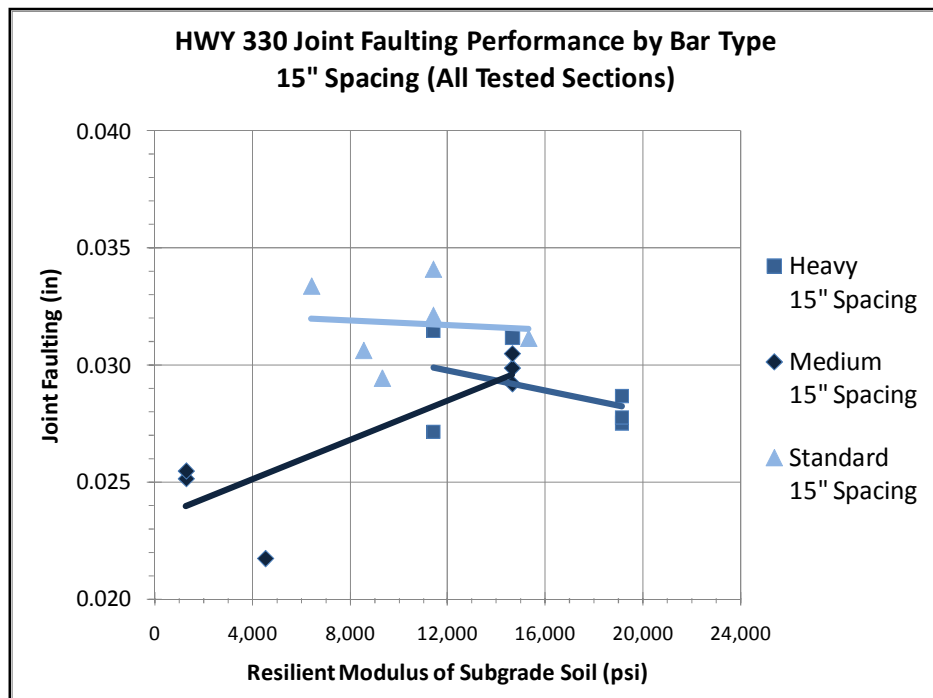
#### 5.4.1.2 Dowel Type - HWY 330 Faulting

The faulting performance of the heavy elliptical, medium elliptical, and standard round dowel bar sections with dowels spaced at 12 inches apart can be seen below in Figure 40. The graph shows medium elliptical bars performing better than standard round dowel bar sections and heavy elliptical dowel sections at the 12 inch spacing. The heavy elliptical dowel bar section has higher faulting values than the medium elliptical and standard round bars. Intuition would say that having a heavier bar with more steel would yield lower faulting values. However, where more steel was used in the joint higher faulting values were observed. This same effect was noticeable in the wheel path basket section earlier. Both standard round and medium elliptical sections with wheel path baskets performed better in terms of faulting than their counterpart full dowel basket sections. This occurrence of more steel equals higher faulting will come up again in later sections.



**Figure 40: HWY 330 Joint Faulting by Bar Type @ 12 inch Spacing**

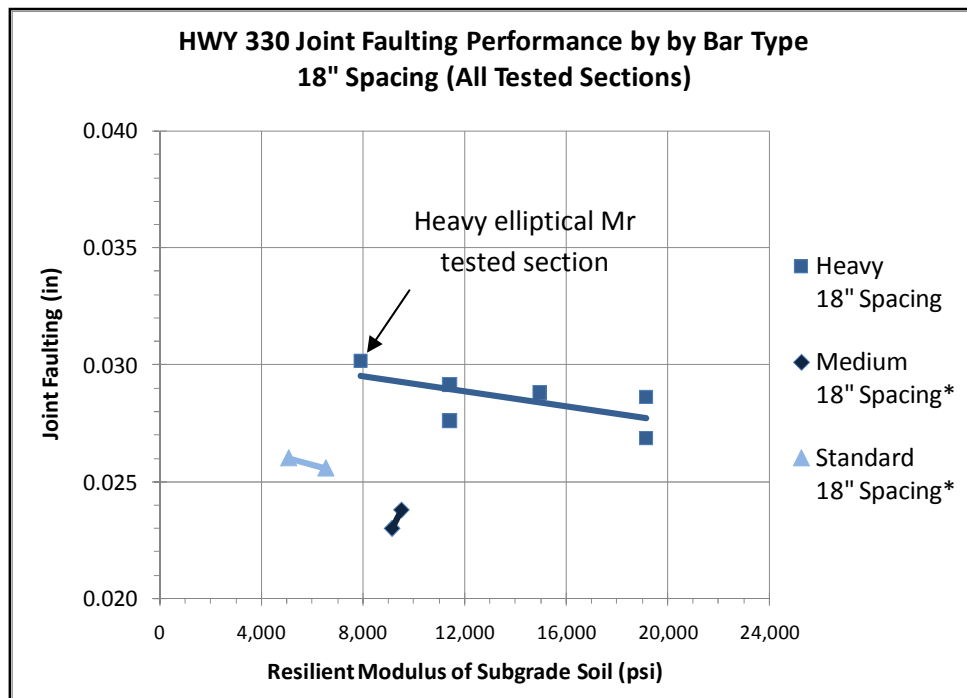
The graph of joint faulting of the different bar types at the 15 inch spacing can be seen below in Figure 41. The data in Figure 41 indicates medium elliptical dowel bars perform better than standard round dowel bars at 15 inch spaced dowel intervals. It also indicates that heavy dowels are performing better than the standard round dowels when spaced at 15 inch intervals. The figure also suggests the possibility that medium elliptical dowels perform just as well as heavy elliptical dowel bars at controlling joint faulting at 15 inch spaced intervals. Something else to consider is no resilient modulus tests were run in sections with heavy bars spaced at 15 inch intervals. A graph of the resilient modulus sections of the points in Figure 41 yields a similar pattern in behavior, with exception to the 15 inch spaced heavy dowels that have no resilient modulus tested sections, only matched sections.



**Figure 41: HWY 330 Joint Faulting by Bar Type @ 15 inch Spacing**



Figure 42 shows the joint faulting performance of the heavy elliptical, medium elliptical, and standard round dowels spaced at 18 inch intervals. The medium elliptical dowel bars did not have a very large range of resilient modulus values. Therefore, only the resilient modulus tested values were shown for the medium elliptical dowel bars. The resilient modulus tested values were shown for the medium elliptical dowel bars. The resilient modulus tested sections were used for the standard round bars as well. The resulting graph indicates similar patterns from previous analysis. The medium elliptical dowels appear to be allowing less joint faulting than the heavy elliptical dowels and the standard round dowels. The sections with more cross-sectional steel may produce more faulting than sections with less cross-sectional steel. The resilient modulus tested section for the heavy elliptical bars spaced at 18 inch intervals is noted in Figure 42. A graph of the original graph with all sections can be found in Appendix C.

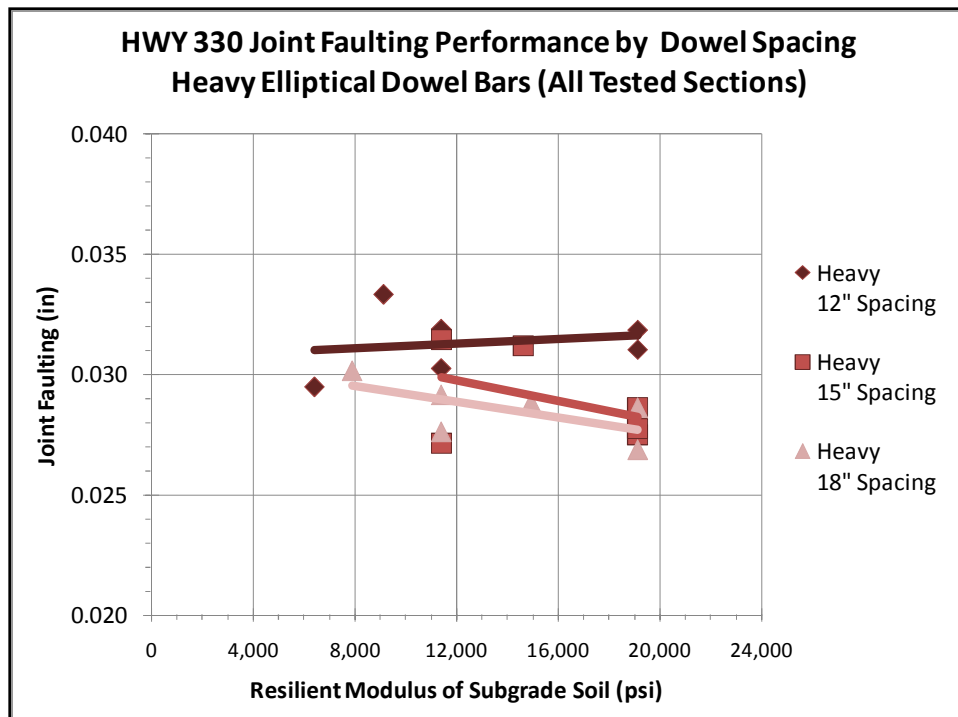


Note: \* means only Mr tested data used

**Figure 42: HWY 330 Joint Faulting by Bar Type @ 18 inch Spacing**

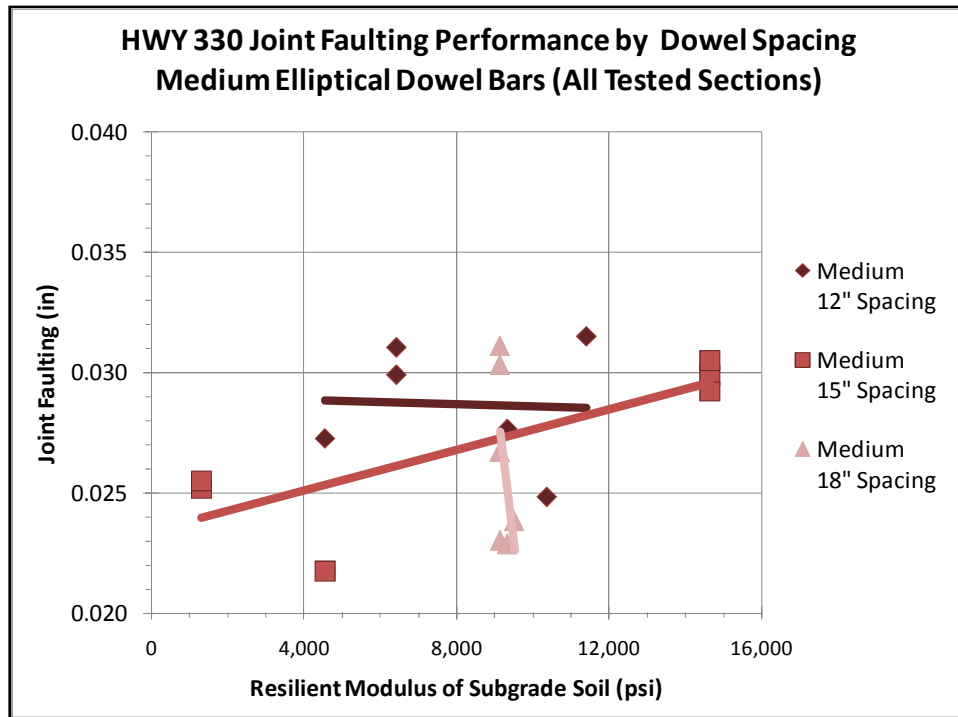
### 5.4.1.3 Dowel Spacing - HWY 330 Faulting

The next thing that was evaluated was the effect of dowel spacing of the individual bar types on joint faulting performance. In Figure 43 below, the heavy elliptical dowel bars are producing more faulting as dowel bars are spaced closer together. This could be caused by an over stiffening of the joint.



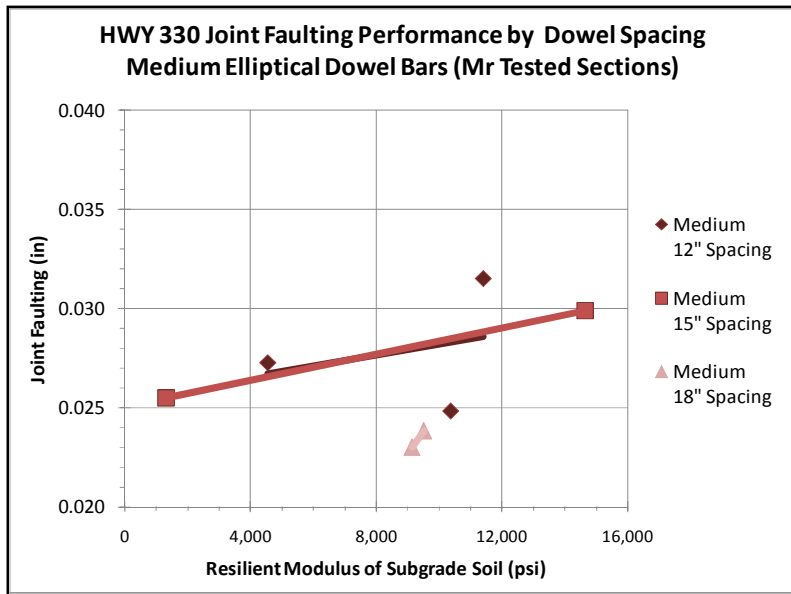
**Figure 43: HWY 330 Joint Faulting by Dowel Spacing – Heavy Elliptical Dowels**

The joint faulting performance of the medium elliptical dowel bars is shown in Figure 44. Similar to the heavy elliptical dowels, Figure 44 shows the sections with dowels at 12 inch spacing performing lower than sections with 15 inch and 18 inch spaced dowels. The results of the 18 inch spaced medium elliptical dowels in Figure 44 should not carry as much weight as the 12 inch and 15 inch spacing since there is a small resilient modulus range to compare over. Again, the wheel path dowel sections were not considered in Figure 44.



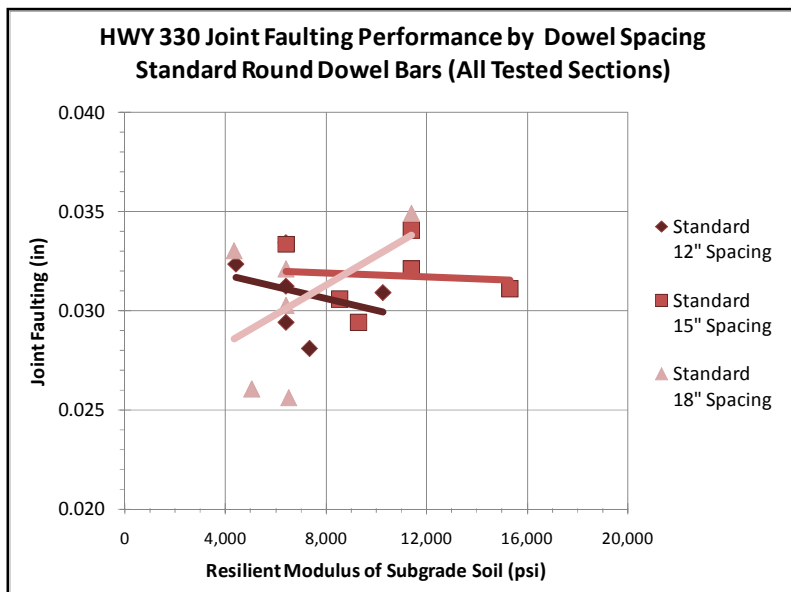
**Figure 44: HWY 330 Joint Faulting by Dowel Spacing – Medium Elliptical Dowels**

If only resilient modulus tested sections are considered in the medium elliptical joint faulting performance by spacing, the results are a little different. Figure 45 shows the 12 inch and 15 inch spaced medium elliptical dowels performing similarly. The 18 inch spaced medium elliptical dowels are performing better in terms of joint faulting than the 12 inch and 15 inch dowel spaced sections. This seems to go along with the same idea from the heavy elliptical dowel bars. The less steel across the joint, the lower the faulting values. One should note that some of the variables of Figure 45 only have two points making up the relationship. This is not optimal, but the figure still seems to give some insight into dowel faulting performance.



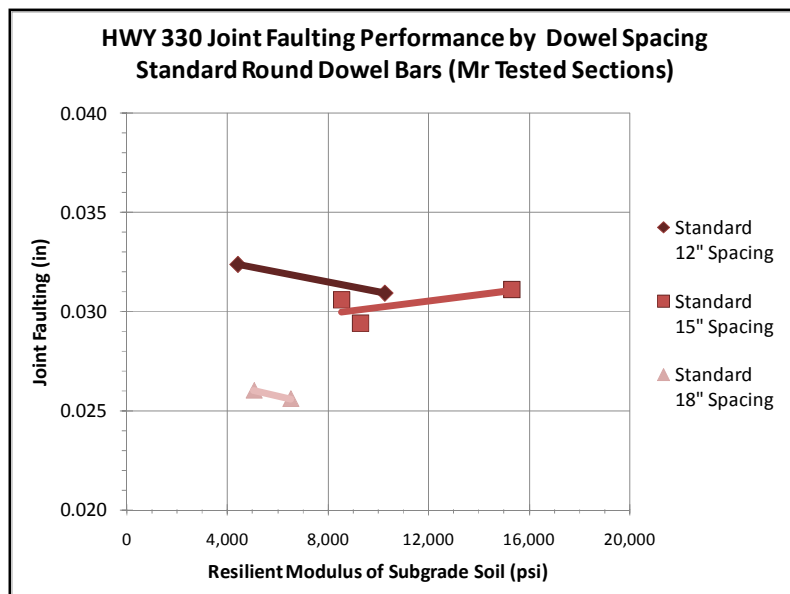
**Figure 45: HWY 330 Joint Faulting Medium Elliptical Dowels (Mr Sections Only)**

The results of the analysis of standard round joint faulting by spacing can be seen in Figure 46 below. This graph shows the standard round dowel sections with 12 inch spacing producing less joint faulting than the 15 inch spaced standard round dowel bars. The sections with 18 inch spaced dowels show varying results.



**Figure 46: HWY 330 Joint Faulting by Dowel Spacing - Standard Round Dowels**

Like before, if only resilient modulus ( $M_r$ ) tested sections are considered in the standard round joint faulting performance by spacing, the results are a little different. Figure 47 now shows the 12 inch spaced dowel sections performing less than or equal to the 15 inch spaced standard round dowel sections. The graph also shows the 18 inch spaced standard round dowel sections are performing better in terms of joint faulting than the 12 inch and 15 inch dowel spaced sections. These are similar finding in terms of faulting to the heavy elliptical and medium elliptical dowel sections. One should note the 18 inch spaced standard round dowel sections only had two sections where resilient modulus was tested. This is not preferred, but the figure still allows some insight into dowel faulting performance.

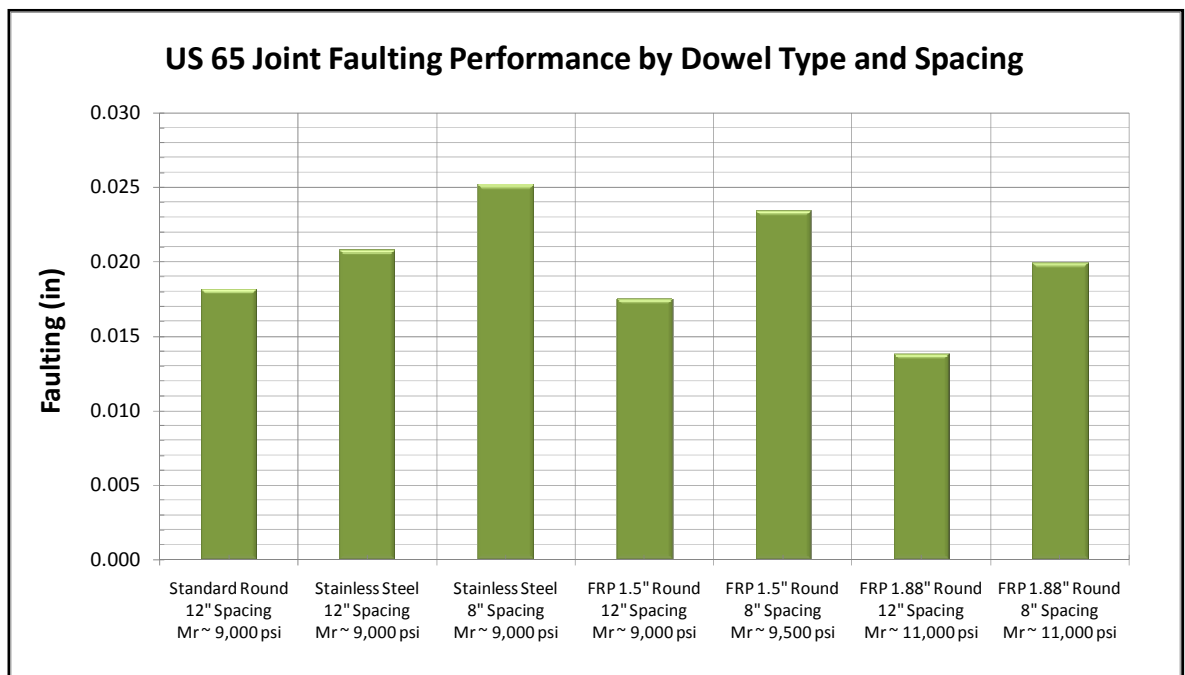


**Figure 47: HWY 330 Joint Faulting Standard Round Dowels (Mr Sections Only)**

#### 5.4.2 US 65 - Faulting

The joint faulting performance of the different dowel types and spacing intervals for US Highway 65 were analyzed. Since the subgrade resilient modulus ( $M_r$ ) conditions were so similar, an overall average of the faulting by section was graphed. The results of the

analysis can be seen in Figure 48 below. The figure also shows the resilient modulus value of the particular sections. Figure 48 shows the stainless steel dowels having the highest faulting. The next highest faulting values by dowel type in descending order are: standard round, 1.5 inch GFRP, and 1.88 inch GFRP dowel bars. The 1.88 inch GFRP bars performed the best in terms of joint faulting of all the bar types used on the US 65 project. A similar event occurred in the joint faulting of these bar types as did in the dowels used on the Iowa Highway 330 project. The dowel sections with closer spaced (more) dowels had higher faulting values than the sections with less dowels.

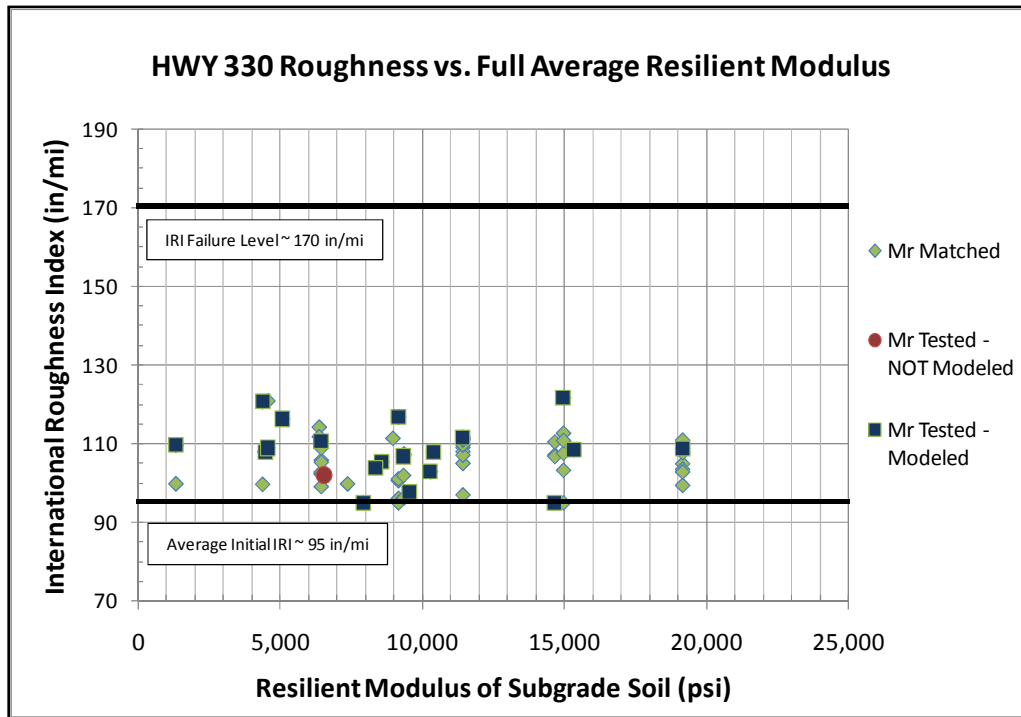


**Figure 48: US 65 Joint Faulting Performance by Dowel Type and Spacing**

### 5.5 HWY 330 Profile/ Roughness

The last data that was analyzed was road profile data from Highway 330. Profile data was not collected during the study of the US 65 section. The road profile data collected on Highway 330 was normalized for temperature during collection. The data was analyzed using

ProVal version 2.7 software (Transtec Group, 2007). ProVal 2.7 converts the profile data readings into a number called the International Roughness Index (IRI), as stated earlier. This is a universal way to quantitatively assign a roughness value to a particular stretch of highway. The roughness value is measured in inches per mile (in/mi). A higher IRI value is indicative of a rougher pavement surface. Since each pavement section has a different initial roughness, due to surface construction finish, there needs to be a way to compare the roughness incurred by the pavement due to post-construction effects. Post-construction effects would be effects caused by dowel type, dowel spacing, and subgrade conditions. In order to compare the different sections, a baseline value was established by which all sections could be standardized. An overall value of initial IRI was calculated to be approximately 95 in/mi. This value was set as the initial IRI for all sections. Then increases in IRI after construction were added to the standardized initial value to accurately assess the relative performance of the different sections. An overall roughness versus resilient modulus graph of all the dowel sections can be seen below in Figure 49. This graph does not differentiate sections with different dowel types and spacing.

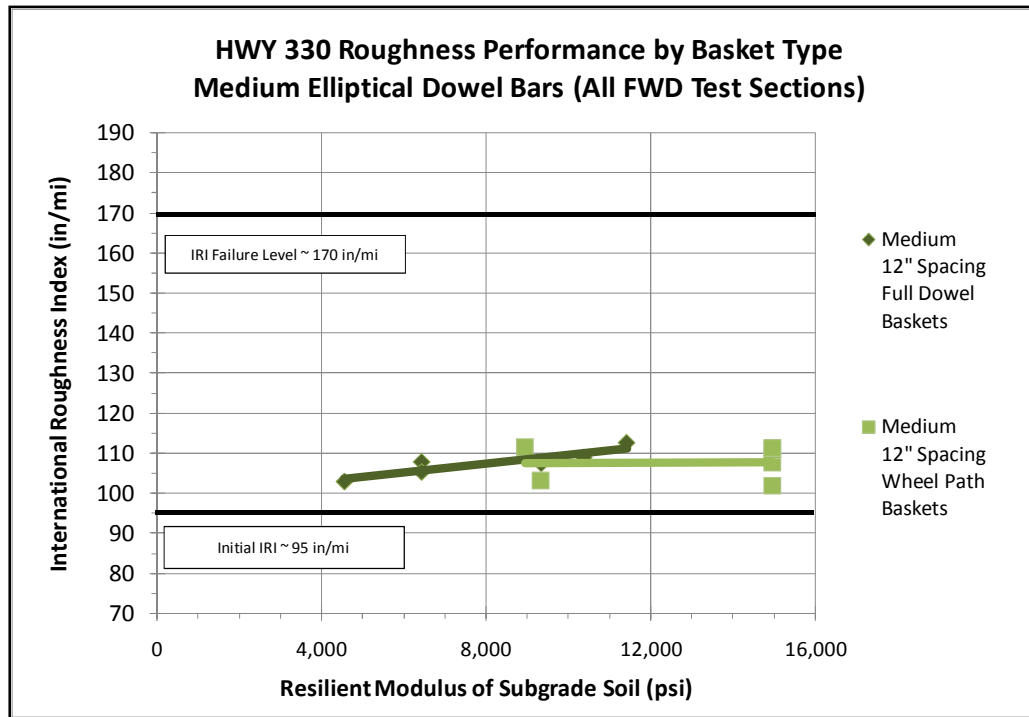


**Figure 49: HWY 330 Roughness vs. Resilient Modulus**

#### 5.5.1 Dowel Basket Type – HWY 330 IRI

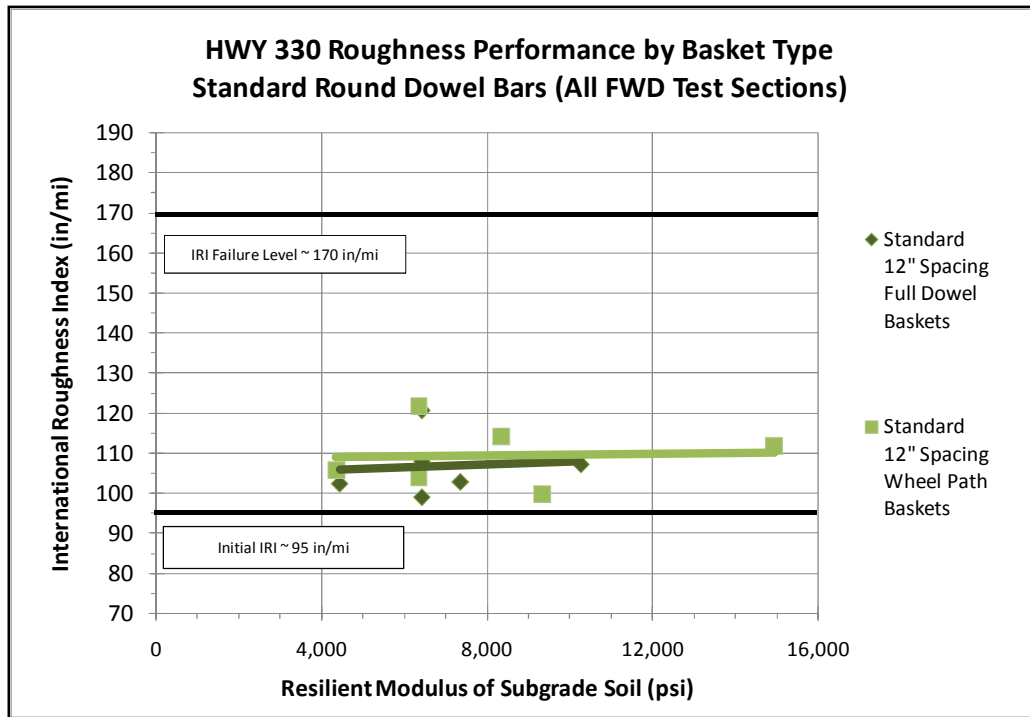
If dowel type and spacing are not considered Figure 49 indicates roughness will not yield any significant trends. However, when the dowel type, dowel spacing, and dowel basket type are considered, meaningful results can be found. Figure 50 below shows full dowel basket sections and wheel path basket sections performance when medium elliptical dowel bars are used. Medium elliptical dowel bars placed in wheel paths provide similar roughness performance as the full dowel basket sections. These results are the product of five years of testing. Continued testing may show different results for medium elliptical wheel path basket sections.





**Figure 50: HWY 330 Roughness by Basket Type - Medium Elliptical Dowels**

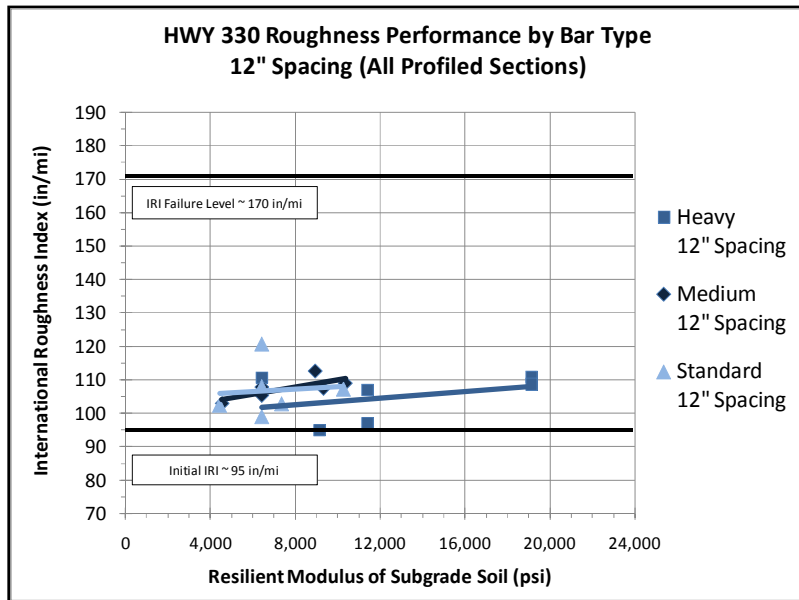
Figure 51 below shows standard round dowel bar roughness performance with full dowel basket sections and wheel path basket sections are used. Standard round dowel bars placed in wheel paths do not provide roughness performance equal to the full dowel basket sections. Notice the increased amount of spread of the standard round wheel path baskets compared with the full baskets. This indicates a degree of irregular behavior of the dowel bars. If the difference in roughness of the wheel path baskets continues at the rate it has been increasing for the last five year, the wheel path sections could be seeing significantly higher, if not failing IRI values as it gets closer to its design life.



**Figure 51: HWY 330 Roughness by Basket Type – Standard Round Dowels**

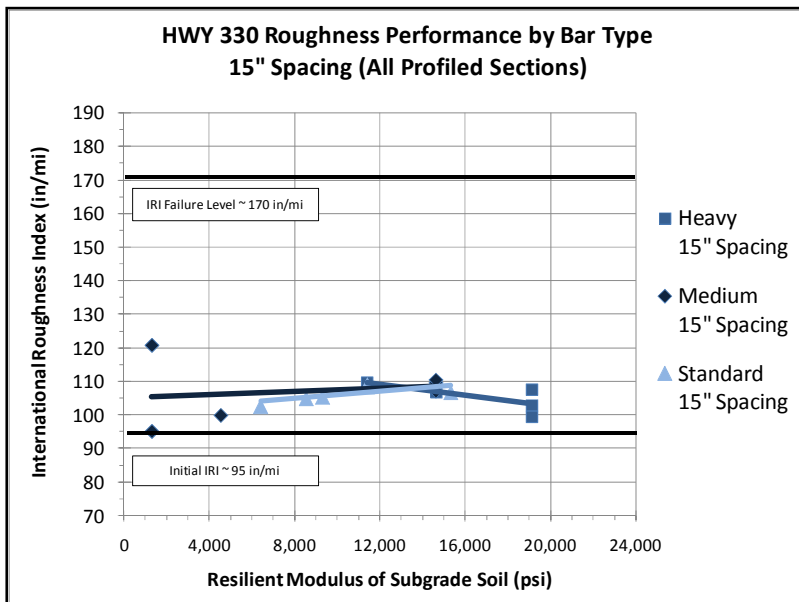
### 5.5.2 Dowel Type – HWY 330 IRI

Figure 52 below shows the heavy elliptical dowel bars outperforming the medium elliptical dowel bars and the standard round dowel bars at a 12 inch spacing. This makes intuitive sense, as the heavy elliptical dowel bars have more cross sectional area and should therefore be performing at a higher level than the medium elliptical and standard round dowel bars. Figure 52 also shows the medium elliptical dowel bars performing the same as standard round dowel bars. Since typical construction practice is to use dowel bars spaced at 12 inch intervals, this graph has good information about practical construction practice. Roughness data in the wheel path sections of the medium elliptical and standard round dowel bars was not graphed with the full basket data contained in Figure 52.



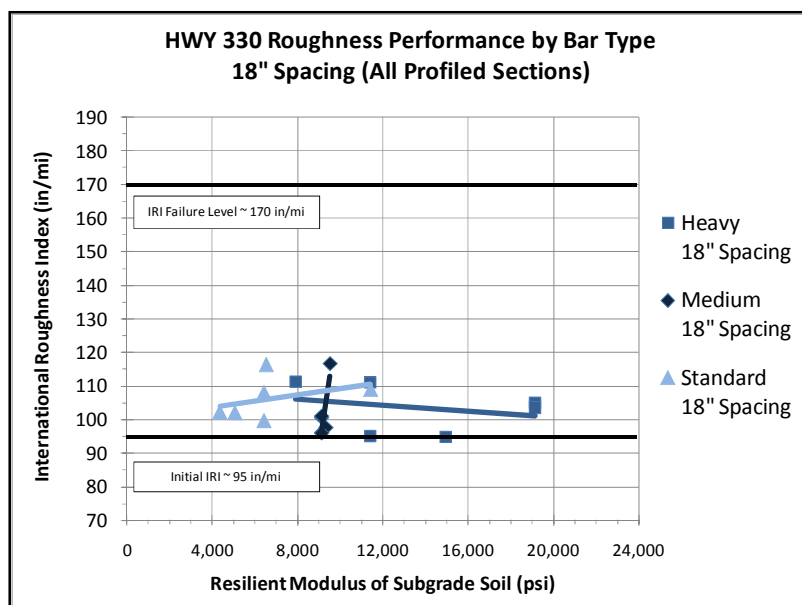
**Figure 52: HWY 330 Roughness Performance by Dowel Type @ 12 inch Spacing**

At the 15 inch spacing, Figure 53 shows that medium elliptical and standard round dowel bars are essentially performing equally in terms of roughness. The roughness performance of the heavy elliptical dowel bars seems to be about the same if not better than the standard round and medium elliptical toward the higher resilient modulus values.



**Figure 53: HWY 330 Roughness Performance by Dowel Type @ 15 inch Spacing**

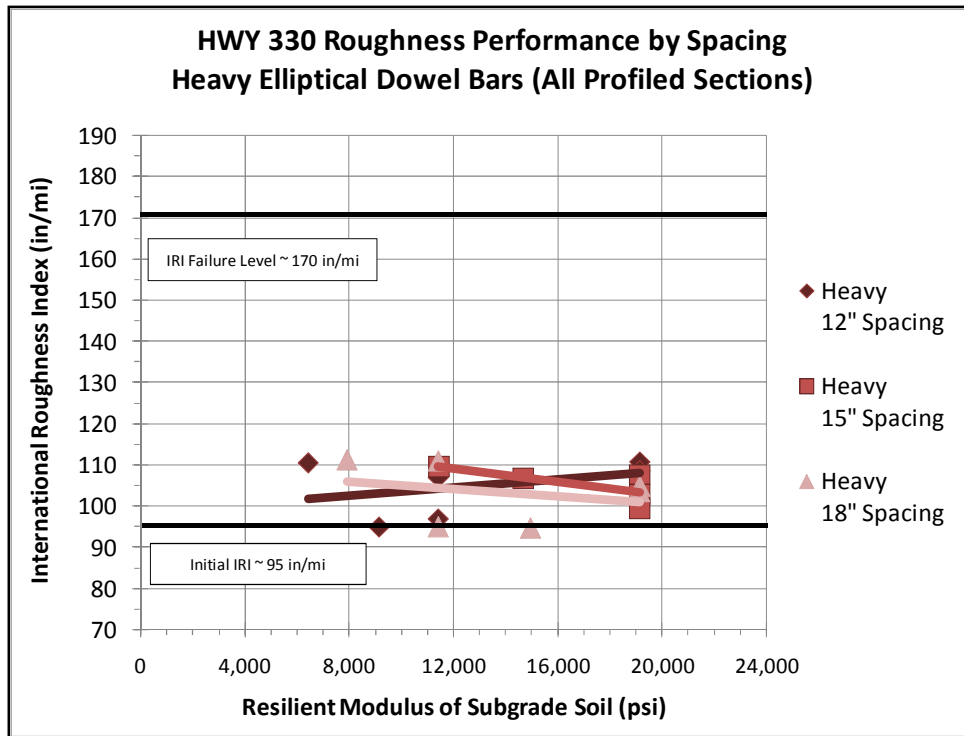
The results of the heavy elliptical, medium elliptical, and standard round dowel bars spaced at 18 inches can be seen in Figure 54 below. Figure 54 shows the heavy elliptical dowels spaced at 18 inches performing just as well as, if not better than the standard round dowels. The resilient modulus of the medium elliptical dowel bars spaced 18 inches apart do not have a large enough range to make confident performance comparisons. However, at the 9,000 to 10,000 psi level, where data was available for the medium elliptical dowels, the medium elliptical dowel bars seem to have performed just as well, if not better than the standard round dowel bars.



**Figure 54: HWY 330 Roughness Performance by Dowel Type @ 18 inch Spacing**

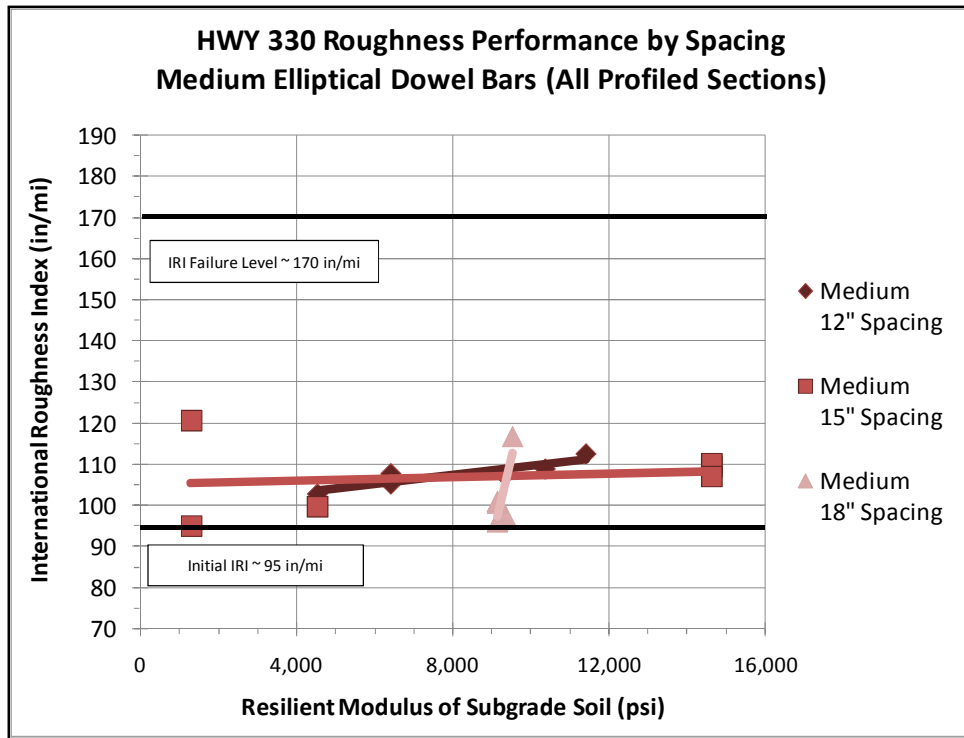
### 5.5.3 Dowel Spacing – HWY 330 IRI

Next, the roughness performance of heavy elliptical dowel bars at different spacing intervals was analyzed. Figure 55 shows that heavy elliptical dowel bars spaced at 15 inches and 18 inches are performing just as well in terms of roughness as the sections with heavy elliptical bars spaced 12 inches apart.



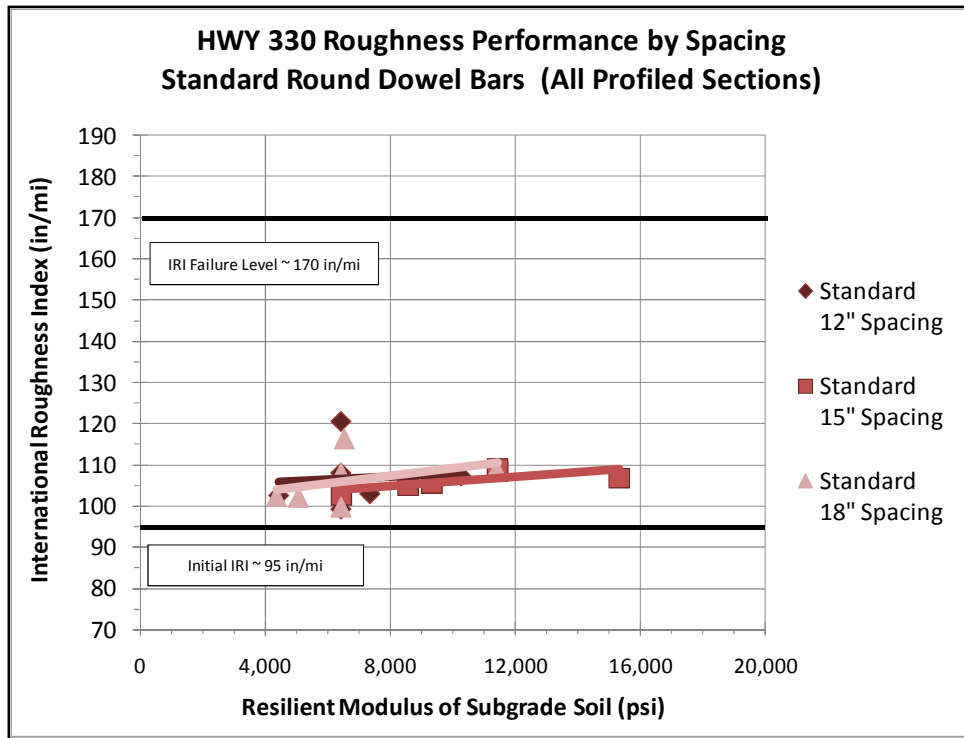
**Figure 55: HWY 330 Roughness by Dowel Spacing - Heavy Elliptical Dowels**

The roughness performance of the medium elliptical dowel bar sections at different spacing intervals was analyzed. The results of Figure 56 show that in terms of roughness, the medium elliptical dowels spaced 12 inches and 15 inches apart performed equally. The sections with wheel path baskets spaced at 12 inches were not included in the results of Figure 56. The data in Figure 56 that was taken at the 18 inch spaced medium elliptical dowel sections looks to have an average in the area of the 12 inch and 15 inch spaced dowels at that particular resilient modulus value. But, the medium elliptical dowel sections with bars spaced 18 inches apart did not have significant spread in resilient modulus, so the performance is not as conclusive.



**Figure 56: HWY 330 Roughness by Dowel Spacing - Medium Elliptical Dowels**

The roughness performance of the standard round dowel bar sections at different spacing intervals was analyzed. The results of Figure 57 show the standard round dowels spaced 15 inches and 18 inches apart performed just as well as the standard round dowels spaced 12 inches apart in terms of roughness. The sections with wheel path baskets spaced at 12 inches were not included in the results of Figure 57.



**Figure 57: HWY 330 Roughness by Dowel Spacing – Standard Round Dowels**

## Chapter 6. Summary and Conclusions

A summary of the performance found on Iowa Highway 330 and US Highway 65 by section can be found in Appendix D.

### 6.1 Load Transfer

#### 6.1.1 *Dowel Basket Type – Load Transfer Conclusions*

Iowa Highway 330 was the only project that contained sections that had a dowel configuration where dowels were placed in the wheel paths. Sections of both medium elliptical and standard round dowels bars were tested with dowels located exclusively in the wheel paths. There were four dowels placed in each wheel path with a spacing of 12 inches between each. These sections were compared with their respective full dowel basket sections. The results showed the medium elliptical dowel bar sections with dowels in the wheel paths only transfer load equally compared to the sections with medium elliptical bars placed in full baskets. This was characterized by a near overlap of the load transfer efficiency vs. resilient modulus graph of medium elliptical full basket and wheel basket sections. The load transfer of these sections ranged from 80 to 85% depending upon the subgrade resilient modulus value.

Sections where standard round dowel bars were placed exclusively in the wheel paths yielded significantly lower load transfer efficiency value than their full basket counterparts. The wheel path dowel sections for the standard round dowel bars were in the range of three to eight percent less effective at transferring load over the short five year study period. These differences would likely be more severe as the pavement reaches the end of its design life.



### 6.1.2 *Dowel Type – Load Transfer Conclusions*

Iowa Highway 330 and US Highway 65 both had varying bar types on the project. Iowa Highway 330 compared the effects of using 1.5 inch standard round epoxy coated steel dowel bars (area = 1.767 in<sup>2</sup>.), with using heavy elliptical (major axis = 1.969 in., minor axis = 1.338 in., and area = 2.084 in<sup>2</sup>.) and medium elliptical (major axis = 1.654 in., minor axis = 1.115 in., and area = 1.473 in<sup>2</sup>.) dowel bars. US Highway 65 compared the effects of using 1.5 inch standard round epoxy coated steel dowel bars with using 1.5 inch stainless steel, 1.5 inch fiber composite, and 1.88 inch fiber composite dowel bars.

In the Iowa Highway 330 project the 12 inch and 15 inch spacing intervals were used to compare the different bar types in performance. The bar types typically demonstrated a range of resilient modulus values, which allowed the plotting of a load transfer efficiency versus resilient modulus value. This makes it possible to see what happens to load transfer with change in bar types, as well as change in resilient modulus of the subgrade. Overall, the medium elliptical dowel bar sections exhibited zero to four percent better load transfer efficiency than the standard round dowel bars. This makes it possible to say that medium elliptical dowel bars perform as well, if not better than standard round dowel bars in terms of load transfer efficiency. Overall, the heavy elliptical dowel bar sections exhibited zero to four percent better load transfer efficiency than the medium elliptical dowel bars at the 12 inch spacing, depending upon the subgrade resilient modulus value. On the other hand, at the 15 inch spacing the heavy elliptical dowel bars performed one to two percent less than the medium elliptical dowel bars in terms of load transfer efficiency depending upon the subgrade resilient modulus value. Overall, the heavy elliptical dowel bars performed best in terms of load transfer, but did not perform significantly better than the medium elliptical

dowel bars. However, the heavy elliptical dowel bars displayed a trait that the other two dowel bar types did not. The heavy elliptical dowel bars seemed to be less sensitive to the resilient modulus value than the medium elliptical and standard round dowel bars. In the range of 6,000 to 19,000 psi resilient modulus at 12 inch spacing the heavy elliptical dowels performed at 84% to 85%. In the 11,000 to 19,000 psi resilient modulus range at 15 inch spacing, the heavy elliptical dowels performed at 83% to 82% load transfer efficiency. In the same 8,000 to 19,000 psi resilient modulus range at 18 inch spacing the heavy elliptical dowels performed at about 80% load transfer efficiency.

In the US Highway 65 project the 12 inch spacing was used to compare the different bar types in performance. Since all the bar types had very similar resilient modulus values, with exception to the 1.88 inch fiber composite bars, they were compared by using an overall average of all the sections over all the test periods. The standard round bars spaced at 12 inches performed better than the other bar types with an overall load transfer efficiency average of 89%. The stainless steel was the next best with an overall average of 86% load transfer efficiency. There was not much difference between the 1.5 inch and 1.88 inch GFRP bars with overall averages right around 79% load transfer efficiency. As stated earlier, the 1.88 inch GFRP sections had a little higher resilient modulus value. This did not change the results of the comparison since a higher resilient modulus value would equate to higher load transfer efficiency. In order to standardize the resilient modulus values, a lower load transfer would be assigned to the 1.88 inch GFRP bars. Since they are already at the bottom of performance, the conclusion is still the same; 1.88 inch GFRP bars do not perform as well as stainless steel or standard round bars in terms of load transfer.

### 6.1.3 Dowel Spacing – Load Transfer Conclusions

In the Iowa Highway 330 project the individual dowels (heavy elliptical, medium elliptical, standard round) were compared at different spacing intervals to see how spacing would affect load transfer performance. The heavy elliptical dowels showed the most consistent data. The heavy dowels appeared to be less sensitive to subgrade resilient modulus as previously stated. The load transfer efficiency of the heavy elliptical dowels at 12 inch spacing in the range of 6,000 to 19,000 psi resilient modulus were 84% to 85%. The 15 inch spaced heavy elliptical dowel sections in the 11,000 to 19,000 psi resilient modulus range performed at 83% to 82% load transfer efficiency. The 18 inch spaced heavy elliptical dowel sections in the 8,000 to 19,000 psi resilient modulus range performed at about 80% load transfer efficiency. The medium elliptical dowel bar sections had the 15 inch spaced dowel sections perform just as well as the 12 inch spaced dowel sections. The 15 inch spaced dowel sections transferred between 82% and 85% of the load between 1,000 and 15,000 psi subgrade resilient modulus. The sections with 12 inch dowel spacing performed slightly lower, but intuition indicates they should be performing as high, if not higher than the dowel sections with 15 inch spaced dowels. Therefore, it is assumed that the 12 inch spaced dowel sections will transfer similar values across the transverse joints. The sections with medium elliptical dowels spaced 18 inches apart had some sporadic results when all the test sections were used.

When only the sections with tested resilient modulus value were used, the results were reasonable and followed the premise that less bars will produce lower load transfer values. The sections with 18 inch spaced medium elliptical dowels had resilient modulus values between 9,000 and 10,000 psi and transferred about 77% to 79% of the load across the

transverse joint. The standard round dowel bar sections had the 12 inch spaced dowel sections perform slightly better than the 15 inch and 18 inch spaced dowel sections. The 12 inch spaced dowel sections transferred about 82% of the load when subgrade resilient modulus values were between 4,000 and 10,000 psi. The 15 inch spaced standard round dowel sections transferred between 80% and 82% of the load with subgrade resilient modulus values ranging from 6,000 and 15,000 psi. Again, sections with dowels spaced 18 inches apart had some inconsistent results when all test sections were used. Therefore, sections where resilient modulus values had been tested were used. The results were in a reasonable range. They showed the sections with 18 inch spaced medium elliptical dowels transfer about 80 % of the load across the transverse joint with a subgrade resilient modulus value between 5,000 and 7,000 psi. These are similar values to the sections with 15 inch spaced dowels. However, due to the inconsistent results coming from the 18 inch spaced dowel sections, it is not recommended to expand the dowel spacing of standard round or medium elliptical dowels for load transfer purposes based on data from Iowa Highway 330.

In the US Highway 65 project the individual dowels were compared at different spacing to see how it would affect load transfer performance. The stainless steel bars sections with bars spaced at eight inch intervals had the highest load transfer of all the other sections. At eight inch spacing the stainless steel dowel bars sections achieved 93% load transfer. This was an overall increase in load transfer of about seven percent with the closer spacing (i.e. more) stainless steel dowel bars. Placing the 1.5 inch GFRP bars at eight inch intervals increased the load transfer efficiency about seven percent to about 86% overall load transfer efficiency. The performance of the eight inch spaced 1.5 inch GFRP bars is approximately

the same load transfer efficiency performance as the stainless steel dowel bars spaced 12 inches apart. Decreasing the spacing of the 1.88 inch GFRP bars from 12 inches to eight inches only yielded a load transfer efficiency increase of about one percent. The 1.88 inch GFRP bars did not seem to effectively transfer load across the transverse joint. The data from the US 65 project suggests there is no benefit to using a 1.88 inch GFRP bar over a 1.5 inch GFRP bar in terms of load transfer efficiency.

## **6.2 Faulting**

### *6.2.1 Dowel Basket Type – Faulting Conclusions*

The medium elliptical wheel path dowel baskets showed an overall performance equal to or better than the full basket medium elliptical dowel sections in terms of joint faulting. All the standard round dowel sections on the Iowa Highway 330 project with dowels in the wheel paths showed lower levels of faulting than the full basket sections. Keep in mind these wheel path dowel baskets had four dowels spaced at 12 inch intervals across each wheel path of the transverse joint. The overall conclusion, based on the data, is the use of medium elliptical, or standard round wheel path baskets is just as good, if not better than full dowel baskets in terms of faulting. The results supported the possibility of faulting increases if too much steel is placed in the joint.

### *6.2.2 Dowel Type – Faulting Conclusions*

In the Iowa Highway 330 project the heavy elliptical, medium elliptical, and standard round dowel types were compared with each other to see how dowel type would affect faulting performance. The results hinted at the possibility that medium elliptical dowels are best of the three types at controlling faulting. The data also suggested the possibility that

heavy dowel bars produce the most faulting. This supports a theory that if too much steel is placed in the joint, faulting may be more prevalent.

In the US Highway 65 project the standard round, stainless steel, 1.5 inch round GFRP, and 1.88 inch round GFRP dowel types were compared with each other to see the effects of changing dowel type on joint faulting performance. The data suggested the order of faulting performance from greatest to least was 1.88 inch round GFRP, 1.5 inch round GFRP, standard round, and stainless steel dowel bars, respectively. Overall the dowel type faulting data for US 65 project seemed to hint at the possibility of a less stiff joint yielding better faulting performance.

### *6.2.3 Dowel Spacing – Faulting Conclusions*

Faulting performance for the Iowa Highway 330 project was analyzed on the individual dowel types at different spacing intervals. The results showed faulting performance for heavy elliptical dowel bars went down as more bars were used across the joint. The 12 inch and 15 inch spaced dowel sections for medium elliptical dowel bars seemed to perform similarly. Yet, the data suggested the 18 inch spaced medium elliptical dowel sections performed better than both the sections with 12 inch and 15 inch spaced intervals. The standard round sections suggested the possibility that the 18 inch spaced dowels had the best faulting performance. Keep in mind all faulting values were at a relatively low level due to the short five year study period. These results may become increasingly different as the pavement ages and encounters more traffic.

The individual dowels on the US Highway 65 project were compared at different spacing to see how dowel spacing would affect faulting performance. All dowel types;

stainless steel, 1.5 inch round GFRP, and 1.88 inch round GFRP, demonstrated higher faulting values as more bars were introduced into the joint. This means the data suggests the use of an eight inch spaced dowel bar configuration for stainless steel, 1.5 inch round GFRP, or 1.88 inch round GFRP results in a higher faulting value than the use of a 12 inch spaced dowel bar configuration.

### **6.3 Profile / Roughness**

#### *6.3.1 Dowel Basket Type – Roughness Conclusions*

The effect on roughness caused by using wheel path dowel baskets instead of full dowel baskets varied depending upon dowel type. On the Iowa Highway 330 project the medium elliptical dowel bars provided equal dowel bar performance to full dowel baskets when wheel path baskets were employed. When wheel path baskets were used in standard round dowel sections, the results were not as favorable. The standard round wheel path basket sections had higher roughness values than the full dowel basket sections. The difference was large enough to potentially decrease the serviceability life of the pavement through the use of standard round dowels placed in wheel paths only.

#### *6.3.2 Dowel Type – Roughness Conclusions*

In the Iowa Highway 330 project the 12 inch, 15 inch and 18 inch dowel spacing intervals were used to compare the different bar types in roughness performance. Overall, the medium elliptical dowel bar sections produced equal to or lower roughness values than the standard round dowel bars at all three dowel spacing intervals. Therefore, the data indicates medium elliptical dowel bars perform as well, if not better than standard round dowel bars in terms of roughness. At the 12 inch dowel spacing interval the heavy elliptical dowel bars

performed significantly better than the medium elliptical and standard round dowel bars in terms of maintaining low roughness values. At the 15 inch and 18 inch dowel spacing intervals the better performance was not as notable. However, the heavy elliptical dowel bars still demonstrated the lowest roughness values of all the dowel bar types on the Iowa Highway 330 project.

### *6.3.3 Dowel Spacing – Roughness Conclusions*

In the Iowa Highway 330 project the individual dowels (heavy elliptical, medium elliptical, standard round) were compared at different spacing intervals to see how dowel spacing would affect pavement roughness. The 12 inch spaced heavy elliptical dowels bars showed the lowest roughness values. There was a fairly significant effect of increasing the dowel spacing for heavy elliptical bars. However, the overall performance of the heavy elliptical bars at the 15 inch and 18 inch spacings were still better than the medium elliptical and standard round dowel bar sections. Dowels spaced at 12 inches and 15 inches did not show considerable differences from each other for medium elliptical or standard round dowel bars in terms of roughness performance. The results showed that 15 inch spaced dowels would maintain roughness just as well as 12 inch spaced dowels for medium elliptical and standard round dowel bars.

## **6.4 Overall Summary and Conclusions**

- Medium elliptical dowels performed just as well or outperformed standard round dowels in load transfer, faulting, and roughness



- Medium elliptical dowels spaced at 15 inch intervals transferred load, controlled faulting, and minimized roughness just as well as medium elliptical dowels spaced at 12 inch intervals
- Heavy elliptical dowel bars typically provided more load transfer than medium elliptical dowel bars, but the small amount of load transfer increase would be hard to justify for the increased cost
- Heavy elliptical, medium elliptical, and standard round bars performed inconsistently in terms of load transfer at the 18 inch spaced interval
- Standard round dowel bar sections with wheel path baskets performed notably worse than standard round dowels with full baskets in terms of load transfer over the course of the five year study
- Medium elliptical dowel bars placed in wheel paths only, performed equal to full medium elliptical dowel baskets in terms of load transfer, faulting, and roughness
- Round epoxy-coated steel dowels performed best of the dowels on US Highway 65 in terms of load transfer
- Stainless steel round dowels performed best of the non-corrosive alternatives to round epoxy-coated dowels on US Highway 65 in terms of load transfer; however, this may be coupled with future faulting issues
- Data indicates 1.5 inch stainless steel spaced at eight inch intervals should only be used in place of standard round epoxy coated dowel bars at 12 inch spacing if there is a significant cost savings

These conclusions are based on a five-year study and may be subject to change with more data collection.

A summary of the amount of steel used in each two-lane joint on the Iowa Highway 330 project can be seen in Table 10 below. The table shows how each bar configuration compares, as a percent of steel used per joint, to the standard round epoxy-coated 1.5 inch bars at 12 inch spaced intervals. Therefore, if the percent of joint steel is higher than 100%, there is more steel being used than the standard round epoxy-coated bars at 12 inch spaced intervals. Likewise, if the percent of joint steel is lower than 100%, there is less steel being used than the standard round epoxy-coated bars at 12 inch spaced intervals. This table is intended to be used for material cost comparison by bar configuration.

**Table 10: HWY 330 Steel Used per Joint by Dowel Type and Spacing**

<b>HWY 330 Dowel Bar Cross-Sectional Steel</b>				
<b>Bar Configuration</b>	<b>Dowel Bar Area (in<sup>2</sup>)</b>	<b># Bars / Joint (2 Lanes)</b>	<b>Total Cross-Sectional Steel Area per Joint (in<sup>2</sup>)</b>	<b>Percent Joint Steel vs. Standard Round @ 12" Spacing</b>
Heavy @ 12"	2.084	26	54.18	118%
Heavy @ 15"	2.084	19	39.60	86%
Heavy @ 18"	2.084	18	37.51	82%
Med @ 12"	1.654	26	43.00	94% *
Med @ 15"	1.654	19	31.43	68% *
Med @ 18"	1.654	18	29.77	65%
<b>Med @ 12" WP</b>	1.654	16	26.46	58% *
Standard @ 12"	1.767	26	45.94	100% ^
Standard @ 15"	1.767	19	33.57	73%
Standard @ 18"	1.767	18	31.81	69%
<b>Standard @ 12" WP</b>	1.767	16	28.27	62%

Note: \* dowel configuration performing notably well

^ dowel configuration acting as the standard for comparison

## Chapter 7. Recommendations

### 7.1 Design Considerations

- It is recommended that medium elliptical steel dowel bars at 12 inch or 15 inch spacing be considered for substitution of standard round dowel bars at 12 inch spacing in JPCP design
- The use of stainless steel dowel bars spaced at eight inch increments may be used in areas where epoxy-coated steel is not sufficient for corrosion resistance

### 7.2 Further Study

- The use of medium elliptical steel dowel bars in wheel path should be further studied as a viable alternative for load transfer mechanism to validate or refute the results of this study
- More study on the use of medium elliptical steel dowel bars at 18 inch spaced dowel intervals should be done to determine if they will perform acceptably
- The time observing pavement performance for both projects was limited to five years. More monitoring of these pavement sections would indicate long term effects of the different dowel types and spacing intervals.
- Specifically, more monitoring of the stainless steel bar sections spaced at 12 inch increments and 1.5 inch GFRP bar sections spaced at eight inch increments is recommended

## References

- AASHTO. (1998). *Supplement to the Guide for Design of Pavement Structures Part II, - Rigid Pavement Design & Rigid Pavement Joint Design*. New York: American Association of State Highway & Transportation Officials.
- AASHTO T-307-99 . (2000). *Determining the Resilient Modulus of Soils and Aggregate Materials , 20th Edition*.
- Andrei, D., Wiczak, M. W., Schwartz, C. W., & Uzan, J. (2004). Harmonized Resilient Modulus Test Method for Unbound Pavement Materials. *Transportation Research Record , No. 1874*, 29-37.
- ARA Inc., E. C. (2004, March). Guide for Mechanistic-Empirical Design of New and Rehabilitated Pavement Structures. NCHRP.
- ARA Inc., E. D. (2000, June). Resilient Modulus as Function of Soil Moisture - Summary of Predictive Models. *Guide for Mechanistic-Empirical Design of New and Rehabilitated Pavement Structures , Appendix DD-1*. NCHRP.
- Brigg, A. (2000, October 1-3). *FWD Operations - The Evolution of Total Quality Control Implementation*. Retrieved November 18, 2008, from FWD User's Group: <http://pms.nevadadot.com/2000.asp>
- Cable, J. K., Porter, M. L., Hoffman, J., Rold, L. L., & Edgar, L. E. (2003). *Demonstration and Field Evaluation of Alternative Portland Cement Concrete Pavement Reinforcement Materials*. Iowa Department of Transportation.
- Cable, J. K., Porter, M., Walker, J., Totman, S. L., & Pierson, N. (2008). *Field Evaluation of Elliptical Steel Dowel Performance*. Iowa State University, Center for Transportation Research and Education. Washington D.C.: Federal Highway Administration.
- Colley, B. E., & Tayabji, S. D. (1968). *Improved Rigid Pavement Joints*. report prepared for Federal Highway Administration.
- Darter, M. I., & Barenberg, E. J. (1977). *Design of Zero Maintenance Plain Jointed Concrete Pavement, Vol. II - Design Manual*. Federal Highway Administration.
- Das, B. M. (2001). *Principles of Geotechnical Engineering* (Fifth Edition ed.). Upper Saddle River: Nelson Education Limited.
- Drumm, E. C., Reeves, J. S., Madgett, M. R., & Trolinger, W. D. (1997, May). Subgrade Resilient Modulus Correction Factor for Saturation Effects. *Journal of Geotechnical and Geoenvironmental Engineering , 663-670*.

- Elliott, R. P., & Thornton, S. I. (1988). Simplification of Subgrade Resilient Modulus Testing. *Journal of Transportation Research Record* (1192), 1-7.
- FHWA. (2008). *Appendix B. MANUAL FOR FAULTMETER MEASUREMENTS*. Retrieved July 23, 2008, from U.S. Department of Transportation - Federal Highway Administration: <http://www.tfhr.gov/pavement/ltp/tp/reports/03031/appb.htm>
- FHWA. (2008). *Pavement Smoothness Methodologies*. Retrieved August 12, 2008, from U.S. Department of Transportation - Federal Highway Administration: [http://www.fhwa.dot.gov/resourcecenter/teams/pavement/pave\\_5psm.cfm](http://www.fhwa.dot.gov/resourcecenter/teams/pavement/pave_5psm.cfm)
- George, K. P. (2004). *Prediction of resilient modulus from soil index properties*. University of Mississippi. University of Mississippi.
- Hall, K. T. (1992). *Backcalculation Solutions for Concrete Pavements*. Long Term Pavment Performance Memo Prepared for SHRP Contract P-020.
- Hoffman, J. G. (2002). Evaluation of Fiber Composite and Stainless Steel as Alternative Dowel Bar Material. *Diss. Iowa State Univ.* Iowa State University.
- Huang, Y. H. (2004). *KENPAVE Pavement Analysis and Design*. Upper Saddle River.
- Huang, Y. H. (2003). *Pavement Analysis and Design. 2nd ed.* Upper Saddle River: Prentice Hall.
- Ioannides, A. M., & Korovesis, G. T. (1992). Analysis and Design of Doweled Slab-on-Grade Pavement Systems. *Journal of Transportation Engineering* , 118 (6), 745-768.
- Kilareski, W. P. (1982). Epoxy Coating for Protection of Reinforcement Steel. In D. E. Tonini, & S. W. Dean, *Chloride Corrosion of Steel in Concrete - STP 629* (pp. 82-88). New York: American Society for Testing & Materials.
- Kim, D., & Siddiki, N. Z. (2006). *Simplification of Resilient Modulus Testing for Subgrades*. Purdue University, Indiana Department of Transportation. U.S. Department of Transportation - Federal Highway Administration.
- Liang, R., & Zeng, S. (2002). Efficient Dynamic Analysis of Multilayered System During Falling Weight Deflectometer Experiments. *Journal of Transportation Engineering* , 366-374.
- Malla, R. B., & Joshi, S. (2007, September). Resilient Modulus Prediction Models Based on Analysis of LTPP Data for Subgrade Soils and Experimental Verification. *Journal of Transportation Engineering* , 491-504.

- May, R. W., & Witzczak, M. W. (1981). Effective granular modulus to model pavement responses. *Transportation Research Record 810* , 1-9.
- McDaniel, L. L. (1998). Using Deflection Basins to Estimate Alternative Joint Reinforcement Load Transfer. *Iowa State University Dissertation* . Iowa State University.
- NRCS. (2008). *Web Soil Survey*. Retrieved June 10, 2008, from United States Department of Agriculture - Natural Resource Conservation Services:  
<http://websoilsurvey.nrcs.usda.gov/app/WebSoilSurvey.aspx>
- Porter, M. L., Guinn Jr., R. J., & Lundy, A. L. (2001). *Dowel Bar Optimization: Phases I and II*. Iowa State University. Ames: Center for Transportation Research and Education & Center for Portland Cement Concrete Pavement Technology.
- Porter, M. L., Guinn Jr., R. J., Lundy, A. L., Davis, D. D., & Rohner, J. G. (2001). *Investigation of Glass Fiber Composite Dowel Bars for Highway Pavement Slabs*. Ames: Submitted to Highway Division of the Iowa Department of Transportation and Iowa Highway Research Board.
- Santha, B. L. (1994). Resilient Modulus of Subgrade Soils: Comparison of Two Constitutive Equations. *Transportation Research Record 1462* , 79-90.
- SAS. (2007). JMP 7.0. Cary, North Carolina.
- Sutherland, E. C., & Teller, L. W. (1935). The Structural Design of Concrete Pavements. *Public Roads* , 16 (8), 67-144.
- Thölen, O. (1982). Falling Weight Deflectometer KUAB 50. *Proc. Int. Conf. on Bearing Capacity of Roads and Airfields*. Trondheim, Norway.
- Transtec Group. (2007). *ProVal Pavement Profile Viewing and Analysis*. Retrieved August 2007, from <http://www.roadprofile.com/>
- Uzan, J. (1985). Characterization of granular material. *Transportation Research Record, 1022* , 52-59.
- Wilson, B. E., Sargand, S. M., Hazen, G. A., & Green, R. (1990). Multiaxial Testing of Subgrade. *Journal of Transportation Research Record (1278)*, 91-95.
- Witzczak, M. W., & Uzan, J. (1988). *The Universal Airport Design System Report I of IV: Granular Material Characterization*. University of Maryland, Department of Civil Engineering, College Park, MD.

## Appendix A

**Table 11: HWY 330 Dowel Basket Locations**

Test Section	Station		Station	Bar Type	Size	Spacing (Inches)
	Proposed	Actual				
1T	1175+44		1176+00	Standard	35 mm	12
2	1176+00	1176+00	1177+20	Standard	1.5 in	12
3T	1177+20		1177+50	Standard	35 mm	12
4	1177+50	1177+51	1178+70	Standard	1.5 in	12
5T	1178+70		1179+00	Standard	35 mm	12
6	1179+00	1179+03	1179+20	Standard	1.5 in	12
7T	1179+20		1180+50	Standard	35 mm	12
8	1180+50	1180+55	1181+70	Standard	1.5 in	15
9T	1181+70		1182+00	Standard	35 mm	12
10	1182+00	1182+00	1183+20	Standard	1.5 in	15
11	1183+50	1183+53	1184+70	Standard	1.5 in	15
12T	1184+70		1187+00	Standard	35 mm	12
13	1187+00	1187+01	1188+20	Standard	1.5 in	18
14T	1188+20		1188+50	Standard	35 mm	12
15	1188+50	1188+55	1189+70	Standard	1.5 in	18
16T	1189+70		1190+00	Standard	35 mm	12
17	1190+00	1190+00	1191+20	Standard	1.5 in	18
18T	1191+20		1191+50	Standard	35 mm	12
19	1191+50	1191+51	1192+70	Medium Elliptical	oval	12
20T	1192+70		1193+00	Standard	35 mm	12
21	1193+00	1193+00	1194+20	Heavy Elliptical	oval	12
22T	1194+20		1194+50	Standard	35 mm	12
23	1194+50	1194+50	1195+70	Medium Elliptical	oval	12
24T	1195+70		1197+00	Standard	35 mm	12
25	1197+00	1197+03	1198+20	Heavy Elliptical	oval	12
26T	1198+20		1198+50	Standard	35 mm	12
27	1198+50	1198+52	1199+70	Heavy Elliptical	oval	12
28T	1199+70		1201+50	Standard	35 mm	12
29	1201+50	1201+55	1202+70	Medium Elliptical	oval	12
30T	1202+70		1204+50	Standard	35 mm	12
31	1204+50	1204+55	1205+70	Heavy Elliptical	oval	15
32T	1205+70		1206+00	Standard	35 mm	12
33	1206+00	1206+01	1207+20	Medium Elliptical	oval	15
34T	1207+20		1209+00	Standard	35 mm	12
35	1209+00	1209+02	1210+20	Medium Elliptical	oval	15
36T	1210+20		1210+50	Standard	35 mm	12

Test Section	Station		Station	Bar Type	Size	Spacing (Inches)
	Proposed	Actual				
37	1210+50	1210+55	1211+70	Heavy Elliptical	oval	15
38T	1211+70		1213+00	Standard	35 mm	12
39	1213+00	1213+05	1214+20	Medium Elliptical	oval	15
40T	1214+20		1214+50	Standard	35 mm	12
41	1214+50	1214+56	1215+70	Medium Elliptical	oval	18
42T	1215+70		1216+00	Standard	35 mm	12
43RG	1216+00	1216+01	1217+20	Medium Elliptical	oval	18
44T	1217+20		1217+50	Standard	35 mm	12
45RG	1217+50	1217+50	1218+70	Medium Elliptical	oval	18
46T	1218+70		1219+00	Standard	35 mm	12
47RG	1219+00	1219+00	1220+20	Heavy Elliptical	oval	12
48T	1220+20		1222+00	Standard	35 mm	12
49	1222+00	1222+01	1223+20	Heavy Elliptical	oval	15
50T	1223+20		1223+50	Standard	35 mm	12
51	1223+50	1123+51	1224+70	Heavy Elliptical	oval	12
52T	1224+70		1225+00	Standard	35 mm	12
53	1225+00	1125+01	1226+20	Heavy Elliptical	oval	18
54T	1226+20		1226+50	Standard	35 mm	12
55	1226+50	1226+51	1227+70	Heavy Elliptical	oval	12
56T	1227+70		1228+00	Standard	35 mm	12
57	1228+00	1228+01	1229+20	Heavy Elliptical	oval	18
58T	1229+20		1229+50	Standard	35 mm	12
59	1229+50	1229+52	1230+70	Heavy Elliptical	oval	15
60T	1230+70		1231+00	Standard	35 mm	12
61	1231+00	1231+03	1232+20	Heavy Elliptical	oval	15
62T	1232+20		1232+50	Standard	35 mm	12
63	1232+50	1232+53	1233+70	Heavy Elliptical	oval	15
64T	1233+70		1237+00	Standard	35 mm	12
65	1237+00	1237+00	1238+20	Heavy Elliptical	oval	18
66T	1238+20		1238+50	Standard	35 mm	12
67	1238+50	1238+54	1239+70	Heavy Elliptical	oval	18
68T	1239+70		1240+00	Standard	35 mm	12
69	1240+00	1240+05	1241+20	Standard	1.5 in	12
70T	1241+20		1241+50	Standard	35 mm	12
71	1241+50	1241+55	1242+70	Standard	1.5 in	12
72T	1242+70		1243+00	Standard	35 mm	12
73	1243+00	1243+03	1244+20	Standard	1.5 in	12
74T	1244+20		1244+50	Standard	35 mm	12
75	1244+50	1244+52	1245+70	Heavy Elliptical	oval	18



Test Section	Station		Station	Bar Type	Size	Spacing (Inches)
	Proposed	Actual				
76T	1245+70		1246+50	Standard	35 mm	12
77	1246+50	1246+51	1247+70	Standard	1.5 in	15
78T	1247+70		1248+50	Standard	35 mm	12
79	1248+50	1248+50	1249+70	Standard	1.5 in	15
80T	1249+70		1250+00	Standard	35 mm	12
81	1250+00	1250+00	1251+20	Medium Elliptical**	oval	12
82T	1251+20		1251+50	Standard	35 mm	12
83	1251+50	1251+50	1252+70	Heavy Elliptical	oval	18
84T	1252+70		1253+00	Standard	35 mm	12
85	1253+00	1253+00	1254+20	Medium Elliptical**	oval	12
86T	1254+20		1254+50	Standard	35 mm	12
87	1254+50	1254+50	1255+70	Medium Elliptical**	oval	12
88T	1255+70		1256+00	Standard	35 mm	12
89	1256+00	1256+06	1257+20	Medium Elliptical**	oval	12
90T	1257+20		1259+00	Standard	35 mm	12
91	1259+00	1259+03	1260+20	Standard**	1.5 in	12
92T	1260+20		1260+30	Standard	35 mm	12
93	1260+30	1260+35	1261+50	Medium Elliptical**	oval	12
94T	1261+50		1261+60	Standard	35 mm	12
95	1261+60	1261+60	1262+80	Standard	1.5 in	15
96T	1262+80		1262+90	Standard	35 mm	12
97	1262+90	1262+85	1263+70	Standard	1.5 in	18
98	1264+00	1264+06	1265+20	Medium Elliptical**	oval	12
99T	1265+20		1265+30	Standard	35 mm	12
100	1265+30	1265+32	1266+50	Standard**	1.5 in	12
101	1266+50	1266+53	1267+70	Standard**	1.5 in	12
102T	1267+70		1275+80	Standard	35 mm	12
103	1275+80	1275+81	1277+00	Standard**	1.5 in	12
104	1277+00	1277+05	1278+20	Standard	1.5 in	18
105T	1278+20		1278+50	Standard	35 mm	12
106	1278+50	1278+54	1279+70	Standard	1.5 in	18
107T	1279+70		1280+00	Standard	35 mm	12
108	1280+00	1280+03	1281+20	Medium Elliptical	oval	12
109T	1281+20		1301+00	Standard	35 mm	12
110	1301+00	1301+01	1302+20	Standard**	1.5 in	12
111T	1302+20		1317+00	Standard	35 mm	12
112	1317+00	1317+03	1318+20	Medium Elliptical	oval	12
113T	1318+20		1318+50	Standard	35 mm	12
114	1318+50	1318+54	1319+70	Medium Elliptical	oval	12

Test Section	Station		Station	Bar Type	Size	Spacing (Inches)
	Proposed	Actual				
115T	1319+70		1320+00	Standard	35 mm	12
116	1320+00	1320+05	1321+20	Medium Elliptical	oval	15
117T	1321+20		1327+00	Standard	35 mm	12
118	1327+00	1327+06	1328+20	Standard**	1.5 in	12
119T	1328+20		1331+00	Standard	35 mm	12
120	1331+00	1331+00	1332+20	Medium Elliptical	oval	15
121T	1332+20		1332+50	Standard	35 mm	12
122	1332+50	1332+52	1333+70	Medium Elliptical	oval	15
123T	1333+70		1339+00	Standard	35 mm	12
124	1339+00	1339+06	1340+20	Medium Elliptical	oval	18
125T	1340+20		1343+50	Standard	35 mm	12
126	1343+50	1343+56	1344+70	Medium Elliptical	oval	18
127T	1344+70		1345+00	Standard	35 mm	12
128	1345+00	1345+05	1346+20	Medium Elliptical	oval	18
129T	1346+20		1360+00	Standard	35 mm	12

Note: Sections designated with a "T" are non-test sections

Test sections designated with a "RG" are located in the rebuilt grading

Test sections with \*\* after bar type are wheel path basket sections

## Appendix B

**Table 12: US 65 Dowel Basket Locations**

Test Section	Boring #	Station		Bar Type	Size	Spacing (Inches)
		Beginning	End			
1	B1	642+16	641+96	Standard	1.5 in	12"
2		641+96	641+76	Standard	1.5 in	12"
3		641+76	641+56	Standard	1.5 in	12"
-	B2		637+00	Stainless Steel	1.5 in	12"
4		635+22	635+02	Stainless Steel	1.5 in	12"
5		635+02	634+84	Stainless Steel	1.5 in	12"
6		634+84	634+64	Stainless Steel	1.5 in	12"
7	B3	632+20	632+00	Stainless Steel	1.5 in	8"
8		632+00	631+80	Stainless Steel	1.5 in	8"
9		631+80	631+60	Stainless Steel	1.5 in	8"
10		630+80	630+60	RJD	1.5 in	12"
11		630+60	630+40	RJD	1.5 in	12"
12		630+40	630+20	RJD	1.5 in	12"
13		629+80	629+60	RJD	1.5 in	8"
14		629+60	629+40	RJD	1.5 in	8"
15		629+40	629+20	RJD	1.5 in	8"
-	B4		628+00	Hughes Brothers	1 7/8"	12"
16		625+23	625+03	Hughes Brothers	1 7/8"	12"
17		625+03	624+83	Hughes Brothers	1 7/8"	12"
18		624+83	624+63	Hughes Brothers	1 7/8"	12"
19	B5	623+23	623+03	Hughes Brothers	1 7/8"	8"
20		623+03	622+83	Hughes Brothers	1 7/8"	8"
21		622+83	622+63	Hughes Brothers	1 7/8"	8"

### Appendix C

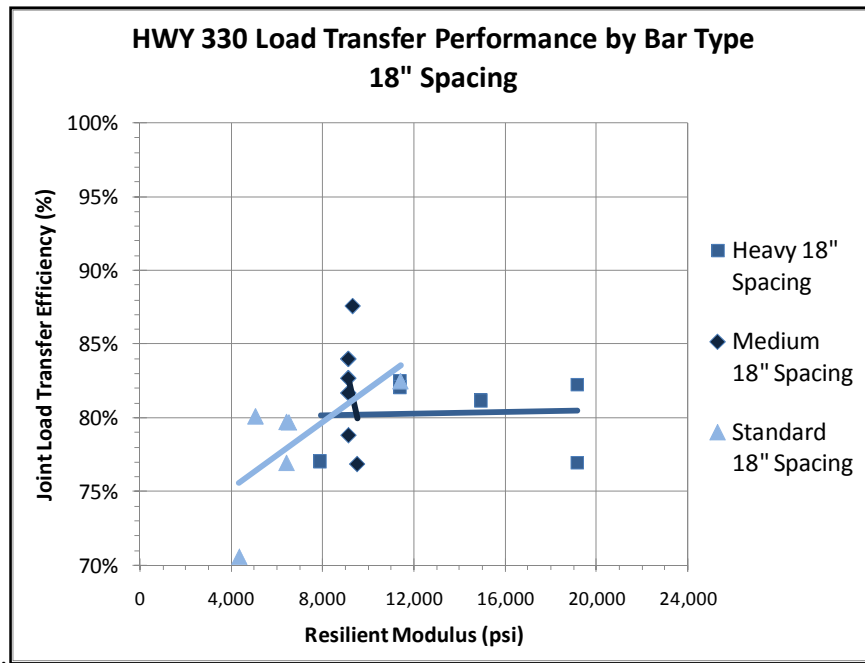


Figure 58: HWY 330 Load Transfer by Bar Type @ 18 inch Spacing

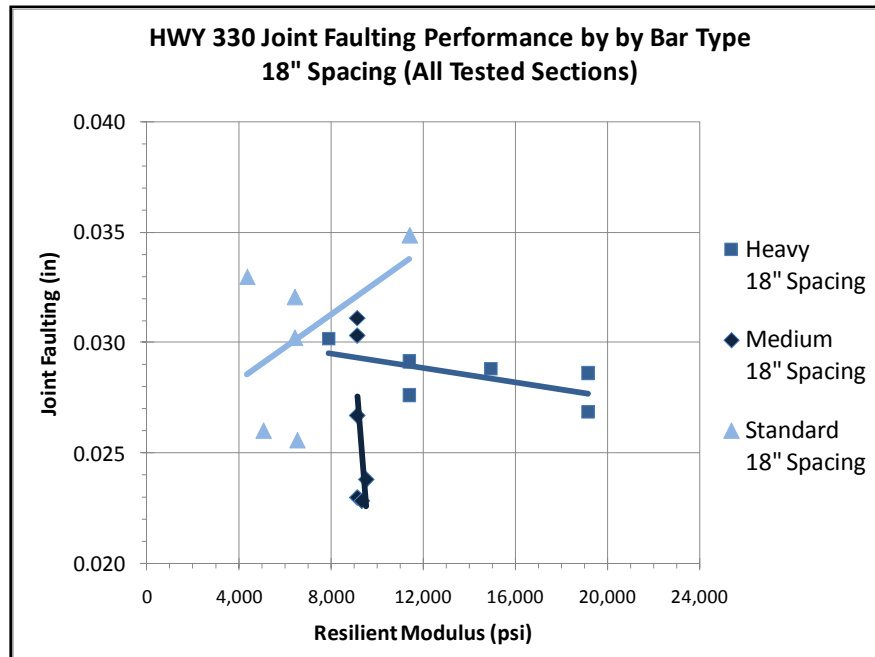


Figure 59: HWY 330 Joint Faulting by Bar Type @ 18 inch Spacing

## Appendix D

**Table 13: HWY 330 Performance Data Summary**

<b>HWY 330 Performance Data Summary</b>											
Test Section	Station		Bar Type	Bar Size	Bar Spacing (in)	Boring #	Boring Station Location	Mr Modeled (psi) *	Load Transfer (%)	IRI (in/mi)	Faulting Average (in)
	Begin	End									
2	1176+00	1177+20	standard	1.5 in	12			6424	84%	106	0.033
4	1177+51	1178+70	standard	1.5 in	12	1	1178+00	6424	82%	102	0.029
6	1179+03	1180+20	standard	1.5 in	12			6424	79%	99	0.031
8	1180+55	1181+70	standard	1.5 in	15			6424	80%	103	0.033
10	1182+00	1183+20	standard	1.5 in	15			11412	83%	105	0.032
11	1183+53	1184+70	standard	1.5 in	15	2	1184+00	11412	78%	109	0.034
13	1187+01	1188+20	standard	1.5 in	18			11412	82%	108	0.035
15	1188+55	1189+70	standard	1.5 in	18			6424	80%	102	0.032
17	1190+00	1191+20	standard	1.5 in	18			6424	77%	109	0.030
19	1191+51	1192+70	medium	oval	12			6424	78%	103	0.030
21	1193+00	1194+20	heavy	oval	12	3	1193+30	6424	83%	111	0.030
23	1194+50	1195+70	medium	oval	12	4	1195+00	6424	82%	105	0.031
25	1197+03	1198+20	heavy	oval	12			11412	87%	107	0.030
27	1198+52	1199+70	heavy	oval	12			11412	86%	97	0.032
29	1201+55	1202+70	medium	oval	12	5	1202+00	11412	86%	112	0.031
31	1204+55	1205+70	heavy	oval	15			11412	84%	110	0.031
33	1206+01	1207+20	medium	oval	15			14649	88%	107	0.029
35	1209+02	1210+20	medium	oval	15			14649	84%	110	0.030
37	1210+55	1211+70	heavy	oval	15			14649	80%	107	0.031
39	1213+05	1214+20	medium	oval	15	6	1213+50	14649	84%	95	0.030
41	1214+56	1215+70	medium	oval	18			9142	84%	101	0.027
43	1216+01	1217+20	medium	oval	18			9142	82%	101	0.030
45	1217+50	1218+70	medium	oval	18	7	1218+00	9142	83%	96	0.031
47	1219+00	1220+20	heavy	oval	12			9142	84%	95	0.033
49	1222+01	1223+20	heavy	oval	15			19147	80%	99	0.028
51	1123+51	1224+70	heavy	oval	12			19147	82%	111	0.032
53	1125+01	1226+20	heavy	oval	18			19147	82%	105	0.027
55	1226+51	1227+70	heavy	oval	12	8	1227+00	19147	83%	109	0.031
57	1228+01	1229+20	heavy	oval	18			19147	77%	104	0.029
59	1229+52	1230+70	heavy	oval	15			19147	80%	108	0.028
61	1231+03	1232+20	heavy	oval	15			11412	84%	110	0.027
63	1232+53	1233+70	heavy	oval	15	9	1233+00	19147	88%	103	0.029

<b>HWY 330 Performance Data Summary</b>											
Test Section	Station		Bar Type	Bar Size	Bar Spacing (in)	Boring #	Boring Station Location	Mr Modeled (psi) *	Load Transfer (%)	IRI (in/mi)	Faulting Average (in)
	Begin	End									
65	1237+00	1238+20	heavy	oval	18			11412	82%	111	0.029
67	1238+54	1239+70	heavy	oval	18			11412	83%	111	0.028
69	1240+05	1241+20	standard	1.5 in	12	10	1240+50	4436	82%	108	0.032
71	1241+55	1242+70	standard	1.5 in	12	11	1242+00	10266	81%	103	0.031
73	1243+03	1244+20	standard	1.5 in	12	12	1243+50	7351	83%	100	0.028
75	1244+52	1245+70	heavy	oval	18	13	1245+00	7910	77%	95	0.030
77	1246+51	1247+70	standard	1.5 in	15	14	1247+00	8557	82%	105	0.031
79	1248+50	1249+70	standard	1.5 in	15	15	1249+00	15314	82%	108	0.031
81	1250+00	1251+20	medium	oval	12			14952	85%	103	0.028
83	1251+50	1252+70	heavy	oval	18			14952	81%	95	0.029
85	1253+00	1254+20	medium	oval	12	16	1253+50	14952	84%	113	0.028
87	1254+50	1255+70	medium	oval	12			14952	79%	108	0.024
89	1256+06	1257+20	medium	oval	12	17	1256+50	14952	88%	111	0.026
91	1259+03	1260+20	standard	1.5 in	12	18	1259+50	14952	83%	122	0.027
93	1260+35	1261+50	medium	oval	12			8948	85%	111	0.029
95	1261+60	1262+80	standard	1.5 in	15	19	1262+00	9321	81%	107	0.029
97	1262+85	1263+70	standard	1.5 in	18	20	1263+20	6531	80%	102	0.026
98	1264+06	1265+20	medium	oval	12			9321	78%	102	0.027
100	1265+32	1266+50	standard	1.5 in	12	21	1266+00	8347	77%	104	0.024
101	1266+53	1267+70	standard	1.5 in	12	22	1267+20	6352	75%	114	0.026
103	1275+81	1277+00	standard	1.5 in	12	23	1276+20	4358	75%	121	0.027
104	1277+05	1278+20	standard	1.5 in	18			4358	71%	100	0.033
106	1278+54	1279+70	standard	1.5 in	18	24	1279+20	5061	80%	116	0.026
108	1280+03	1281+20	medium	oval	12	25	1280+70	10372	81%	108	0.025
110	1301+01	1302+20	standard	1.5 in	12	26	1301+70	9337	80%	107	0.026
112	1317+03	1318+20	medium	oval	12	27	1317+50	9337	81%	107	0.028
114	1318+54	1319+70	medium	oval	12	28	1318+80	4547	81%	109	0.027
116	1320+05	1321+20	medium	oval	15			4547	81%	121	0.022
118	1327+06	1328+20	standard	1.5 in	12	29	1327+70	6352	76%	112	0.024
120	1331+00	1332+20	medium	oval	15			1305	83%	100	0.025
122	1332+52	1333+70	medium	oval	15	30	1333+00	1305	84%	110	0.025
124	1339+06	1340+20	medium	oval	18	31	1339+50	9337	88%	96	0.023
126	1343+56	1344+70	medium	oval	18	32	1344+00	9525	77%	98	0.024
128	1345+05	1346+20	medium	oval	18	33	1345+50	9149	79%	117	0.023

Note: \* resilient modulus data for two psi confining pressure and two psi deviator stress

**Table 14: US 65 Performance Data Summary**

<b>US 65 Performance Data Summary</b>										
Test Section	Station		Bar Type	Bar Size	Bar Spacing (in)	Boring #	Boring Station Location	Mr Modeled (psi) *	Load Transfer (%)	Faulting Average (in)
	Begin	End								
1	642+16	641+96	Standard	1.5"	12"	1	642+00	9053	91%	0.0210
2	641+96	641+76	Standard	1.5"	12"			9053	91%	0.0203
3	641+76	641+56	Standard	1.5"	12"			9053	89%	0.0131
-	-	-	-	-	-	2	637+00	13562	-	-
4	635+22	635+02	Stainless Steel	1.5"	12"			9166	83%	0.0276
5	635+02	634+84	Stainless Steel	1.5"	12"			9166	88%	0.0177
6	634+84	634+64	Stainless Steel	1.5"	12"			9166	88%	0.0171
7	632+20	632+00	Stainless Steel	1.5"	8"	3	632+00	9166	93%	0.0269
8	632+00	631+80	Stainless Steel	1.5"	8"			9166	93%	0.0361
9	631+80	631+60	Stainless Steel	1.5"	8"			9166	92%	0.0125
10	630+80	630+60	GFRP	1.5"	12"			9166	72%	0.0223
11	630+60	630+40	GFRP	1.5"	12"			9166	84%	0.0171
12	630+40	630+20	GFRP	1.5"	12"			9166	81%	0.0131
13	629+80	629+60	GFRP	1.5"	8"			9166	87%	0.0223
14	629+60	629+40	GFRP	1.5"	8"			9763	89%	0.0203
15	629+40	629+20	GFRP	1.5"	8"			9763	83%	0.0276
-	-	-	-	-	-	4	628+00	9763	-	-
16	625+23	625+03	GFRP	1 7/8"	12"			11052	75%	0.0230
17	625+03	624+83	GFRP	1 7/8"	12"			11052	87%	0.0125
18	624+83	624+63	GFRP	1 7/8"	12"			11052	74%	0.0059
19	623+23	623+03	GFRP	1 7/8"	8"	5	623+00	11052	84%	0.0157
20	623+03	622+83	GFRP	1 7/8"	8"			11052	71%	0.0190
21	622+83	622+63	GFRP	1 7/8"	8"			11052	85%	0.0249

Note: \* resilient modulus data for two psi confining pressure and two psi deviator stress